

PAULA REEMANN

The effects of microenvironment
on skin cells



PAULA REEMANN

The effects of microenvironment
on skin cells



Department of Physiology, Institute of Biomedicine and Translational Medicine, University of Tartu, Tartu, Estonia

Dissertation is accepted for the commencement of the degree of doctor philosophiae in Neuroscience on March 19, 2015, by the Council of the commencement of Doctoral Degree in Neuroscience

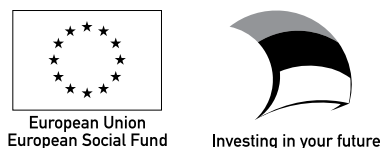
Supervisors: Sulev Kõks, MD, PhD, Professor, Department of Pathophysiology, Institute of Biomedicine and Translational Medicine, University of Tartu, Estonia
Küllü Kingo, MD, PhD, Professor, Department of Dermatology, University of Tartu, Estonia
Viljar Jaks, MD, PhD, Senior Researcher, Institute of Molecular and Cell Biology, University of Tartu, Estonia
Olavi Vasar, MD, FESPS Consultant, Plastic and vascular surgeon Hospital of Reconstructive Surgery, Tallinn, Estonia

Reviewers: Tarmo Annilo, PhD, Senior Research Fellow, Estonian Genome Center, University of Tartu, Estonia
Pille Säälük, PhD, Research Fellow, Laboratory of Cancer Biology, Institute of Biomedicine and Translational Medicine, University of Tartu, Estonia

Opponent: Esko Kankuri, MD, PhD, Docent, Principal Investigator, Head of Laboratory, Faculty of Medicine, Pharmacology, University of Helsinki, Finland

Commencement: May 22, 2015

This research was supported by the institutional research funding (grants IUT20-46 and IUT2-25) and personal research grants PUT4 and PUT177 of the Estonian Ministry of Education and Research; by the research grant ETF8932 of Estonian Science Foundation; by the European Union through the European Social Fund, and through the European Regional Development Fund via projects “Carbon Nanotube Reinforced Electrospun Nano-fibres and Yarns” (3.2.1101.12-0018), “SmaCell” (3.2.1101.12-0017) and via Centre of Translational Medicine (3.2.0101.08-0008), Centre of Excellence “Mesosystems: Theory and Applications” (3.2.0101.11-0029), Centre of Translational Genomics of University of Tartu (SPIGVARENG); by the integration grant from the European Molecular Biology Organization (MLOMR09003).



ISSN 1736-2792
ISBN 978-9949-32-800-0 (print)
ISBN 978-9949-32-801-7 (pdf)

Copyright: Paula Reemann, 2015

Tartu Ülikooli Kirjastus
www.tyk.ee

CONTENTS

LIST OF ORIGINAL PUBLICATIONS	8
ABBREVIATIONS	10
INTRODUCTION	11
REVIEW OF LITERATURE	13
1. Skin structure	13
1.1. Epidermis	13
1.2. Dermis	14
1.3. Hypodermis	15
2. Skin cells	15
3. The role of interleukin-10 (IL-10) family cytokines in defense mechanisms of the skin	16
4. Extracellular matrix	17
5. Skin grafting	18
6. Skin substitutes	19
7. Biomaterial surfaces	20
8. The design of extracellular matrix	21
8.1. Polymers	21
8.2. Natural polymers. Gelatin.	22
AIMS OF THE STUDY	24
MATERIALS AND METHODS	25
1. Human subjects (Papers I–IV)	25
1.1. Tissue samples	26
2. Isolating and growing skin cells (Papers I–IV)	26
2.1. Lipopolysaccharide stimulation	27
3. RNA extraction (Papers II, IV)	27
3.1. RNA extraction for whole transcriptome sequencing	27
3.2. RNA extraction for qRT-PCR	27
4. Whole Transcriptome sequencing (Paper IV)	27
5. Gene expression analysis by qRT-PCR (Paper II)	28
6. Immunohistochemistry (Paper II)	28
7. Fibroblast cultivation on sol–gel prepared nanopatterned silica surfaces (Paper I).....	28
7.1. Preparing silica structures	28
7.2. Atomic force microscopy	29
7.3. Fibroblast cultivation on silica structures	29
7.4. Fluorescent microscopy	29
7.5. Senescence associated β -galactosidase staining	30
8. Fibroblast cultivation on thermally cross-linked glucose-containing electrospun gelatin meshes (Paper III).....	30
8.1. Designing fibrous glucose-containing gelatin meshes	30

8.2. Assessment of biological properties	31
8.2.1. Glucose measurement	31
8.2.2. Quantification of viable cells	31
8.2.3. Protein mass spectrometry (MS)	31
8.2.4. In vitro degradation of scaffolds	31
9. Scanning electron microscopy (SEM) (Papers I, III)	32
9.1. SEM of cells grown on silica surfaces	32
9.2. SEM of fibrous gelatin meshes	32
9.3. SEM of adult's skin biopsy	32
10. Statistical analysis (Papers I, II, VI)	33
10.1. Analysis of RNA-Seq data	33
10.1.1. Modeling background regions	33
10.1.2. Differential expression analysis of gene expression	33
10.1.3. Pathway analysis of differentially expressed genes	34
10.2. Statistical analysis for qRT-PCR analyses	34
RESULTS	35
1. Interleukin-10 family cytokines in the skin and skin cells (Paper II).....	35
2. Whole transcriptome sequencing (Paper IV)	41
2.1. Overall differences between cultivated melanocytes, keratinocytes, fibroblasts and whole skin tissue	42
2.2. Pathway analysis of the skin cells and whole skin	43
2.3. Characterization of gene expression pattern of juvenile keratinocytes, melanocytes and fibroblasts	46
3. Cells on nanopatterned surfaces (Paper I)	51
3.1. Surface design	51
3.2. Cell morphology	52
3.3. The induction of cell senescence on nanopatterned surfaces	54
3.4. The regulation of cell proliferativity by nanopatterned surfaces	54
3.5. Scanning electron microscopy (SEM) and focused ion beam (FIB) imaging of the cells grown on sol-gel prepared silica surface	55
4. Design of thermally cross-linked glucose-containing electrospun gelatin meshes (Paper III)	56
4.1. Glucose measurements	58
4.2. Biological degradation	59
4.3. Cell proliferation	59
4.4. Cell morphology	60
DISCUSSION	62
1. IL-10 family cytokines	62
2. Cell type-specific differences in the skin transcriptome	63
2.1. Tumorigenesis	65
2.2. Inflammation	65
2.3. Stemness-related processes	66
2.4. Extracellular matrix	67
3. Biocompatible surfaces	67

4. Gelatin scaffolds modified by glucose-assisted thermal cross-linking	69
5. Concluding thoughts and future prospects	70
Normal versus artificial condition. 2D versus 3D environment	70
CONCLUSIONS	73
REFERENCES	74
SUMMARY IN ESTONIAN	82
ACKNOWLEDGEMENTS	84
ORIGINAL PUBLICATIONS	85
CURRICULUM VITAE	139
ELULOOKIRJELDUS	142

LIST OF ORIGINAL PUBLICATIONS

- I Reemann, P.; Kangur, T.; Pook, M.; Paalo, M.; Nurmis, L.; Kink, I.; Porosaar, O.; Kingo, K.; Vasar, E.; Kõks, S.; Jaks, V.; Järvekülg, M. (2013). **Fibroblast growth on micro- and nanopatterned surfaces prepared by a novel sol-gel phase separation method.** *Journal of Materials Science: Materials in Medicine*, 24: 783–792.
- II Reemann, P.; Reimann, E.; Suutre, S.; Paavo, M.; Loite, U.; Porosaar, O.; Abram, K.; Silm, H.; Vasar, E.; Kõks, S.; Kingo, K. (2014). **Expression of Class II Cytokine Genes in Children's Skin.** *Acta Dermato-Venereologica*, 94: 386–392.
- III Siimon, K.; Reemann, P.; Pöder, A.; Pook, M.; Kangur, T.; Kingo, K.; Jaks, V.; Mäeorg, U.; Järvekülg, M. (2014). **Effect of glucose content on thermally cross-linked fibrous gelatin scaffolds for tissue engineering.** *Materials Science and Engineering C*, 42: 538–545.
- IV Reemann, P.; Reimann, E.; Ilmjärv, S.; Porosaar, O.; Silm, H.; Jaks, V.; Vasar, E.; Kingo, K.; Kõks, S. (2014). **Melanocytes in the skin – comparative whole transcriptome analysis of main skin cell types.** *PLOS ONE*, 9(12): e115717.

Contribution of the author:

- I The author designed the biological part of the study, performed all cell culture and histochemistry experiments, prepared samples for scanning electron microscopy, performed stainings for fluorescent microscopy, carried out some of imaging, participated in statistical analysis process and writing the biological part of the manuscript, and handled correspondence.
- II The author participated in designing the study, performed the cell culture experiment (jointly with Ene Reimann), carried out RNA extraction and majority of the quantitative real-time PCR, performed data analysis and statistical analysis, wrote most parts of the manuscript, and handled correspondence.
- III The author designed the biological part of the study, performed the majority of the cell culture experiments and assessment of cellular properties (preparing cell-containing for scanning electron microscopy, glucose and biological degradation measurement) (jointly with Annika Pöder), carried out data analysis of the biological part, co-wrote the manuscript.

- IV The author participated in designing the study, performed all cell culture experiments, performed RNA extraction, carried out the whole transcriptome sequencing (jointly with Ene Reimann), carried out some parts of the statistical analysis, wrote the manuscript with input from co-authors, and handled correspondence.

ABBREVIATIONS

cDNA	complementary DNA
DMEM	Dulbecco's Modified Eagle's medium
DNA	deoxyribonucleic acid
DNase	deoxyribonuclease
FB	fibroblasts
FBS	foetal bovine serum
FIB	focused ion beam
<i>Hprt1</i>	hypoxanthine guanine phosphoribosyl transferase 1 gene
IL	interleukin
KC	keratinocytes
LPS	lipopolysaccharide
MC	melanocytes
mRNA	messenger ribonucleic acid
qRT-PCR	quantitative real-time polymerase chain reaction
RNA	ribonucleic acid
SEM	scanning electron microscopy

INTRODUCTION

Human tissues are well-organized systems. They consist of thousands of smaller functional modules, which all have crucial parts to play to achieve faultless functioning of the body. In order to understand how our body works one has to break the system down into small units, investigate them individually and try to merge the results into a big picture. The smallest functional unit in the body is a cell. This is why we tend to think of cells as the key building blocks of living systems. However, equally important are extracellular components, which by virtue of being arranged into elaborate systems allow cells to function properly and perform organ-specific tasks.

In the present study, the focus is on skin tissue, where cells and extracellular structures exhibit an extensive network of interactions and a well-organized structure (Figure 1).

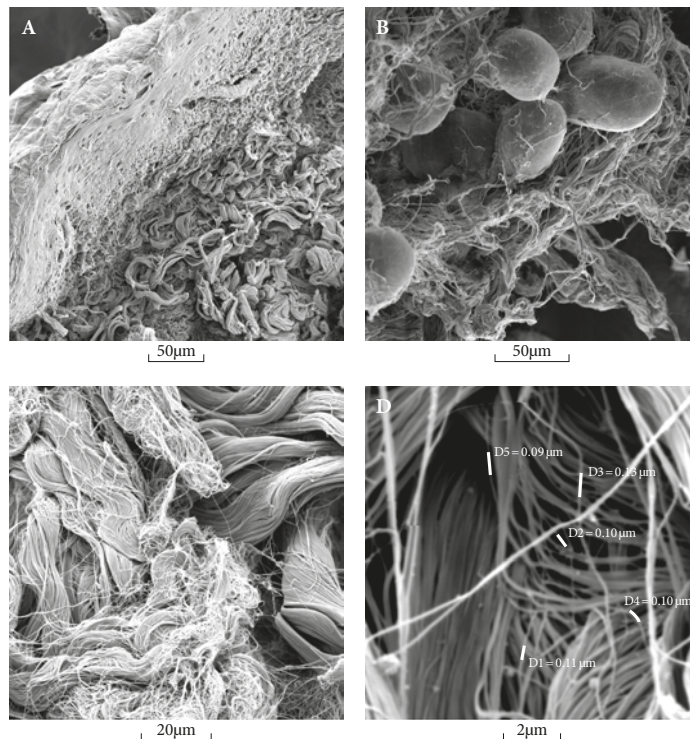


Figure 1. Scanning electron microscopy (SEM) imaging of adult's whole skin tissue (by Paula Reemann and Triin Kangur). SEM image shows layers and structural components of the skin: cross-section of the epidermis and dermis (A), hypodermis (B), fibrillary proteins in dermis (C), magnification of collagen fibres (D).

The beauty of the skin structure has fascinated me for a long time and has inspired me to study the workings of this intricate system. It also raised the question, whether it can be mimicked artificially in order to provide some relief for the problems caused by the limited amount of donor skin.

Studies linked to the current dissertation began with harvesting and describing the most common cell types of the skin – keratinocytes, melanocytes and fibroblasts. We sequenced the transcriptomes of cultured keratinocytes, melanocytes, fibroblasts and whole skin biopsies. The purpose of this study was to extend the existing knowledge about the background and functioning of these three skin cell types, often used for tissue engineering purposes.

We took a detailed look at interleukin-10 family cytokines and their receptor expression in the skin as one of the most important aspects in tissue engineering is to avoid immunological responses, which interfere with regeneration and cause rejection of grafts. A number of IL-10 family cytokines have both pro-inflammatory and anti-inflammatory roles, they can improve the healing process in injured skin, limit infection-induced damage or modify inflammation (Ouyang et al., 2011). Our study identified specific cytokine expression profiles for each cell type studied, and helped to explain the roles of different cells in the regulation of inflammatory response in the skin.

Tissue-engineered products make extensive use of juvenile skin cells due to their excellent proliferative capacity. For the same reason we used juvenile fibroblasts to investigate the biocompatibility of novel sol-gel silica surfaces. Next, we studied glucose cross-linked fibrous gelatin scaffolds, which were found to possess favourable mechanical properties for skin tissue engineering purposes. Cultivation of juvenile fibroblasts on these matrices had significant impact on the proliferation and morphology of the cultured cells suggesting their enhanced biocompatibility when compared to conventional monolayer cell culture.

REVIEW OF LITERATURE

I. Skin structure

Skin is the largest organ of human body and constitutes about 15–20% of the body's total mass (Gartner and Hiatt, 2001). Skin is defined as an organ because it has different tissues that work together to perform its specific functions. Four main tissue types can be found in the skin – (a) different epithelial tissues (keratinized stratified squamous epithelium such as epidermis; simple squamous epithelium as endothelium in blood vessels; glandular epithelium and simple or stratified cuboidal epithelial cells in sweat gland; glandular epithelium and cornifying squamous epithelium in sebaceous gland; hair follicle epithelial cells), (b) extracellular matrix-rich connective tissues (dense irregular connective tissue such as dermis; loose connective tissue in blood vessels and nerves; fat tissue; blood and immune system cells), (c) nerve tissue (bundles of axons which form peripheral nerves and are connected to variety of sensory and motor nerve endings like free nerve endings, Merkel's cells, Meissner's corpuscles, Pacinian corpuscles, Ruffini endings and hair follicle receptors), and (d) muscle tissue (smooth muscle incorporated in the walls of the arterioles and erectors of hairs) (Burgdorf et al., 2009, Arend et al., 1994, Alberts et al., 2008, Gartner and Hiatt, 2001).

At the same time the term “skin tissue” is very often used in literature. Usually it refers to two most prominent tissue layers in the skin: the outer epidermis with keratinocytes and melanocytes and the deeper dermis with fibroblasts and extracellular matrix. A hypodermis below the dermis, which is composed of subcutaneous adipose tissue, is occasionally also encompassed by this term (Burgdorf et al., 2009).

In the present study we use the term “skin tissue” to incorporate all three layers: epidermis, dermis and hypodermis and concentrate mostly on the three main skin cell types: keratinocytes, melanocytes and fibroblasts and the extracellular matrix of the dermis.

I.1. Epidermis

Epidermis is a cell-dense, but relatively thin skin layer: in most of the body parts it is 70 μ m – 1.2mm (except palms and soles (Gartner and Hiatt, 2001)). Despite this, the undamaged epidermis prevents most infectious agents and harmful substances from entering the body. The epidermis has several layers (Figure 2) – (a) stratum corneum, composed of dead keratinized cell sheets, (b) stratum granulosum, a keratinized stratified squamous epithelium, (c) stratum spinosum, consisting of polygonal cells, where keratinization begins and (d) stratum basale (basal layer), which consists of mitotic cells (keratinocyte stem cells) which are attached to the basement membrane (Gartner and Hiatt, 2001). After division, the daughter keratinocytes start to migrate upward towards the

surface of the skin. The outermost layer of the skin consisting of dead cells constantly sheds off (Gartner and Hiatt, 2001), therefore, keratinocytes are responsible for the continuous renewal of the skin. Pigment producing melanocytes and antigen-presenting Langerhans cells, which detect foreign substances are located between the basal keratinocytes (Gartner and Hiatt, 2001).

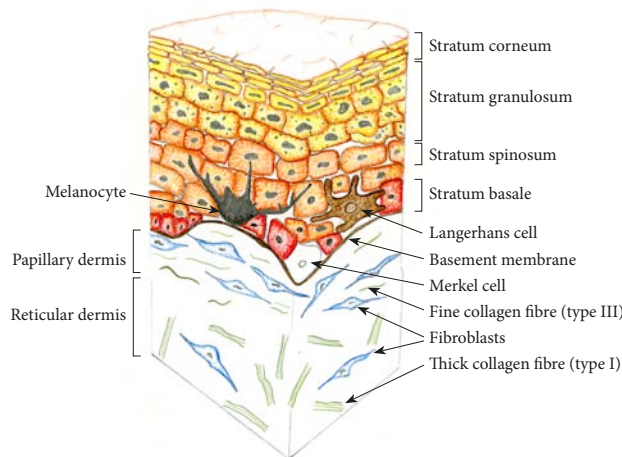


Figure 2. Schematic illustration of epidermis and dermis (based on Gartner and Hiatt (Gartner and Hiatt, 2001) and Young and Heath (Young and Heath, 2000)).

1.2. Dermis

The thickness of dermis is approximately 0.6–3 mm, depending on the body site (Gartner and Hiatt, 2001). As it is not sharply demarcated from underlying hypodermis, the exact thickness is difficult to determine. The dermis consists of two functional layers of connective tissue: the superficial papillary layer and the deeper reticular layer, again without a clear margin between them (Gartner and Hiatt, 2001). The papillary layer is relatively thin, forming invaginations into the epidermis (dermal papillae). Compared to the reticular layer, it is more cell-dense (Janson et al., 2012) and contains mainly fine collagen type III (less than 5 μm) (Geneser, 1986) intertwined with fine elastic fibres. It also contains small blood and lymph vessels and nerves. The reticular layer of the dermis is relatively thick, containing irregularly orientated collagen (mainly type I) fibres (5–10 μm) (Geneser, 1986), which arrange into bundles (up to 100 μm) (Geneser, 1986) and coarse elastic fibres (Sorrell and Caplan, 2004, Gartner and Hiatt, 2001). It also contains large vascular plexus, lymph vessels and nerves penetrating the reticular dermis.

The main cell type in the dermis is the fibroblast, but as in epidermis, cells from the other structures penetrating the skin tissue are also present: perineural Schwann cells, endothelial cells of blood vessels, some adipocytes, macrophages, mast cells etc. (Gartner and Hiatt, 2001).

1.3. Hypodermis

Hypodermis (subcutaneous) is thickest layer of the skin. It invaginates into the dermis and is mainly formed by adipose cells held together by fibrous tissue. Each adipocyte is encircled by small capillaries, which bunch together to form bigger arteries and veins locating in the major fibrous septa (Gartner and Hiatt, 2001).

2. Skin cells

Keratinocytes and fibroblasts form the main cellular mass in the skin (7×10^5 – 9×10^5 keratinocytes per mm^2 (Bauer et al., 2001, Hoath and Leahy, 2003) and 2×10^3 mid-dermis fibroblasts (Miller et al., 2003) to 10^5 papillary fibroblasts per mm^3 (Randolph and Simon, 1998). The average number of pigment-producing melanocytes depends on the body site and is estimated to be between 500 to 2000 melanocytes per mm^2 (Gartner and Hiatt, 2001, Thingnes et al., 2012).

Keratinocytes make up the majority of the cellular mass (95%) of the epidermis (Haake et al., 2001) and they have several roles in a mammalian organism. They form a hydrophobic envelope acting as a mechanical barrier against external pathogens. Keratinocytes secrete different kinds of cytokines and signal molecules, thereby modulating immunological and regenerative status of the skin (Burgdorf et al., 2009). Additionally, they keep other epidermal cells in place.

Another important cell type in the epidermis is the pigment-producing melanocyte. These cells are located on the basement membrane together with keratinocyte stem cells. It is estimated that there is one melanocyte per five to six basal keratinocytes in the basal layer (Park et al., 2012). Melanocytes are highly influenced by surrounding keratinocytes, which regulate melanocyte survival, dendricity, melanogenesis, and the expression of cell surface receptors (Park et al., 2012). Individual variation in the melanocyte number is remarkably small (Gartner and Hiatt, 2001). Melanocytes are highly outnumbered by keratinocytes, which makes it difficult to study them in whole skin biopsies and increases the likelihood that their role in different pathological processes will be underestimated. Besides the pigment synthesis, melanocytes have both local and systemic functions: they are able to secrete a wide range of signaling molecules, e.g. proinflammatory cytokines, immunosuppressive molecules, neuromediators etc. (Slominski, 2009, Park et al., 2012).

Fibroblasts constitute the majority of the cells in the middle layer of the skin – the dermis. Fibroblasts originate from mesenchymal stem cells and are normally found in many tissues (Arend et al., 1994). A dermal fibroblast differs from fibroblasts originating from other tissues by having less cellular plasticity: their reprogramming to other fibroblast types is far less likely. At least two subpopulations of dermal fibroblasts have been described: papillary and reticular (Sorrell and Caplan, 2004). These are located in papillary and reticular dermis, respectively. These two cell populations have multiple differences at the gene expression level (Janson et al., 2012), in the production of factors that

regulate epithelial and mesenchymal cells interactions, cellular proliferation and extracellular matrix production (Sorrell and Caplan, 2004). In addition, they can be distinguished by morphology: reticular fibroblasts have more polygonal appearance, while papillary fibroblasts tend to be spindle-shaped (Janson et al., 2012). Papillary fibroblasts are more proliferative than reticular fibroblasts (Azzarone and Macieira-Coelho, 1982, Janson et al., 2013, Harper and Grove, 1979) and the loss of papillary fibroblasts might play a role in skin aging (Mine et al., 2008).

3. The role of interleukin-10 (IL-10) family cytokines in defense mechanisms of the skin

The most important roles of the skin are protection, sensation, thermoregulation and metabolism. Protection against pathogens and other harmful agents includes providing an impenetrable barrier to the outer world and the ability to control adequately immune and inflammatory responses to environmental factors. The IL-10 family cytokines are crucial players in host defense mechanisms. They can improve the healing process, limit infection-caused damage or modify inflammation by promoting innate immune responses in epithelial tissue (Mosser and Zhang, 2008, Cao et al., 2006, Sonnenberg et al., 2010). Recent results suggest that the IL-10 family of cytokines is involved in the function of skin as well as in the pathogenesis of major skin diseases (e.g. psoriasis and atopic dermatitis) (Mosser and Zhang, 2008, Ouyang et al., 2011)

The IL-10 family includes a number of cellular cytokines: IL10, IL19, IL20, IL22, IL24, IL26, IL28A, IL28B, and IL29. This classification is based on distinctive six-alpha-helix structure that is common to all mature IL-10 family members (Trivella et al., 2010). They also share up to 28% of their amino acid level (Dumoutier and Renauld, 2002, Fickenscher et al., 2002). However, receptor-binding domains of IL-10 family cytokines are variable and define their interaction with different receptors (Ouyang et al., 2011, Sheppard et al., 2003) (Table 1).

Table 1. The interaction of IL-10 family cytokines with cytokine receptors. IL-10 family cytokines have been shown to exert their function through different receptors by partly sharing receptor subunits or whole receptor complexes (Ouyang et al., 2011, Sheppard et al., 2003).

Gene	IL10	IL19	IL20	IL22	IL24	IL26	IL28B	IL29
IL10RA	√							
IL10RB	√			√		√	√	√
IL20RA		√	√		√	√		
IL20RB		√	√		√			
IL22RA1			√	√	√			
IL22RA2				√				
IL28RA							√	√

The variability of the receptor affinities is likely to cause differences in the biological functions of these interleukins. All receptors of IL-10 family cytokines (IL10RA, IL10RB, IL20RA, IL20RB, IL22RA1, IL22RA2 and IL28RA) belong to class II cytokine receptor family commonly composed of ligand-binding alpha subunit and signal-transducing beta or gamma chain subunits (Ouyang et al., 2011, Langer et al., 2004).

4. Extracellular matrix

Cells are always interacting with surrounding structures in the living tissue – other cells, supporting structures, loose connective tissues etc. In multicellular organisms, cells are supported by the extracellular matrix (ECM). It is composed of numerous proteins and polysaccharides, which are assembled into a scaffold (Alberts et al., 2008). The structure and mechanical properties of ECM are highly tissue-specific and provide the necessary environment for the cells. For example, in bone tissue the calcium-containing ECM is strong and provides mechanical support for the whole body, while in skin the ECM is elastic and stretchable (Alberts et al., 2008). The mechanical properties of the ECM dictate the mechanical properties of the whole tissue (Thomas et al., 2010) – the skin has an elastic modulus of 0.1–10 kPa, the brain 0.5 kPa and the muscle tissue 12 kPa (Achterberg et al., 2014). The amount of ECM found in different organs also varies to a great extent. In the cartilage and bone, it is the major component of the tissue, but in the brain it is only a minor constituent (Alberts et al., 2008).

Two forms of ECM are found in human tissues – stromal matrix and basement membrane (Alberts et al., 2008). Both these structures are present in skin. The basement membrane is the most prominent ECM structure in the epidermis and separates the outer epidermis from the underlying dermis (Alberts et al., 2008). Keratinocytes in the multilayered epidermis are closely linked to each other by a very complex interaction system, which is formed by specialized junctions (anchoring junctions, tight junctions and gap junctions) (Alberts et al., 2008). Therefore, the extracellular spaces between keratinocytes are very narrow (Arend et al., 1994). Although the ECM between epidermal cells cannot be directly visualized by simple light microscopy, the intra-keratinocyte space is filled with hyaluronan (Tammi et al., 1988) and a small amount of proteoglycans (epican) and lipids (Comper, 1996, Arend et al., 1994). Nevertheless, speaking about the epidermal ECM, it usually comprises the basement membrane.

The basement membrane is a highly organized structure and contains the following proteins – laminin, type IV and VII collagen, bullous pemphigoid antigens, entactin/nidogen and proteoglycans (perlecan, heparan sulfate family members) (Alberts et al., 2008, Krieg and Aumailley, 2011, Giudice et al., 1993). It plays a crucial role in pathological processes such as wound healing and tumor cell or pathogen invasion (Alberts et al., 2008).

In epidermis, the cells (keratinocytes, melanocytes) are lined onto the ECM (basement membrane); in dermis, however, the cells (fibroblasts) are dispersedly embedded into ECM. The ECM of dermis is a mixture of numerous components such as fibrillary proteins (collagens, elastin), other proteins (fibronectin, laminins, etc.) and more than 40 different proteoglycans (protein-linked polysaccharides) e.g. glycosaminoglycans (hyaluronan, chondroitin sulfate, dermatan sulfate, heparan sulfate, and keratan sulfate) (Alberts et al., 2008, Krieg and Aumailley, 2011).

The fibrous components of dermal ECM form a continuous network where the predominant orientation of the fibres is parallel to the skin surface and follows Langer's tension lines (Leesion et al., 1985).

For many years the ECM was considered a relatively inert scaffold for the tissue and the cells were thought to play the most important role in the functioning and regeneration of the tissue. Now it is clear that the extracellular environment is actually much more active in regulating cell viability and tissue-specific functioning. For instance, it is known that the ECM attracts sodium ions due to its high glycosaminoglycan content and is therefore crucial in regulating fluid balance in the body (Alberts et al., 2008).

5. Skin grafting

The management of patients with extensive skin defects resulting from burns, trauma, chronic wounds and congenital defects is a challenging situation in the clinic and often requires skin coverage or replacement.

The use of autologous skin grafts (donor tissue from the same individual) goes back thousands of years whereas the first published scientific reports came from late nineteenth century (Aziz and Shushan, 2010). Both split-thickness skin graft, which includes the entire epidermis and a part of the dermis and full-thickness skin graft, which involves all the layers of the skin are nowadays in clinical use. Although autologous skin grafting yielded good results, the areas where the skin can be harvested are usually limited, especially in case of large burns. The alternatives to autologous skin grafting are the use of allograft tissues (tissue from the other individual, including cadaver) and xenografts (skin from other species) (Aziz and Shushan, 2010). Soon it became clear that the latter two approaches often caused graft rejection due to immunological incompatibility (Aziz and Shushan, 2010). In case of cadaver tissue the main issue is its limited availability.

In the late 1970s, Rheinwald and Green began experimenting with creation of artificial skin that could be permanently grafted onto patients. It started with simple experiments where cells were isolated and seeded onto the damaged tissue site (Aziz and Shushan, 2010). Soon scientists began to realize that using only cells does not lead to sufficient skin replacement and a scaffold for forming the functional tissue is needed.

Now such medical devices, named “skin substitutes” are manufactured by seeding human cells onto a matrix containing proteins and growth factors, which simulate the cells to form a properly organized tissue (Altala et al., 2011).

Despite decades of research on skin substitutes, we still face similar problems as in the beginning of skin grafting. Skin autografting is still the gold standard procedure and although skin substitutes are available there are still problems concerning immunological rejection. Furthermore, no dermo-epidermal skin substitute, which can fully mimic the natural environment, is available for clinicians to date.

6. Skin substitutes

Skin substitutes are used to improve wound closure, control associated pain, prevent excessive scar formation and facilitate functional skin tissue regeneration. An optimal skin substitute should provide one-step replacement and it should be produced in large-scale at a reasonable price.

There are both permanent and temporary devices available (Altala et al., 2011). A temporary dressing material protects against pathogens and water loss, acting as a simple mechanical barrier. Amniotic membrane, Oasis® (porcine small intestine wall), synthetic polymer sheet or sprays and also combined materials – Transcyte® (human fibroblast on silicon film) and Biobrane® (silicone-nylon mesh with porcine collagen) – are a few examples. These products protect the wound only for a short time and are meant to be peeled off when the wound has re-epithelialized. “Permanent” substitutes are used to replace the full thickness of skin layers for a longer period, but are usually fully or partially degradable by host tissues over the time. The permanent skin substitutes include EpiCel® (cultured epithelial autograft grown in the presence of proliferation-arrested mouse fibroblasts), Integra® (silicone with porous matrix of cow collagen and glycosaminoglycan), OrCel® (human keratinocytes and dermal fibroblasts, cultured in separate layers into a bovine collagen sponge).

Dieckmann et al. have suggested that skin substitutes can be divided into two main categories: a) biomaterial and b) cellular (Dieckmann et al., 2010). Biomaterials are acellular and produced from natural or synthetic sources. Natural skin substitutes are for instance human cadaver skin or decellularized bovine or porcine xenografts (e.g. Alloderm®, Stratice®), but also engineered tissue using biological materials including polypeptides, hydroxyapatites, glycosaminoglycans (including hyaluronan), fibronectin, collagen, chitosan and alginates, which all originate mainly from animal sources. Synthetic skin substitutes, which are made from various biodegradable and non-degradable combinations of natural and synthetic polymers, are described in detail in the next paragraph.

The majority of the clinically available skin substitutes are natural biomaterials, which do not contain any cells. Only a few skin substitutes in clinical

use are tissue engineered and contain viable cells and either natural or synthetic extracellular matrix.

Apligraf®, StrataGraft® and OrCel® are dermo-epidermal composite grafts, which contain fibroblasts and keratinocytes seeded into a combined collagen matrix. Similarly, epidermal substitute Epicel® contains human keratinocytes and proliferation-arrested mouse fibroblasts seeded onto nonporous silicon film. Dermal substitutes Transcyte® and Dermagraft® contain human fibroblasts, which are seeded onto bioabsorbable polyglactin mesh.

Above-mentioned materials are the most popular commercially available skin/dermal substitutes, which are currently in clinical use (Zhang and Michniak-Kohn, 2012). US Food and Drug Administration (FDA) has specific regulations concerning skin substitutes of different origin and composition. The regulations concerning human cells and tissue products are applied on products derived from human materials, but additional and the most strict requirements have been set for products containing manipulated cells and tissues. For this reason, only a few such products are available on the market.

These demanding needs and strict regulations have caused the researchers to focus on manipulating the subcellular environment (gene and protein expression, cell morphology etc.) and studying the responses of cells to the changes in nano- and microscale environment.

7. Biomaterial surfaces

The widely used definition for “biomaterials” given by the American National Institute of Health postulates them as substance or combination of substances (drugs not included), synthetic or natural in origin, which augments or replaces partially or totally any tissue, organ or function of the body and therefore interacts with living tissue. There are several possibilities to develop these biomaterials. A basic example is a biocompatible surface. Well-known examples of biocompatible surfaces are the different coatings for bone or joint metal implants where interactions with the surrounding tissue are crucial (Altala et al., 2011). The advanced form of biomaterial is a bioactive or biofunctional surface, which can improve the adhesiveness or interaction between cells and surrounding environment. This can be achieved by using different nanoscale patterns, adding chemical groups or organic/inorganic compounds to natural matrix components, modifying hydrophilicity of the biomimetic surfaces etc. Finally, there are biomimetic materials, which are inspired by specific properties of natural structures.

Sol-gel technique has been shown to be suitable for designing the nano- and microstructure of surfaces with various mechanical properties as well as chemical composition and functionality (Dirè et al., 2011, Saal et al., 2011). Sol-gel approach is based on the hydrolysis and polymerization reactions of silicon and metal alkoxides.

SiO₂ has been widely used in bone tissue engineering for enhancing adhesion between bone cells and for preventing the formation of non-adherent fibrous capsule around the implant (Hollinger, 2011). Different production methods of SiO₂ result with different properties of the material (Hollinger, 2011). Biocompatible glass surfaces are conventionally produced by melting. This technique produces a dense surface with minimal porosity whereas sol-gel method allows fabrication of thin film coatings, different nanoparticles, porous materials and fibres. Sol-gel polymerization of tetraethylorthosilicate (Si(OC₂H₅)₄; TEOS) is a well established and widely used method of producing silicon dioxide: $\text{Si}(\text{OC}_2\text{H}_5)_4 \rightarrow \text{SiO}_2 + 2 (\text{C}_2\text{H}_5)_2\text{O}$. In the present work we have applied a novel sol-gel phase separation-based synthesis for designing micro- and nanopatterned surfaces with structural biofunctionality. In this method, silicon alkoxide domains are nucleated in continuous liquid phase, leading to the formation of dome-shape silica micro- and nanostructures on a substrate as the liquid phase is removed. Silicon alkoxide condensates into gel and silica surface features are formed after ageing and thermal treatment. This method produces round patterns and therefore represents a more biomimetic approach compared to edged nano- and micropatterns obtained by conventional lithography methods.

8. The design of extracellular matrix

The manufacturing of artificial organs depends on our ability to prepare a suitable scaffold, which mimics the structure of the specific tissue and sustains the characteristic properties of the cells, which are necessary for this particular tissue to function (Altala et al., 2011). Taken together, this artificial scaffold should provide all the functions of the extracellular matrix of the particular tissue.

The ideal matrix for skin substitute should: (a) enhance interaction of the matrix and host tissue, (b) mimic natural skin structure, (c) permit diffusion of nutrients, gases and growth agents to supply the cells, (d) provide support for adhesion, promote proliferation and tissue-specific functioning, (e) lack immunogenicity and toxicity, (f) possess controllable biodegradability.

Thus, choosing proper biomaterials is a crucial step in the development process. A wide range of synthetic and natural materials has been reported.

8.1. Polymers

As a raw material source, synthetic polymers usually possess superior stability – their shape, size, nanostructure, porosity, mechanical and chemical properties are easily reproducible and they are also less expensive than natural materials (Place et al., 2009). A number of different synthetic polymers have been reported as suitable materials for skin tissue engineering. The studies using synthetic polymers for skin substitutes concentrate on two main sub-classes –

degradable (polylactide (PLA), polyglycolide (PGA), poly-lactic-co-glycolic acid (PLGA), polycaprolactone (PCL)) and non-degradable (polytetrafluoroethylene (PTFE), polyethylene terephthalate (PET), polypyrrole (PPy), polyurethane PU)) materials (Place et al., 2009, Altala et al., 2011). The non-degradable materials are mainly used as temporary dressing for wounds. Polyurethane and nylon are the two most widely and extendedly used synthetic materials, which have proven to be highly tolerated by human organism (e.g. surgical dressings and sutures). PTFE is the basic ingredient in several implants of blood vessels and heart valves (Altala et al., 2011).

An alternative approach to fully synthetic skin substitute is to polymerize or co-polymerize naturally occurring metabolites into larger molecules. Such polymers are degraded after a certain time period into compounds normally present in our body. For example, lactide and PLGA are converted into lactic acid and glycolic acid – the by-products of several metabolic pathways in the body. Degradable and non-degradable polymers can be combined into scaffolds with novel mechanical and chemical properties and, as a result, the material previously characterized as non-degradable might become partially or fully degradable like in the case of PPy-PLA combination (Shi et al., 2004).

Natural polymers can interact with cells and modulate their biological activity due to their nature as biologically active molecules. For example, synthetic materials, which are initially produced as static scaffolds can be modulated by surface reactions promoting the bonding of the materials with surrounding tissue (e.g. bioactive glass) (Altala et al., 2011).

8.2. Natural polymers. Gelatin.

Natural macromolecules, mainly proteins (collagens, gelatin, elastin, silk, fibrinogen, keratin, actin, myosin) and polysaccharides (glycosaminoglycans, chitosan, cellulose, amylose, dextran) have in many cases been used for skin engineering (Altala et al., 2011).

Gelatin is a mixture of proteins and polypeptides derived by hydrolysis of collagen, a naturally occurring protein, which is the most abundant protein of the extracellular matrix in connective tissue (Gorgieva and Kokol, 2011). Both collagen and gelatin have been widely used in tissue engineering scaffolds. Approximately 30 types of collagens have been described. In the skin, collagens are largely secreted by fibroblasts, but can also originate from other cells (Alberts et al., 2008). Collagen is the major component of skin and bone, constituting up to 25% of the total protein mass of the body (Alberts et al., 2008). Collagen is usually purified from animal tissues (swine, bovine) and its properties have been well examined. It has proven to be biocompatible, non-toxic and biodegradable material, which is very good at supporting cell growth. Therefore, numerous forms of collagen have been designed – coatings, sheets, beads, capsules, meshes, fibres, sponges etc. (Gorgieva and Kokol, 2011).

However, there are certain disadvantages of using collagen derived from natural sources, such as poor stability (swelling and contraction *in vivo*) and poor resistance to mechanical loading.

Compared to collagen, gelatin is less prone to evoke immune responses due to the absence of aromatic groups found in collagen (Gorgieva and Kokol, 2011). Gelatin is a mixture of several proteins and their fragments and its main constituent is type I collagen (Gorgieva and Kokol, 2011), which was also confirmed in our study (Table 7). The exact composition of gelatin depends on the extraction method as well as the origin of the raw material (Gorgieva and Kokol, 2011). Gelatin hydrates in aqueous environment and is fully degradable *in vivo* (Gorgieva and Kokol, 2011). To overcome the problems with stability and durability of this material and also to reduce swelling, cross-linking of gelatin chains is used. Cross-linking decreases solubility by creating chemical bonds between polymer chains (Gorgieva and Kokol, 2011).

Several cross-linking techniques have been described – chemical methods (using dialdehydes, phenolic compounds, genipin etc. (Zhang et al., 2010, Panzavolta et al., 2011, Gorgieva and Kokol, 2011), enzymatic (Bertoni et al., 2006) and physical methods (UV, temperature) or a combination of these (Gorgieva and Kokol, 2011, Birshtein and Tulchinskii, 1982). However, a large proportion of chemical cross-linkers are toxic to a varying degree and therefore their use is limited in tissue engineering application (Gorgieva and Kokol, 2011).

In our study we used a combination of glucose and thermal cross-linking, which results in a higher extent of covalent bounds between gelatin molecules and thereby provide better mechanical stability to the material. Additionally, glucose in the physiological range is non-toxic and is naturally used in the body as a cross-linker.

AIMS OF THE STUDY

The purpose of this study was to design novel biocompatible materials for the skin tissue engineering and to evaluate the suitability of these materials with different physical and chemical properties for the growth of primary cells isolated from human skin.

The specific aims of the study were to:

1. Describe the expression of interleukin-10 family cytokines and their receptors in keratinocytes, melanocytes and fibroblasts in order to describe their inflammatory and healing potential.
2. Characterize the main cell types in the skin – keratinocytes, melanocytes and fibroblasts by gene expression profiling.
3. Evaluate the effects of micro- and nanopatterned silica surfaces on fibroblast viability and morphology.
4. Investigate the biological properties of a novel biomimetic extracellular matrix for skin.

MATERIALS AND METHODS

I. Human subjects (Papers I–IV)

In our study, we used 25 pediatric foreskins obtained from healthy circumcised patients (aged 5 months to 10 years) and punch-biopsies from 15 healthy adult volunteers (aged 19 to 79 years). Pediatric patients were recruited from elective patients present at the Department of Pediatric Surgery, Tallinn Children’s Hospital. Adult volunteers were recruited from patients attending the outpatient clinic of the Department of Dermatology of the University of Tartu. All procedures were carried out in accordance with the ethical standards. This study has been approved by Research Ethics Committee of the University of Tartu (approval number 178/T-19).

A written informed consent (approved by Research Ethics Committee of the University of Tartu) was obtained from all adult volunteers and from all parents or caretakers of patients under 18 years. Additionally, a separate written informed consent was obtained from all patients aged 8–17 years.

We only used circumcised tissue samples from healthy children with no concurrent diseases and signs of infection. Pediatric tissue samples were by-products of circumcision procedures and no additional intervention was incurred.

One biopsy sample (ø 4 mm) from non-sun-exposed skin was taken from a healthy adult volunteer with no concurrent diseases.

All samples were coded and information of the donor identity was only available to the physician. All patient related information was stored separately from the samples and the data. Schematic diagram of sample processing in the study can be found on Figure 3.

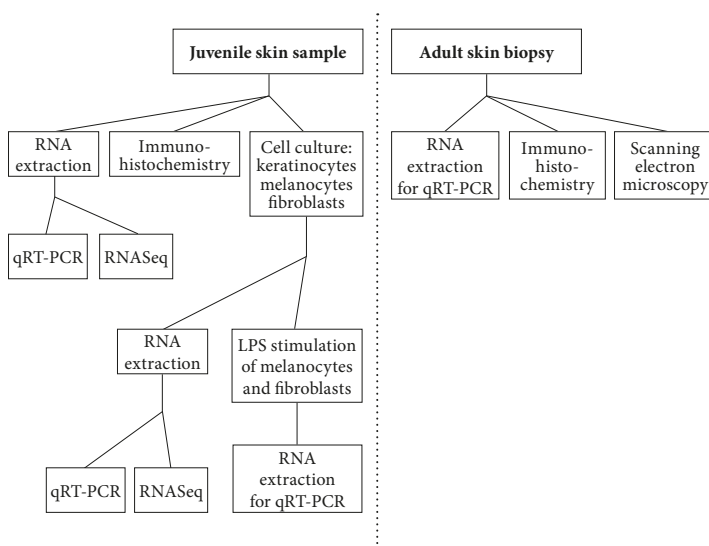


Figure 3. Schematic diagram of sample processing in the study.

1.1. Tissue samples

0.9% NaCl solution was used to stabilize the juvenile samples during the transport to the laboratory at 4°C. Pediatric tissue was divided into two parts. 4–5 mm³ piece was transferred into RNALater (Life Technologies) for RNA extraction and the remaining tissue part used for extraction of cells. Adult biopsy samples were instantly frozen in liquid nitrogen and stored at 80°C until RNA extraction. Samples for immunohistochemistry were instantly inserted into 10% formalin for fixation. One adult biopsy sample was fixed in Karnovsky fixative for scanning electron microscopy.

2. Isolating and growing skin cells (Papers I–IV)

We isolated keratinocytes, melanocytes and fibroblasts from pediatric foreskins. Skin pieces were rinsed in phosphate-buffered saline (PBS, without Ca, Mg, PAA Laboratories GmbH). Subcutaneous fat was removed and tissue was incubated in dispase II (2.4 U/ml in PBS, Sigma-Aldrich) at 4°C overnight. Epidermis as a source of keratinocytes and melanocytes was peeled off from the dermis, transferred into 0.05% trypsin-0.02% ethylenediaminetetraacetic acid (EDTA) (Life Technologies) for 3 min at 37°C. Enzymatic process was stopped with trypsin inhibitor (Sigma-Aldrich). Cell suspension was divided into two parts – one for the isolation keratinocytes and the other for the isolation of melanocytes.

We used cell-specific selective media to isolate a particular cell type: EpiLife[®] basal medium with human keratinocyte growth supplement (Life Technologies) for keratinocytes and growth medium M2 with supplement mix (PromoCell) for melanocytes. Melanocyte culture dishes were precoated with gelatin.

The remaining piece of dermis was used for isolation of fibroblasts via migration method. The dermis was rinsed in PBS, cut into approximately 4x4 mm pieces and attached onto a culture dish, covered with 10 ml of Dulbecco's Modified Eagle's medium (DMEM) (PAA Laboratories GmbH) with 10% foetal bovine serum (FBS, Sigma-Aldrich), penicillin (100 UI/ml), streptomycin (100 µg/ml) (PAA Laboratories GmbH) and amphotericin B 250 ng/ml (Sigma-Aldrich; added only at the isolation step). The media were changed every second day throughout the study.

The subculture (passage) of cells was done with 65–70% (in case of keratinocytes) and with 80–95% (in case of melanocytes and fibroblasts) cellular confluence in the Petri dish. Cells with passage number 2–3 were used for subsequent isolation of RNA. The remaining cells were cryopreserved in 10% dimethyl sulfoxide (DMSO, Sigma-Aldrich) diluted in FBS upon on-demand usage. Prior to usage on designed surfaces, growth curve was determined at different densities to obtain optimal seeding density of the cells.

2.1. Lipopolysaccharide stimulation

Reaching approximately 90% confluence, melanocytes and fibroblasts were incubated in lipopolysaccharide (LPS) (*E. coli* 0111:B4, Sigma-Aldrich) and media solution (10 ng/ml) for 12 h and with media alone (controls). After treatment, the cells were washed with PBS and used for the isolation of RNA for qRT-PCR.

3. RNA extraction (Papers II, IV)

3.1. RNA extraction for whole transcriptome sequencing

The skin cells underwent lysis and RNA extraction process using Trizol® (Invitrogen) and RNeasy mini columns (Qiagen) combined protocol.

The tissue samples were homogenized using Precellys® 24 system and total RNA was isolated from tissues with RNeasy Fibrous Tissue Mini Kit (Qiagen) according to the manufacture's protocol.

Extraction of RNA for whole transcriptome sequencing was performed accompanied with DNase I (Qiagen) treatment. The purity and concentration of samples was checked with both Qubit spectrophotometer and Nano Drop ND-1000 and the integrity of the RNA (RIN) was evaluated using Agilent 2100 Bioanalyzer.

3.2. RNA extraction for qRT-PCR

The skin cells underwent lysis and RNA extraction process using Trizol® (Invitrogen) and RNeasy mini columns (Qiagen) combined protocol. The skin biopsies were homogenised using T10 basic homogeniser (IKA Labortechnik) and total RNA was isolated from tissues with RNeasy Fibrous Tissue Mini Kit (Qiagen) according to the manufacture's protocol. The RNA content and quality was determined by spectrophotometry (Nano Drop ND-1000).

4. Whole Transcriptome sequencing (Paper IV)

We chose 12 total RNA samples, with the highest RIN (9–10), extracted from four keratinocyte, four melanocyte, two fibroblast and two whole skin samples for library preparation. Extracted RNA was enriched using RiboMinus™ Eukaryote kit (Invitrogen) according to the manufacturer's instructions. The final quantity of RNA was 10 µg per reaction. The cDNA library was size-selected in the range of 150–250 bp and bar-coded according to a protocol provided by Applied Biosystems. Samples were sequenced using SOLiD 5500xl platform with 75 bp forward and 35 bp reverse primers.

5. Gene expression analysis by qRT-PCR (Paper II)

Approximately 500 ng of each RNA sample was used to synthesize cDNA using High Capacity cDNA Reverse Transcription Kit (Life Technologies) according to the manufacturer's protocol. Gene expression was detected using qRT-PCR (7900 Fast QRT-PCR, Life Technologies). Two primers exon 6 (5'-GACTTTGCTTTCCTTGGTCAGG-3') and exon 7 (5'-AGTCTGGCTTA TATCCAACACTTCG-3') and labelled probe (VIC-5'-TTTCACCAGCAAG CTTGCGACCTTGA-3'-TAMRA) were used to detect the mRNA expression level of the reference gene hypoxanthine phosphoribosyl-transferase-1 (*HPRT-1*). Expression levels of other genes under investigation were detected using the following 20x probe assays (Life Technologies): *IL10* (Hs00174086_m1), *IL10RA* (Hs00155485_m1), *IL10RB* (Hs00175123_m1), *IL19* (Hs00203540_m1), *IL20* (Hs00218888_m1), *IL22* (Hs00220924_m1), *IL20RA* (Hs00205346_m1), *IL20RB* (Hs00376373_m1), *IL22RA1* (Hs00222035_m1), *IL22RA2* (Hs00364814_m1), *IL24* (Hs00169533_m1), *IL26* (Hs00218189_m1), *IL29* (Hs00601677_g1), *IL28RA* (Hs00417120_m1) and *IL28B* (fw 5'-AGAGGG CCAAAGATGCCTTAG-3', rv 5'-GGGAGCGGCACTTGCA-3', FAM-5'-AGAGTCGCTTCTGCTG-3'-MGB).

6. Immunohistochemistry (Paper II)

Skin tissue samples (n=5, both juvenile and adults) were fixed in 10% formalin for 24 h and embedded in paraffin. Deparaffinized sections were treated with 3% H₂O₂ followed by REAL Antibody Diluent (Dako) to block non-specific binding. After blocking, sections were incubated with rabbit polyclonal antibody to IL29 (ab38569) 1:100, IL28 receptor alpha (ab83865) 1:200, IL22 RA2 (ab96341) 1:500, IL26 (ab102977) 1:200 or IL10RB (ab106282) 1:200 overnight at 4°C (all antibodies were purchased from Abcam Ltd.). Visualisation of the primary antibodies was performed by using REAL™ EnVision™ Detection System (Dako). The washing steps were carried out with PBS containing 0.07% of Tween 20. Thionine blue (Sigma-Aldrich) was used for background staining. No immunohistochemical staining was noted in negative controls where the primary antibody was omitted.

7. Fibroblast cultivation on sol-gel prepared nanopatterned silica surfaces (Paper I)

7.1. Preparing silica structures

Patterned substrates were prepared from solutions of partially hydrolyzed tetraethylorthosilicate (TEOS) in different solvents (propanol, methanol, ethanol and hexane). All chemicals were purchased from Sigma-Aldrich. Conventional acid-catalyzed hydrolysis and polymerization of TEOS was carried to prepare

sols on 12 mm borosilicate glass cover slips. The corresponding used sols were: TEOS:propanol = 1:5 (resulting samples are referred to as S1 below); TEOS: ethanol = 1:5 (S2); TEOS:methanol = 1:2 (S3); TEOS:methanol = 1:5 (S4). Spin coating resulted in the formation of patterns of different size nano- and micro-domes. For a reference sample, smooth silica surfaces were prepared from a sol: TEOS:hexane = 1:10 (Smooth). All samples were subsequently heated at 200 °C for 20 h to transform gel material into oxide. The preparing process of the silica structures has been described in more detail in Paper I.

7.2. Atomic force microscopy

For investigating the morphology of structured surfaces, atomic force microscope (AFM) images were obtained with Dimension® Edge™ AFM System (Veeco Instruments Inc.) in tapping mode at room temperature. Height of the surface features was estimated by using the Gwyddion 2.30 software. AFM imaging was performed by Triin Kangur.

7.3. Fibroblast cultivation on silica structures

Previously isolated and cryopreserved fibroblasts were resuspended in a fresh culture medium (DMEM) and cultivated for 1–3 days. Cells were seeded onto nanopatterned cover slips and a flat borosilicate glass (12 mm diameter) at density of 3,000 cells/cm² in a 24-well plate for antibody and SA-b-gal staining and 10,000 cells/cm² for scanning electron microscopy.

7.4. Fluorescent microscopy

Ki67 and γ -actin staining was performed on the fifth day of culture. For actin antibody staining, fibroblasts on glass and nanopatterned coverslips were briefly washed with PBS followed by fixation in cold methanol (Naxo) and acetone (POCH), both for 5 min. For Ki67 antibody staining the cells were fixed with 3.7 % formaldehyde (Scharlab) in PBS for 7 min at room temperature. Fixed tissues were rehydrated, washed with PBS/0.25 % Triton X-100-PBS and blocked for 1 h with PBS/Triton X-100-PBS containing 5% normal donkey serum (Jackson ImmunoResearch Inc.). Incubation with mouse monoclonal IgG1 anti- γ -actin primary antibody (Santa Cruz Biotechnology Inc.; 1:200) and Ki67 rabbit monoclonal antibody (Epitomics Inc.; 1:500) was performed in 2% blocking solution for 45 min at room temperature and overnight at 4 °C. After washing, the slides were incubated with Alexa Fluor® 488-labelled donkey anti-mouse IgG (H + L) secondary antibody and Alexa Fluor® 594-labeled donkey anti-rabbit IgG (H + L) secondary antibody (both 1:500, Life Technologies), respectively. Nuclei were counterstained with DAPI (AppliChem; 1 lg/ml), followed by washing in PBS and ultra pure water and mounting in

fluorescence mounting medium (Dako). Immunofluorescence microscopy was carried out with an Olympus FluoView FV1000 microscope, with a 60x objective and images were acquired with Olympus FV10-ASW 1.6a software. For counting of adhered cells, Zeiss Axiovert S100 inverted microscope with 5x and 10x objectives and AxioVision Rel. 4.8.2, software were used. Typically, data was collected from four randomly chosen fields from four cover slips. Images were analyzed with ImageJ 1.45s software. Statistical analysis was performed using Microsoft Excel software.

7.5. Senescence associated β -galactosidase staining

Senescence associated β -galactosidase staining at pH 6.0 was performed as previously described (Debacq-Chainiaux et al., 2009). To avoid confluence-induced SA- β -gal activity, staining was carried out on subconfluent fibroblast populations on the fifth experimental day. Cells on glass and nanopatterned cover slips were washed with PBS and fixed with 2% formaldehyde-0.2% glutaraldehyde (Naxo) in PBS for 5 min at room temperature. Followed by washing, the cells were transferred into freshly prepared staining buffer for 16 h at 37°C. After incubation the cover slips were washed with PBS and methanol (Naxo) and air-dried. For imaging we used an Olympus BX50 light microscope (Olympus Company Ltd.) and the Cell Imaging System Software (Olympus Company Ltd.).

8. Fibroblast cultivation on thermally cross-linked glucose-containing electrospun gelatin meshes (Paper III)

8.1. Designing fibrous glucose-containing gelatin meshes

Gelatin type A from porcine skin (Sigma-Aldrich) and gelatin type B from bovine skin (Sigma-Aldrich) were used for electrospinning of fibrous scaffolds.

Gelatins were mixed with D-(+)-glucose at different ratios (approximately 0%, 5%, 10%, 15%, 20%, 25%, 30% of glucose in total weight of the glucose and gelatin powder mix; $x\% = \text{mass of glucose} / (\text{mass of glucose} + \text{mass of gelatin})$). The mixtures were dissolved in 10 M aqueous acetic acid (Sigma-Aldrich) solution at about 40°C by vigorous stirring to obtain solutions containing 25% gelatin. A syringe containing gelatin solution was mounted on a New Era Pump Systems NE-511 pump operating at speeds between 6 and 8 $\mu\text{l}/\text{min}$. High voltage between 17 and 18 kV was applied to metallic syringe needle using Heinzinger LNC 30,000 high voltage power supply. A grounded target was placed 14 cm away from the needle tip. Fibrous meshes were collected from the target after electrospinning and stored for further treatment.

Gelatin scaffolds were cross-linked thermally by placing them in an oven for 3 h. In order to avoid thermal degradation of gelatin while obtaining proper cross-linking (Birshtein and Tulchinskii, 1982) and to operate above melting

point and caramelization temperature of glucose, cross-linking was carried out at 170–175°C. Additionally, pieces of some scaffolds were removed from the oven after various times between 5 min and 3 h and analyzed to monitor the cross-linking process.

8.2. Assessment of biological properties

8.2.1. Glucose measurement

Quantitative glucose oxydase and peroxidase kit (Spinreact) was used according to the manufacturer's protocol in order to detect possible leaching of glucose from the scaffolds. The forming hydrogen peroxide binds to chromogenic oxygen acceptor (phenol) and indicates the amount of glucose. Scaffolds were soaked in phenol red free medium DMEM (PAA Laboratories GmbH) for 8 hours at 37°C. Incubated medium was removed for glucose measurements and followed by replacement with fresh medium for the next 8 hours. DMEM was removed before glucose detection. Spectrophotometer (Tecan) with Magellan (Tecan Group Ltd.) software was used at 505 nm wavelength to detect the intensity of a red quinoeimine dye, which is proportional to glucose concentration in the samples.

8.2.2. Quantification of viable cells

CellTiter-Glo® Luminescent Cell Viability Assay® (Promega) was used to quantify the number of viable cells grown on the scaffolds according to the manufacturer's protocol. Cell viability tests were performed 16 hours and 7 days after seeding. The readings were detected using Tecan Infinite M200Pro luminometer.

8.2.3. Protein mass spectrometry (MS)

Protein MS was performed by using LTQ Orbitrap XL (Thermo Fisher) mass spectrometer. MaxQuant 1.4.0.8 software was used for protein identification according to the manufacturer's protocol. Samples were incubated overnight at 4°C and purified with StageTips (C18) after in-solution digestion with proteases lysC and trypsin in 8 M urea. Nano liquid chromatography-tandem MS analysis was performed using acetonitrile 8–40% gradient and 0.5% acetic acid.

8.2.4. In vitro degradation of scaffolds

The biological stability of the fibrous scaffolds was evaluated by exposing them to collagenase type II (2 units/ml; PAA Laboratories GmbH), collagenase type IV (160 units/ml; Gibco) and 0.25% trypsin-0.1% EDTA (Invitrogen) for 24 hours. Degradation tests were performed at 37°C in a horizontal shaker

9. Scanning electron microscopy (SEM) (Papers I, III)

9.1. SEM of cells grown on silica surfaces

Primary fibroblasts with density 2700 cells/cm² were seeded onto silica surfaces and onto flat borosilicate glass (control). SEM was performed on the third experimental day of cell culture. Samples were briefly washed with PBS and fixed in Karnovsky buffer for 30 min at room temperature. After washing in PBS, the cells were dehydrated through alcohol gradient starting at 50% ethanol up to 100% ethanol. Samples were subsequently transferred to 100% hexamethyldisilazane (AppliChem) (drying agent, alternative to critical point drying) for 3 min and air-dried at room temperature. The samples were sputter coated with a 5 nm layer of gold using a Polaron SC7640 High Resolution sputter coater. SEM micrographs were acquired with FEI SEM Helios Nanolab 600, Focused Ion Beam, EDX (Oxford instruments) with an accelerating voltage of 5 kV and cross-sections of samples were previously cut using focused ion beam (FIB).

9.2. SEM of fibrous gelatin meshes

SEM of the fibrous gelatin scaffolds were carried out on plain meshes (without seeded cells) and on scaffolds previously seeded with fibroblast.

Fibroblasts with density of 2700 cells/cm² were seeded onto fibrous scaffolds previously attached to glass cover slips for easier handling. Scaffolds with fibroblasts were collected 24h and 7 days after seeding, washed in PBS and fixed with Karnovsky buffer for 30 min at room temperature. After washing again, the cells were dehydrated through alcohol gradient starting at 50 % ethanol up to 100% ethanol and dried using Leica EM CPD300 critical point drier. Samples were sputter coated with a 5 nm layer of gold. Several images of every scaffold were recorded and fibre diameters were measured from three representatives at 21,000 times magnification with and imaged by Tescan SEM Vega II.

9.3. SEM of adult's skin biopsy

One adult's whole skin sample was used for SEM imaging the physiological ECM sample of skin. The skin sample was fixed in freshly made Karnovsky buffer (with Na-cacodylate) for 4 hours. After fixation, the sample was washed three times in 0.2M Na-cacodylate (Sigma-Aldrich) buffer, each time for 10 min. Postfixation was performed with 2% osmiumtetroxide-0.2M Na-cacodylate buffer for 1 hour. The sample was washed twice in 0.2M Na-cacodylate buffer and followed by critical point drying procedure. The skin sample was imaged by Tescan SEM Vega II.

10. Statistical analysis (Papers I, II, VI)

10.1. Analysis of RNA-Seq data

Sequencing of cDNA libraries resulted in 24,842,284 to 44,324,428 paired reads per sample. For greater mapping quality, the initial 75 bp F3 and 35 bp F5 reads were trimmed to 45 and 25 base pairs, respectively. All color-spaced reads were aligned to human reference genome (Ensembl, release 73) using TopHat v2.1.0 (Kim et al., 2013) that used Bowtie version 1.0.0 (Langmead et al., 2009). RPKM values for gene expression levels were calculated with Cufflinks v2.0.2 (Roberts et al., 2011) and raw counts were retrieved with HTSeq version 0.5.3p9 (<http://www-huber.embl.de/users/anders/HTSeq/>) using gene annotations of protein coding genes downloaded from Ensembl (release 73). Differential expression was estimated on raw counts with edgeR (Robinson et al., 2010). All programs were used with their default parameters with TopHat set to not to find novel junctions.

10.1.1. Modeling background regions

To estimate the number of truly expressed genes we modeled intergenic regions using a methodology described in (Ramskold et al., 2009). Models of intergenic regions are expected to reflect the level of background expression (noise), which is taken as the baseline when estimating the number of expressed genes. For each gene, the length of the background region was equal to the gene's longest combined transcript (the sum of all transcribed nucleotides) and it extended upstream from position -1000 relative to the transcription start site. Only background regions that did not overlap with any expressed sequence tags (EST) were used in the analysis. A gene was considered as expressed only if the RPKM value in all samples of the corresponding cell type was above the cutoff (0.95). Conversely, the gene was labeled as not expressed if the RPKM value was below 0.95 in at least one of the samples. EST annotations were downloaded using UCSC Table Browser (<http://genome.ucsc.edu/cgi-bin/hgTables>)

10.1.2. Differential expression analysis of gene expression

Differential expression between melanocytes and samples from keratinocytes, fibroblasts and the whole skin was estimated using edgeR (Robinson et al., 2010). A gene was considered as differentially expressed if the FDR-adjusted p-value was below 0.05 and if the gene was expressed in at least one of the cell types. To identify a gene as expressed only in melanocytes and not in keratinocytes, fibroblasts (termed as “uniquely expressed in melanocytes”) it had to meet the following requirements: 1) RPKM > 0.95 in melanocytes (gene is labeled as expressed in melanocytes), 2) RPKM < 0.95 in keratinocytes, fibroblasts (gene is labeled as not expressed in keratinocytes, fibroblasts), 3)

differential expression $FDR < 0.05$ (gene is differentially expressed in melanocytes with respect to keratinocytes and fibroblasts).

10.1.3. Pathway analysis of differentially expressed genes

Gene ontology enrichment analysis of differentially expressed genes was performed using g:GOST (<http://biit.cs.ut.ee/gprofiler/index.cgi>) (Reimand et al., 2011). Based on the p-values of g:GOST analysis, GOsummaries package were used to generate word clouds of gene names (<http://cran.r-project.org/web/packages/GOsummaries/index.html>). The word sizes in word clouds are defined by the p-values. Additionally, multidimensional scaling test for visualizing the level of similarity of individual samples in study groups was performed using edgeR. The results confirm the homogeneity and purity of cell populations.

10.2. Statistical analysis for qRT-PCR analyses

Relative gene expression levels were calculated using $2^{-\Delta CT}$ method utilising the housekeeping gene HPRT-1 as an internal control (Livak and Schmittgen, 2001). The data of all studied genes that followed normal distribution (using D'Agostino & Pearson omnibus normality test) were parametrically tested by unpaired *t*-test and the data not following normal distribution by Mann-Whitney *t*-test.

RESULTS

I. Interleukin-10 family cytokines in the skin and skin cells (Paper II)

Interleukin-10 family cytokines, which have been shown to mediate pro- and anti-inflammatory signals in several skin disorders (Ouyang et al., 2011) are also considered to be important players in regulating immune tolerance and, thereby, transplant rejection.

Since the main goal of my research was to contribute to the discovery of novel materials for skin replacement therapies, we first focused on studying the IL-10 family of cytokines (Paper II). Among other processes, the cytokines regulate how cells respond to contacts with foreign materials. First, we studied the baseline gene expression profiles of juvenile keratinocytes, melanocytes and fibroblasts grown in standard tissue culture conditions.

We saw that the mRNAs corresponding to selected IL-10 family cytokines (*IL10*, *IL19*, *IL20*, *IL22*, *IL24*, *IL26*, *IL28B*, *IL29*) and their receptors (*IL10RA*, *IL10RB*, *IL20RA*, *IL20RB*, *IL22RA1*, *IL22RA2*, *IL28RA*) were differentially expressed between cultivated melanocytes, keratinocytes and fibroblasts.

IL10 was not detectable in any of these cell types. In melanocytes and fibroblasts cultures, *IL10RA* was expressed at a very low level while in keratinocytes the expression level was below the detection limit (Figure 4a). In contrast, *IL10RB* was expressed at a high level in melanocytes, keratinocytes and fibroblasts. *IL20* could be detected only in keratinocytes (Figure 4c). Interestingly, the IL20 receptors *IL20RA* and *IL20RB* had significantly higher expression in keratinocytes compared to fibroblasts and melanocytes, suggesting the existence of an autocrine positive feedback loop. The expression level of *IL22RA1* was similar in keratinocytes and fibroblasts, whereas no expression could be detected in melanocytes (Figure 4f). At the same time, no expression of *IL22RA2* as well as *IL26* could be detected in any of the three cultures (data not shown). *IL24* was the most prominent cytokine in melanocytes within the studied IL-10 family cytokines. However, *IL24* was hardly detectable in keratinocytes and fibroblasts (Figure 4g). To mimic an inflammation-like state, we treated the cells with lipopolysaccharide (LPS), which is a strong pro-inflammatory agent. Notably, *IL24* was the only studied gene induced by low concentration of LPS stimulation in cell culture, increasing up to 10 times in melanocytes (Figure 4g). *IL28RA* gene expression was significantly higher in keratinocytes compared to melanocytes and no expression was detectable in fibroblasts (Figure 4h).

Immunohistochemistry (IHC) in skin sections demonstrated that the expression of IL10RB protein (Figure 6a) and corresponding mRNA (Figure 5c) correlated well in juvenile skin. IL10RB protein could be detected in all skin layers (Figure 6a) and correspondingly, the *IL10RB* mRNA expression was similar in cultured melanocytes, keratinocytes and fibroblasts cells (Figure 4b).

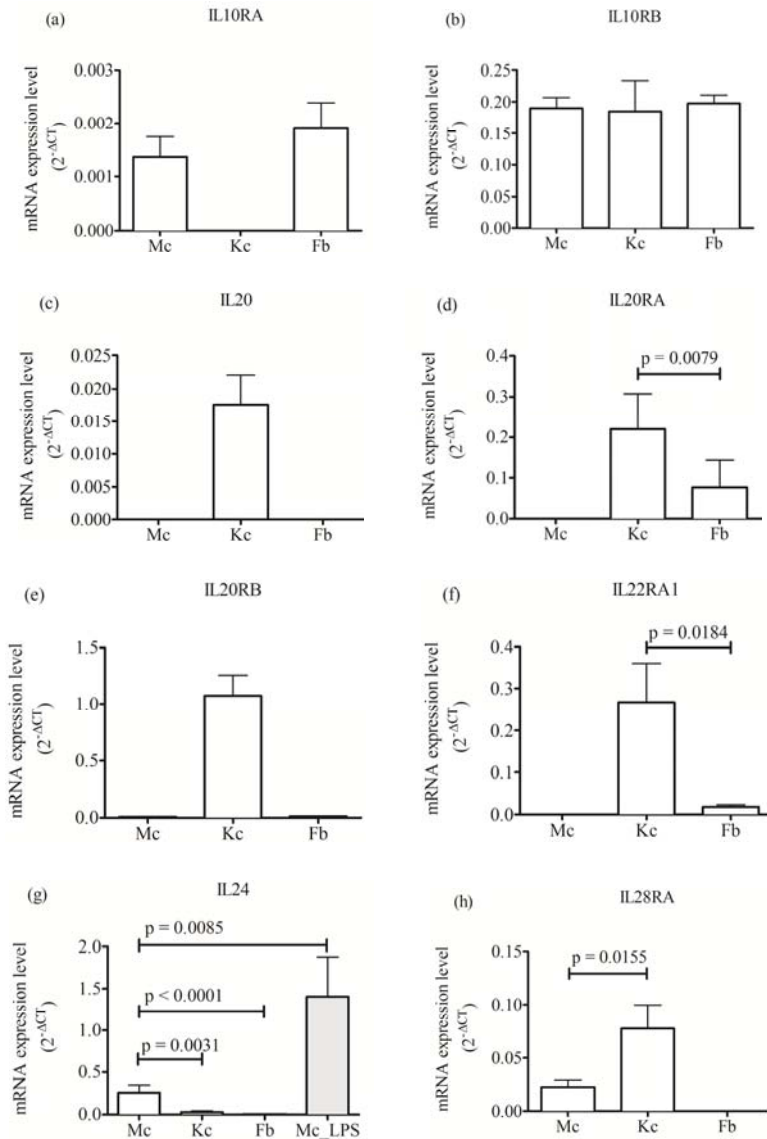


Figure 4. mRNA expression of *IL10RA*, *IL10RB*, *IL20*, *IL20RA*, *IL20RB*, *IL22RA1*, *IL24*, *IL28RA* in cultivated melanocytes (Mc), keratinocytes (Kc), fibroblasts (Fb) and LPS stimulated melanocytes (Mc_LPS). Data is plotted as the mean \pm SD of 15 replicates. *p*-values are shown on graphs. Statistical methods used: d, g, h: Mann-Whitney *t*-test, f: Unpaired *t*-test.

Due to excellent viability and high proliferation rate the cells extracted from juvenile skin are often used for tissue engineering purposes. At the same time, the tissue-engineered products containing juvenile cells are used to a large extent in adults. For this reason, the knowledge about the molecular differences between adult and juvenile skin cells is of utmost importance.

IL10, *IL10RA*, *IL10RB*, *IL20*, *IL20RA*, *IL20RB*, *IL22RA1*, *IL22RA2*, *IL26*, *IL28RA* were all expressed in the juvenile skin. However, *IL10*, *IL20* and *IL26* had extremely low and varying expression level (Figure 5). In the adult skin we detected the expression of *IL10*, *IL10RA*, *IL10RB*, *IL20RA*, *IL20RB*, *IL22RA1*, *IL22RA2*, *IL28RA* mRNAs. In contrast to the juvenile skin, *IL20* and *IL26* were not detectable in adult skin (Figure 5). IHC revealed no detectable IL26 staining in juvenile and adult skin (Figure 6c, i). Furthermore, gene expression of *IL28RA* was present in keratinocytes culture (Figure 4h), but the respective IHC analysis did not reveal any staining in the epidermis (Figure 6d). In the adult skin, IHC analysis revealed IL28RA positive staining in juvenile epidermis (Figure 6j).

IL10RB was expressed at detectable levels in both adult and juvenile skin, however, its expression was considerably higher in the adult skin (Figure 5c). This was also confirmed by IHC, which revealed clearly stronger immunoreactivity in the adult skin (Figure 6a, g). *IL24* RNA was not detectable in juvenile and adult whole skin (data not shown). Similarly, the gene expression of *IL19*, *IL22*, *IL28B* and *IL29* was not detectable neither in whole skin samples nor in the cultured cells (data not shown). Further, we could not detect the presence of IL22RA2, IL26 and IL29 protein in skin sections (Figure 6b, c, e) and the corresponding mRNAs were not detected in any of the cell cultures (data not shown).

A summary of the IL-10 family expression in adult and juvenile whole skin and in cultured juvenile skin cells is presented in Table 2.

Table 2. Overview of the expression levels of the IL-10 family genes in adult and juvenile whole skin, as well as in juvenile skin cells. +: mean $2-\Delta\text{CT}$ 0.001–0.009; ++: mean $2-\Delta\text{CT}$ 0.01–0.09; +++: mean $2-\Delta\text{CT} \geq 0.1-0.9$; ++++: mean $2-\Delta\text{CT} \geq 1$.

Genes	Children	Adults	Keratinocytes	Melanocytes	Fibroblasts
<i>IL10</i>	++	++	–	–	–
<i>IL10RA</i>	+++	+++	–	+	+
<i>IL10RB</i>	+++	++++	+++	+++	+++
<i>IL19</i>	–	–	–	–	–
<i>IL20</i>	++	–	++	–	–
<i>IL20RA</i>	+++	+++	+++	–	++
<i>IL20RB</i>	++++	++++	++++	+	++
<i>IL22</i>	–	–	–	–	–
<i>IL22RA1</i>	++++	+++	+++	–	++
<i>IL22RA2</i>	+++	++	–	–	–
<i>IL24</i>	–	–	++	+++	+
<i>IL26</i>	++	–	–	–	–
<i>IL28RA</i>	+++	++	++	++	–
<i>IL28B</i>	–	–	–	–	–
<i>IL29</i>	–	–	–	–	–

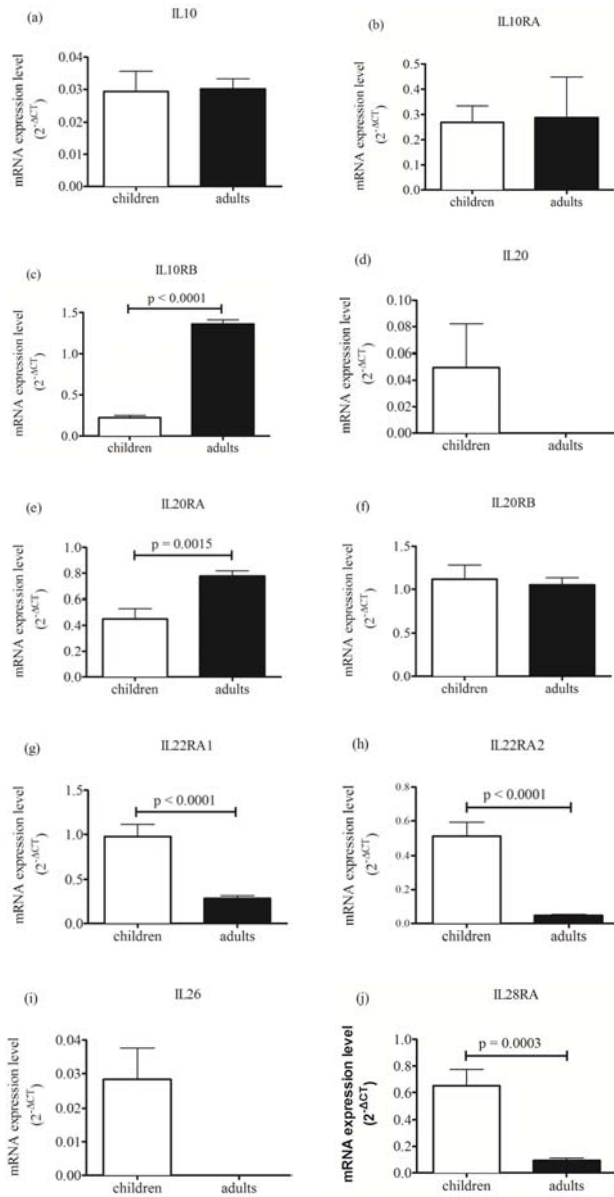


Figure 5. mRNA expression of *IL10*, *IL10RA*, *IL10RB*, *IL20*, *IL20RA*, *IL20RB*, *IL22RA1*, *IL22RA2*, *IL26* and *IL28RA* in adult and juvenile whole skin samples. Data is plotted as the mean of 15 replicates \pm SD. *p*-values are shown on graphs. Statistical methods used: c, g h and j: unpaired *t*-test. e: Mann-Whitney *t*-test.

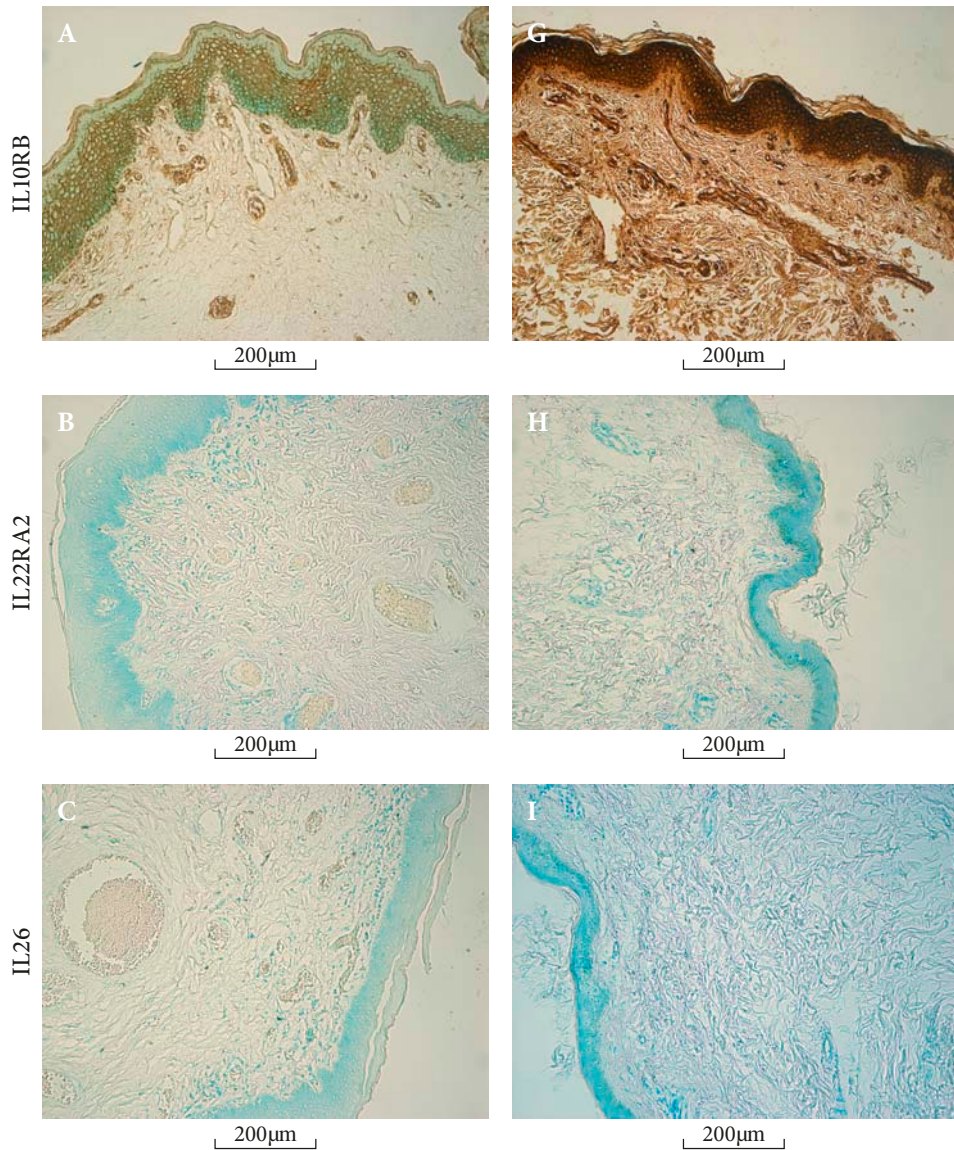


Figure 6. Immunohistochemistry (IHC) staining of juvenile and adult whole skin sample. Skin specimens (n = 5, both in juvenile (A–F) and adult (G–L) group) were stained with thionine blue (blue background staining) and the antibodies for IL10RB, IL22RA2, IL26, IL28RA, IL29 (brown color indicates positive antibody reaction); IL10RB (A, G) antibody staining was present in all layers of adult and juvenile skin, but a significantly weaker antibody reaction in juvenile samples was observable. We detected IL28RA-positive antibody reaction (D, J) in adult epidermis, but no significant staining in juvenile skin. No observable antibody staining of IL22RA2, IL26 and IL29 was detected. Negative control for antibody staining is shown in (F, L). Scale bars: 200 mm.

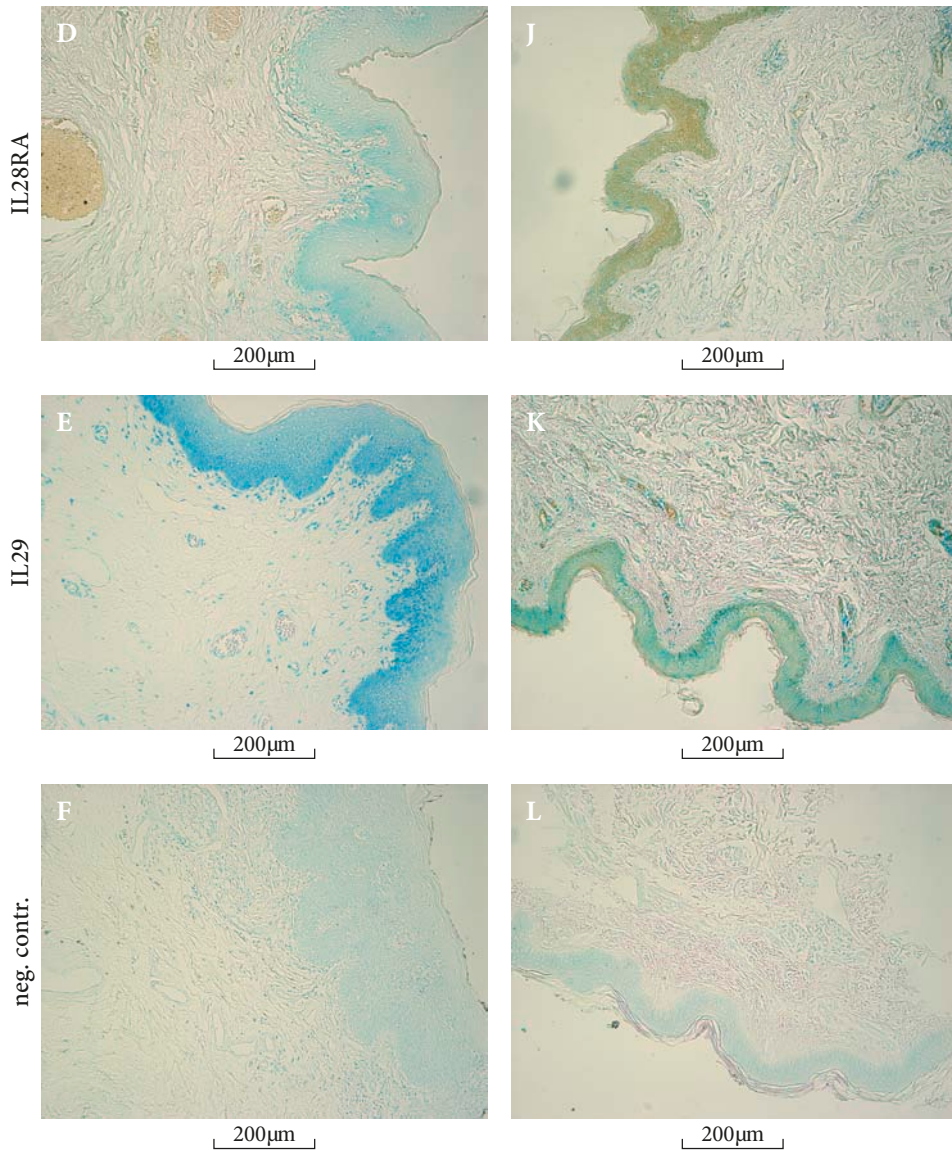


Figure 6 (continued)

2. Whole transcriptome sequencing (Paper IV)

In order to describe more systematically the global differences in the gene expression profiles of the main skin constituents and to expand our knowledge about the intracellular pathways active in these cells when grown in standard tissue culture conditions, we performed a comparative whole transcriptome analysis of cultivated keratinocytes, fibroblasts and melanocytes. In Paper IV we outlined the specific features of melanocytes compared to keratinocytes,

fibroblasts and the whole skin. In parallel, we investigated the differences between keratinocytes and fibroblasts and compared their transcriptome to that of the whole skin.

2.1. Overall differences between cultivated melanocytes, keratinocytes, fibroblasts and whole skin tissue

As expected, the total number of expressed genes was the highest in whole skin samples (10,871 genes), since other cell types besides keratinocytes, melanocytes and fibroblasts (epithelial cells, Merkel cells, Langerhans cells etc.) are present in whole skin biopsy (Table 3). Interestingly, the total number of expressed genes was the lowest in keratinocytes (Table 3). Thereat, 7,766 genes were commonly expressed in all study groups (whole skin and keratinocytes, melanocytes and fibroblasts). The list of the detected genes and their RPKM values can be found in <http://journals.plos.org/plosone/article/asset?unique&id=info:doi/10.1371/journal.pone.0115717.s002>. Similarly, the number of genes considered as uniquely expressed was the largest in the whole skin sample (290 genes, Table 3).

Table 3. The number of detected and uniquely expressed genes.

	Total number of expressed genes	Uniquely expressed genes
Skin	10871	290
Keratinocytes	8937	138
Melanocytes	9903	122
Fibroblasts	10420	277

When comparing specific cell populations, fibroblasts had a higher number of uniquely expressed genes compared to melanocytes and keratinocytes (277, 122, 138 uniquely expressed genes, respectively) (Table 3). It is likely that the true number of uniquely expressed genes is higher as we applied a relatively strict cut-off criterion (RPKM > 0.95) when calling gene expression as present or absent.

Based on the differential gene expression analysis, we identified significantly fewer similarities between melanocytes and whole skin gene expression patterns than when comparing keratinocytes or fibroblasts to the whole skin. In melanocytes, 6,231 genes were differentially expressed compared to the whole skin. Of those, 3,680 were upregulated in melanocytes and 2,551 downregulated in melanocytes (Figure 7). The number of differentially expressed genes when compared to whole skin was 4,480 in keratinocytes and 4,454 in fibroblasts (Figure 7). This finding can be explained by the relatively small proportion of melanocytes of the total skin cell number. The entire list of differentially expressed genes can be found in <http://journals.plos.org/plosone/article/asset?unique&id=info:doi/10.1371/journal.pone.0115717.s003>.

Additionally, there are more upregulated genes in melanocytes and fibroblasts than in keratinocytes when these cells were compared to each other – 2,239 genes were upregulated in fibroblasts, but only 1,377 genes were upregulated in keratinocytes and 2,498 genes in melanocytes in comparison with keratinocytes where only 1,855 genes were upregulated (Figure 7). At the same time the number of differentially upregulated genes did not differ significantly when melanocytes and fibroblasts were compared: 1,230 *versus* 1,511 upregulated genes, respectively (Figure 7).

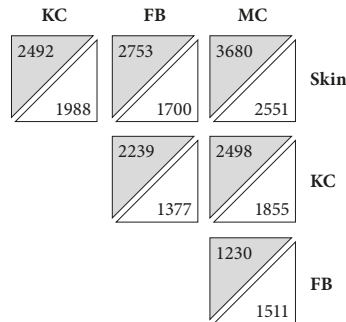


Figure 7. The number of differentially expressed genes in each study group – melanocyte (MC), keratinocyte (KC), fibroblast (FB) and whole skin (Skin). For example, comparing gene expression in keratinocytes and whole skin samples – 2,492 genes were upregulated in keratinocytes (grey triangle) compared to whole skin samples (white triangle), where only 1,988 genes were upregulated (Figure 7).

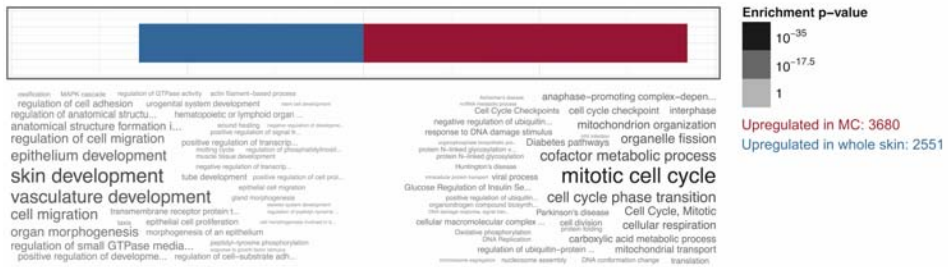
2.2. Pathway analysis of the skin cells and whole skin

Pathway analysis brought forth the most characteristic differences between melanocytes, keratinocytes, fibroblasts and whole skin (Figure 8). In Paper IV, we focused on the pathway analysis of melanocytes. List of pathways (based on differentially expressed genes), prominent in MC compared to KC, FB and whole skin can be accessed via <http://journals.plos.org/plosone/article/asset?unique&id=info:doi/10.1371/journal.pone.0115717.s004>. The analysis revealed that cultured melanocytes could be described as an active and intensively dividing cell population (Figure 8). In addition to the genes involved in melanosome organization and pigment synthesis, we identified a number of genes that were characteristic for ongoing regenerative process and could be related to cell division: genes regulating mitotic activity and cell cycle; DNA replication and chromatin assembly; assembly and metabolism of different cellular components (cytoskeleton, structural macromolecules), formation of lysosome and Golgi complex (Figure 8). Consequently, gene expression profile corresponding to enhanced metabolic activity could be also observed (Figure 8).

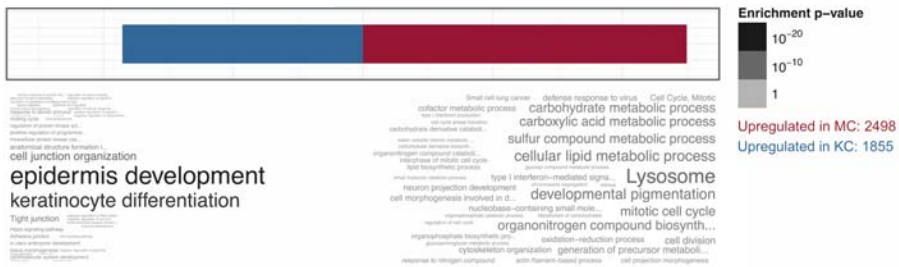
Additionally, we saw that in melanocytes and fibroblasts the upregulated genes represented a more heterogeneous list of pathways than in keratinocytes where the upregulated genes were mostly related to the differentiation of kerati-

nocytes, development of epidermis and formation of intercellular connections (tight junction) in the epidermis (Figure 8). In the case of fibroblasts the up-regulated genes were mostly part of the pathways, which regulate the organization of the extracellular matrix and the development of anatomical structures and are related to cell motility and migration processes.

A melanocytes vs skin



B melanocytes vs keratinocytes



C melanocytes vs fibroblasts

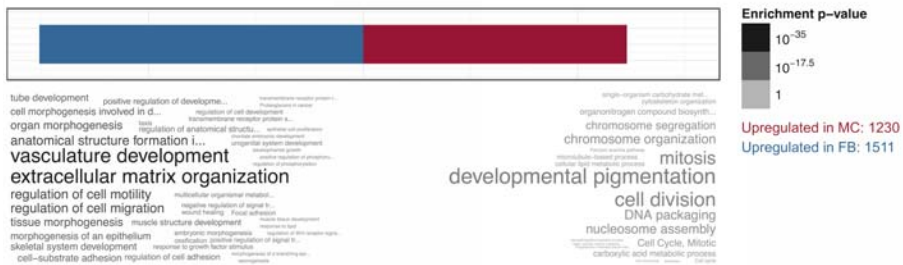
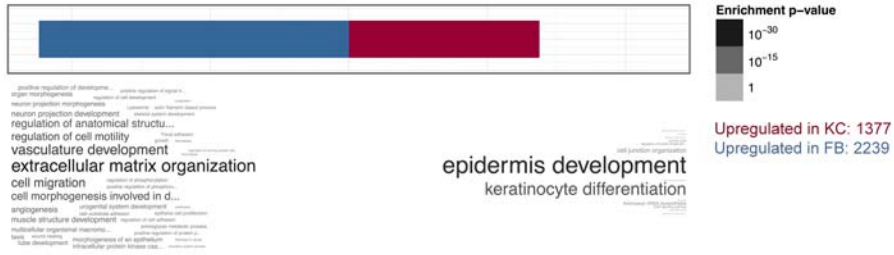
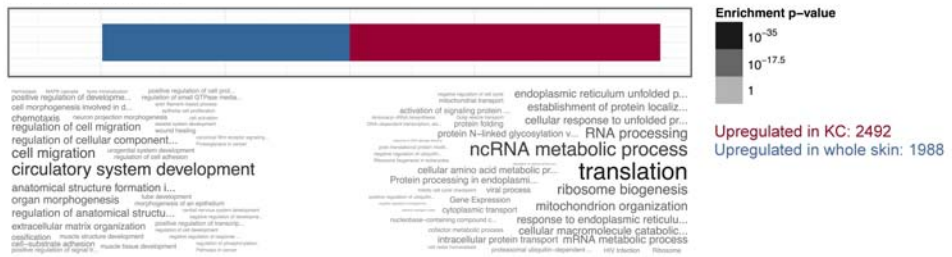


Figure 8. Comparative pathway analysis of melanocytes, keratinocytes, fibroblasts and whole skin. On plots A, B and C, red squares indicate pathways, which were prominently expressed in melanocytes (MC) and blue squares mark pathways, which were downregulated in melanocytes and concomitantly upregulated in the whole skin (A), keratinocytes (KC) (B) and fibroblasts (FB) (C), respectively. On plots D and E red squares indicates pathways, which were prominently expressed in keratinocytes and blue squares, which were upregulated in fibroblast and whole skin, respectively. On plot F red square marks upregulated pathways in fibroblasts compared to whole skin, the upregulated pathways of which are marked by blue color. The word sizes in word clouds were defined by their p-values.

D keratinocytes vs fibroblasts



E keratinocytes vs skin



F fibroblasts vs skin

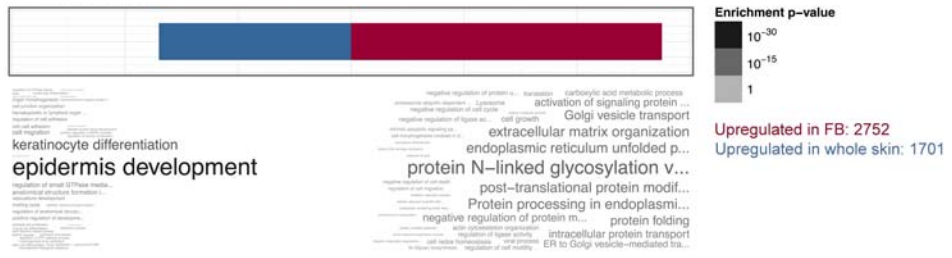


Figure 8 (continued)

2.3. Characterization of gene expression pattern of juvenile keratinocytes, melanocytes and fibroblasts

Comparing melanocytes, keratinocytes and fibroblasts, we found several gene groups, which distinguish cultured melanocytes from other skin cells.

The most prominent group of genes differentially expressed in melanocytes compared to fibroblasts was that of encoding various histone proteins (*HIST1H1A*, *HIST1H1B*, *HIST1H2AA*, *HIST1H2AE*, *HIST1H2AG*, *HIST1H2AI*, *HIST1H2BB*, *HIST1H2BH*,

HIST1H2BI, *HIST1H2BN*, *HIST1H3D*, *HIST1H3F*, *HIST1H3H*, *HIST1H3J*, *HIST1H4D*, *HIST1H4I*, *HIST1H4L*, *HIST2H3D*, *HIST3H2A*, *HIST3H2BB* and *HIST4H4*). Another group of genes differentially expressed between melanocytes and fibroblasts was related to cell division cycle (*CDC20*, *CDC25A*, *CDC25C*, *CDC6*, *CDCA2*, *CDCA5* and *CDCA8*). Additionally, a set of kinesin family genes (*KIF13B*, *KIF20B*, *KIF21A*, *KIF22*, *KIF24*, *KIF2C*, *KIFC1*) was differentially expressed in melanocytes compared to fibroblasts. Also, significantly higher expression of calcium-binding proteins *S100A1*, *S100A14*, *S100A8*, *S100A9* and *S100B* genes was observable in melanocytes compared to fibroblasts.

When compared to keratinocytes, melanocytes expressed a set of major histocompatibility complex protein genes such as *HLA-B*, *HLA-DMA*, *HLA-DPB1*, *HLA-DRA* and *HLA-F*. In addition, interferon-induced protein genes *IFI27*, *IFI35*, *IFI44*, *IFI44L*, *IFI6*, *IFIT1*, *IFIT2*, *IFIT3*, *IFITM1*, *IFITM2* and *IFITM3*, which are related to viral and bacterial infection defense mechanism (Itsui et al., 2006), were highly expressed in melanocytes when compared to keratinocytes. So far the keratinocytes have been shown to be the key players in modulating the immunological status of normal and diseased skin by being the first sensors of harmful agents, secreting inhibitory and stimulating cytokines, and activating other immune competent cells (e.g. Langerhans cells) (Burgdorf et al., 2009). Our data suggest that the role of melanocytes in cutaneous immune system regulation might be more extensive than anticipated so far.

Importantly, we could identify a set of melanocytes-specific genes previously not described by other researchers (Table 4). In many cases the functions of these genes are poorly characterized and further experiments are needed to identify their precise role in melanocytes. A number of genes that were unique for melanocytes (*CA8*, *CHRNA6*, *CTTNBP2*, *EPHA5*, *FAXC*, *KCNN2*, *SCG2*, *SLITRK2*) refer to melanocytes' origin from the neural crest (Kos et al., 2001, Chakrabarty et al., 2012, Jiao et al., 2005, Chen and Hsueh, 2012, Akaneya et al., 2010, Szatanik et al., 2008, Hotta et al., 2009, Yim et al., 2013, Hill et al., 1995) (Table 4).

Table 4. Uniquely expressed genes in melanocytes. The list of genes, expressed in melanocytes, but not in keratinocytes and fibroblasts.

Uniquely expressed genes in melanocytes							
Symbol	Gene name	Symbol	Gene name	Symbol	Gene name	Symbol	Gene name
<i>ADCK1</i>	aarF domain containing kinase 1	<i>EME1</i>	essential meiotic endonuclease 1 homolog 1 (S. pombe)	<i>LSM11</i>	LSM11, U7 small nuclear RNA associated	<i>SCG2</i>	secretogranin II
<i>ADCY2</i>	adenylate cyclase 2 (brain)	<i>ENTHD1</i>	ENTH domain containing 1	<i>LYPD1</i>	LY6/PLAUR domain containing 1	<i>SEPT4</i>	septin 4
<i>ANKRD37</i>	ankyrin repeat domain 37	<i>EOMES</i>	comesodermin	<i>LZTSL1</i>	leucine zipper, putative tumor suppressor 1	<i>SFMBT2</i>	Scm-like with four mbt domains 2
<i>ANO5</i>	anoctamin 5	<i>EPHA5</i>	EPH receptor A5	<i>MC1R</i>	melanocortin 1 receptor	<i>SHC4</i>	SHC family, member 4
<i>ARL9</i>	ADP-ribosylation factor-like 9	<i>ESR2</i>	estrogen receptor 2 (ER beta)	<i>MCF2</i>	MCF2 cell line derived transforming sequence	<i>SHROOM4</i>	shroom family member 4
<i>ASB9</i>	ankyrin repeat and SOCS box containing 9	<i>EVI2A</i>	ecotropic viral integration site 2A	<i>MCOLN2</i>	mucolipin 2	<i>SLAMF9</i>	SLAM family member 9
<i>BAIAP2L2</i>	BAI1-associated protein 2-like 2	<i>EVI2B</i>	ecotropic viral integration site 2B	<i>MDGA2</i>	MAM-containing glycosylphosphatidylinositol anchor 2	<i>SLC16A10</i>	solute carrier family 16, member 10
<i>BCL2</i>	B-cell CLL/lymphoma 2	<i>FABP7</i>	fatty acid binding protein 7, brain	<i>MGAT5B</i>	mannosyl-glucosaminyltransferase, isozyme B	<i>SLC19A1</i>	solute carrier family 19 (folate transporter), member 1
<i>BHLHE41</i>	basic helix-loop-helix family, member e41	<i>FAM124A</i>	family with sequence similarity 124A	<i>MMP8</i>	matrix metalloproteinase 8 (neutrophil collagenase)	<i>SLC19A3</i>	solute carrier family 19, member 3
<i>BMPRI1B</i>	bone morphogenetic protein receptor, type IB	<i>FAM69B</i>	family with sequence similarity 69, member B	<i>NPM2</i>	nucleophosmin/nucleoplasmin 2	<i>SLC22A18AS</i>	solute carrier family 22, member 18 antisense
<i>BST2</i>	bone marrow stromal cell antigen 2	<i>FAXC</i>	failed axon connections homolog (Drosophila)	<i>NR4A3</i>	nuclear receptor subfamily 4, group A, member 3	<i>SLITRK2</i>	SLIT and NTRK-like family, member 2

Uniquely expressed genes in melanocytes							
Symbol	Gene name	Symbol	Gene name	Symbol	Gene name	Symbol	Gene name
<i>C11ORF96</i>	chromosome 11 open reading frame 96	<i>FCGR2A</i>	Fc fragment of IgG, low affinity IIa, receptor (CD32)	<i>PAEP</i>	progesterone-associated endometrial protein	<i>SORBS1</i>	sorbin and SH3 domain containing 1
<i>C2ORF88</i>	chromosome 2 open reading frame 88	<i>FOXD3</i>	forkhead box D3	<i>PDE3A</i>	phosphodiesterase 3A, cGMP-inhibited	<i>SSUH2</i>	ssu-2 homolog (C. elegans)
<i>C8ORF46</i>	chromosome 8 open reading frame 46	<i>FOXRED2</i>	FAD-dependent oxidoreductase domain containing 2	<i>PDE7B</i>	phosphodiesterase 7B	<i>ST6GALNAC3</i>	N-acetylglucosaminide alpha-2,6-sialyltransferase 3
<i>CA8</i>	carbonic anhydrase VIII	<i>FRMD5</i>	FERM domain containing 5	<i>PDLIM3</i>	PDZ and LIM domain 3	<i>ST8SIA1</i>	Alpha-N-Acetyl-Neuraminidase Alpha-2,8-Sialyltransferase 1
<i>CADM3</i>	cell adhesion molecule 3	<i>GAPDHS</i>	glyceraldehyde-3-phosphate dehydrogenase, spermatogenic	<i>PGBD5</i>	piggyBac transposable element derived 5	<i>TCN1</i>	transcobalamin I (vitamin B12 binding protein)
<i>CD200</i>	CD200 molecule	<i>GJB1</i>	gap junction protein, beta 1, 32kDa	<i>PKN3</i>	protein kinase N3	<i>TFF3</i>	trefoil factor 3 (intestinal)
<i>CDH19</i>	cadherin 19, type 2	<i>GOLGA7B</i>	golgin A7 family, member B	<i>PKNOX2</i>	PBX/knotted 1 homeobox 2	<i>THEM6</i>	thioesterase superfamily member 6
<i>CGREF1</i>	cell growth regulator with EF-hand domain 1	<i>GPR19</i>	G protein-coupled receptor 19	<i>PLA1A</i>	phospholipase A1 member A	<i>TLR1</i>	toll-like receptor 1
<i>CHRNA6</i>	cholinergic receptor, nicotinic, alpha 6 (neuronal)	<i>GPRN3</i>	GPRN family member 3	<i>PLEKHH1</i>	pleckstrin homology domain containing, family H, 1	<i>TMEM169</i>	transmembrane protein 169
<i>CMPK2</i>	cytidine monophosphate (UMP-CMP) kinase 2	<i>GREB1</i>	growth regulation by estrogen in breast cancer 1	<i>PPM1H</i>	protein phosphatase, Mg ²⁺ /Mn ²⁺ dependent, 1H	<i>TMEM229B</i>	transmembrane protein 229B

Uniquely expressed genes in melanocytes							
Symbol	Gene name	Symbol	Gene name	Symbol	Gene name	Symbol	Gene name
<i>CRISPLDI1</i>	cysteine-rich secretory protein LCCL domain containing 1	<i>HELZ2</i>	helicase with zinc finger 2, transcriptional coactivator	<i>PRDM7</i>	PR domain containing 7	<i>TMEM56</i>	transmembrane protein 56
<i>CSGALNA3CT1</i>	chondroitin sulfate N-acetylgalactosaminyltransferase 1	<i>HOXB7</i>	homeobox B7	<i>PRKCB</i>	protein kinase C, beta	<i>TMEM71</i>	transmembrane protein 71
<i>CSPG4</i>	chondroitin sulfate proteoglycan 4	<i>HPDL</i>	4-hydroxyphenylpyruvate dioxygenase-like	<i>RAB20</i>	RAB20, member RAS oncogene family	<i>TMPRSS5</i>	transmembrane protease, serine 5
<i>CTTNBP2</i>	contactin binding protein 2	<i>HSF4</i>	heat shock transcription factor 4	<i>RNF157</i>	ring finger protein 157	<i>TRIM6</i>	tripartite motif containing 6
<i>CXORF57</i>	chromosome X open reading frame 57	<i>IL16</i>	interleukin 16	<i>RNF182</i>	ring finger protein 182	<i>TSPAN10</i>	tetraspanin 10
<i>CYTL1</i>	cytokine-like 1	<i>ITPR1</i>	inositol 1,4,5-trisphosphate receptor, type 1	<i>ROPNI</i>	rhophilin associated tail protein 1	<i>TTYH2</i>	twenty homolog 2 (Drosophila)
<i>DISC1</i>	disrupted in schizophrenia 1	<i>KCNK2</i>	potassium intermediate/small conductance calcium-activated channel, subfamily N, member 2	<i>RTKN2</i>	thoketin 2	<i>WDR17</i>	WD repeat domain 17
<i>DNMT3A</i>	DNA (cytosine-5-)methyltransferase 3 alpha	<i>KIAA1211</i>	KIAA1211	<i>RTP4</i>	receptor (chemosensory) transporter protein 4	<i>ZNF280B</i>	zinc finger protein 280B
<i>DPY19L2</i>	dpy-19-like 2 (C. elegans)	<i>LPL</i>	lipoprotein lipase	<i>RUNX3</i>	runt-related transcription factor 3		
<i>EGFL8</i>	Epidermal growth factor-like protein 8; Lysosomal thioesterase PPT2	<i>LRRCA5</i>	leucine rich repeat containing 45	<i>RXRG</i>	retinoid X receptor, gamma		

As already indicated by the pathway analysis, fibroblasts are the crucial players in extracellular matrix synthesis and degradation processes. In Table 5 we have pointed out the expression of genes coding extracellular matrix proteins in fibroblasts. In our study, a gene was considered as expressed only if the RPKM value in all samples of the corresponding cell type was above the cutoff (0.95). We could detect *COL1A1*, *COL1A2*, *COL3A1*, *COL4A1*, *COL4A2*, *COL4A5*, *COL5A1*, *COL5A2*, *COL5A3*, *COL6A1*, *COL6A2*, *COL6A3*, *COL7A1*, *COL8A1*, *COL8A2*, *COL12A1*, *COL13A1*, *COL14A1*, *COL15A1*, *COL16A1*, *COL17A1*, *COL18A1*, *COL21A1* and *COL27A1* in cultivated fibroblasts. In addition to collagen, we also detected genes, which encode laminin chains *LAMA1*, *LAMA2*, *LAMA3*, *LAMA4*, *LAMB1*, *LAMB2*, *LAMB3*, *LAMC1*, *LAMC2* in fibroblasts (Table 5). However, besides fibroblasts, the keratinocytes and melanocytes also synthesize the components of the ECM. For example, laminin alpha 1 gene *LAMA1* was highly expressed in melanocytes when compared to keratinocytes and fibroblasts suggesting that melanocytes might have a role in ECM formation and remodeling and might refer to a higher potential of melanocytes to transform into tumorous cells since *LAMA1* is expressed predominantly in embryonic tissues (Ekblom et al., 2003). The list of the RPKM values can be accessed via <http://journals.plos.org/plosone/article/asset?unique&id=info:doi/10.1371/journal.pone.0115717.s002>.

3. Cells on nanopatterned surfaces (Paper I)

During the cultivation of different skin cell types we identified fibroblasts as the most accessible and easy-to-grow cell population, which yields a homogeneous cell culture. For this reason juvenile skin fibroblasts were used as a model system for testing the cell-compatibility of novel biofunctional surfaces.

In Paper I we compared the growth properties of normal human primary fibroblasts on silica surfaces with round nano- and micropatterns of different sizes. As a reference we used smooth sol-gel prepared silica surface and untreated borosilicate glass inserts commonly used for cell culturing. Our goal was to evaluate the biocompatibility of these materials and to study how the micro- and nanopatterns with different configurations on substrate influence the spreading and growth of cultivated primary cells.

3.1. Surface design

Substrate patterns of different size nano- and micro-domes were prepared using different solvents (propanol (S1), ethanol (S2), methanol (S3) and methanol (S4)), in TEOS-based precursors. The surface of smooth samples, prepared using solvent – hexane, showed no noticeable roughness in relevant lateral scale in SEM analysis. The characteristics of different silica surfaces can be found in Table 6. The hydrophilic properties of surfaces were characterized by water droplet contact angle method. Relatively small contact angle of S3 is due to the rather flat dome structure (Figure 9C).

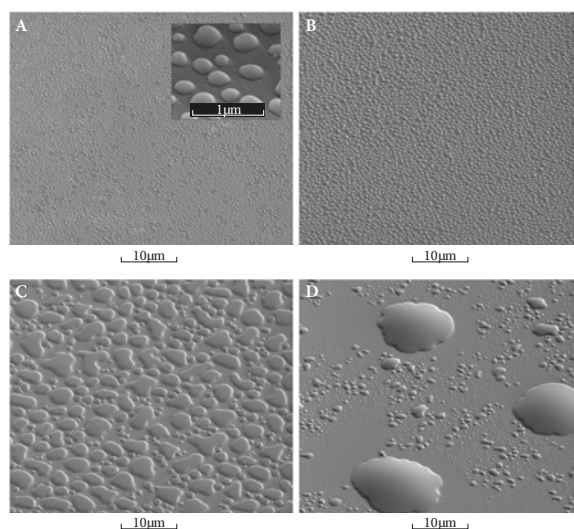


Figure 9. Scanning electron microscopy analysis of silica domes S1 (A), (B), S3 (C) and S4 (D). The inset on the picture “A” shows a magnification of the S1 surface.

Table 6. The characteristics of different silica surfaces.

	Mean diameter of the dome	Mean height of the dome (nm)	Number of domes per 10 000 μm^2	Surface-dome contact angle ($^\circ$)
S1	200 nm	90	51,000	48
S2	500 nm	210	24,000	54
S3	1 μm	200	4,300	15
S4	10 μm	920	18	34

3.2. Cell morphology

Primary fibroblasts adhered, grew and proliferated on all studied surfaces, indicating that the composition of the used material is compatible with cells. However, the cells grown on surfaces with different topography displayed changes in morphology showing a role for surface roughness in regulating cell growth (Figure 10A–C, G–I.) On a flat surface, fibroblasts usually maintain their “normal” spindle-shaped morphology (Figure 10n). However, on S3 and S4, a portion of cells were either spread out showing drastically increased cell size or, alternatively, became stretched out and obtained a narrow cytoplasm and an oval nucleus (Figure 10M, O). It has been shown that such cells do not proliferate and represent most probably either senescent or stressed cells, respectively (Chen et al., 2000).

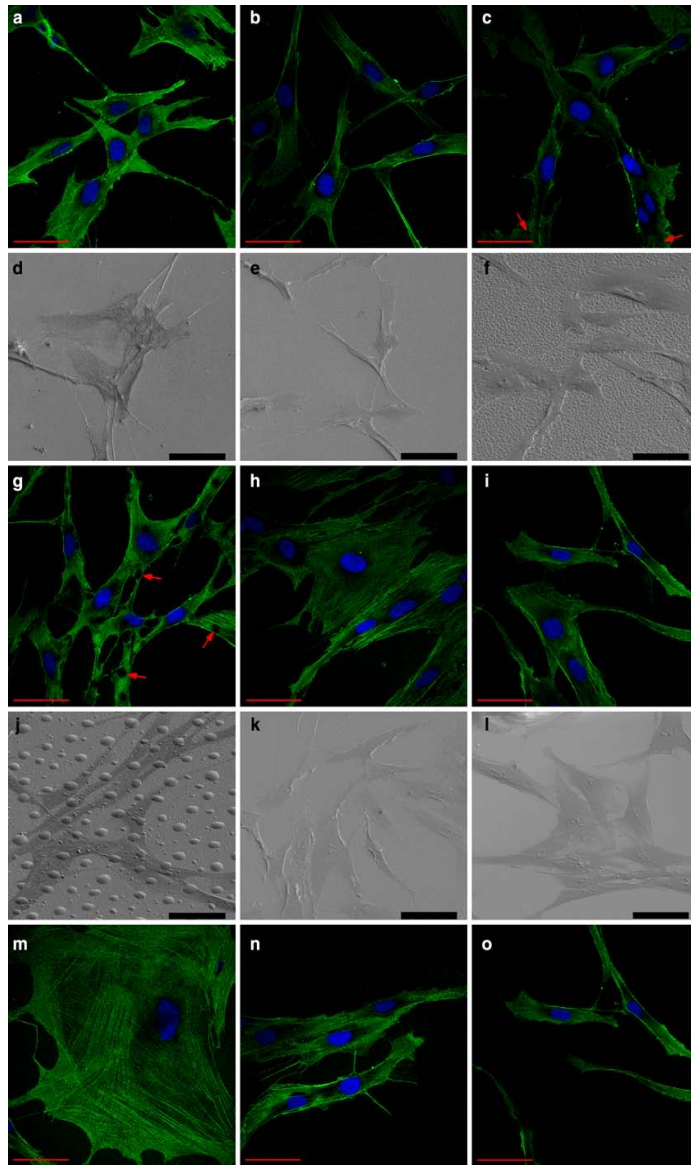


Figure 10. Confocal fluorescence microscopy images of normal human dermal fibroblasts cultured on silica domes S1 (A), S2 (B), S3 (C), S4 (G), smooth surface (H), borosilicate glass (I). SEM micrographs of cultured fibroblasts on silica domes S1 (D), S2 (E), S3 (F), S4 (J), smooth silica surface (K) and borosilicate glass (L). Confocal fluorescence images of fibroblasts with different morphology (M–O): M – enlarged cell; N – spindle-shaped normal cells; O – narrowed cells. The cytoskeleton of the cells is labeled with anti-gamma actin (green) and nuclei are labeled with DAPI (blue). Red arrows mark the domes. Scale bar: 50 μm .

3.3. The induction of cell senescence on nanopatterned surfaces

Senescence-associated beta-galactosidase (SA-b-gal) activity allows to detect cells undergoing a limited number of doublings in culture before irreversibly arresting proliferation (becoming senescent) (Debacq-Chainiaux et al., 2009). We used this method to study whether different nanopatterned surfaces could inhibit the proliferation of cells via induction of senescence. We could confirm the presence SA-b-gal staining in significantly enlarged cells, which occasionally had a surface up to 10 times larger than of normal cells (data not shown).

The number of senescent cells grown on S1 and S2 substrates was similar to the number of such cells on flat surfaces (Figure 11A). In contrast, cells grown on S3 and S4 substrates displayed an increased proportion of enlarged cells and decreased proportion of cells with narrow cytoplasm (Figure 11A). Furthermore, the amount of fibroblasts positive for SA-b-gal staining was increased when cells were grown on S3 and S4, suggesting that increasing the dome size of the surface increases the induction of cell senescence (Figure 11B).

3.4. The regulation of cell proliferativity by nanopatterned surfaces

Ki67 antibody staining recognizes a proliferation-specific nuclear antigen expressed by proliferating cells in late G1, S, G2 and M phases, but not in resting cells (Kill, 1996, Gerdes et al., 1984). It has been used widely for the estimation of the growth fraction of normal cells in culture. Previous studies have shown that the level of Ki67-positive cells decreased with time of culture and number of cell passages (Knuchel et al., 1990). To avoid this tendency, cells from the third and fourth passage were used in our experiment.

In concordance with the presence of the increased number of senescent cells on S3 and S4 surfaces, we found that the number of Ki67-positive nuclei was slightly decreased in the cells grown on S3 and S4 (Figure 11C).

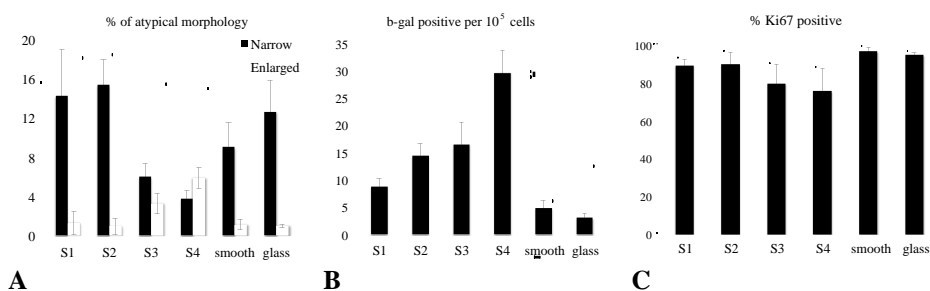


Figure 11. Regulation of cell senescence and cell proliferativity by nanopatterned surfaces. Graphs describe the percentage of cells with atypical morphology (A), ratio of SA-b-gal positive per 10⁵ normal cells (B) and mean percentage of Ki-67-positive cells per total number of cells (C). Error bars: \pm SD.

3.5. Scanning electron microscopy (SEM) and focused ion beam (FIB) imaging of the cells grown on sol-gel prepared silica surface

To obtain more detailed insight into the possible reasons behind the morphology changes described above, we performed SEM imaging of the cells grown on different surfaces (Figure 10D–F, J–L). One striking difference between cells grown on S3 and S4 is the lack of filopodia of cells grown on S3 (Figure 10F). Instead, the cells grown on S4 stretch out long filopodia (Figure 10J).

To investigate the attachment of cells to the nanopatterned surface, we imaged the vertical cuts of the cell-substrate interface by FIB. The cells grown on S1 displayed tight attachment to the substrate with no gaps present between the cell membrane and the material (Figure 12A). Cells grown on S2 attached incompletely to the substrate with occasional gaps present (Figure 12B). These changes were more pronounced in the cells grown on S3, where cells were attached only to the domes and contact with the substrate in between the domes was practically absent (Figure 12C). The cells grown on S4 attached both to the domes and to the space between them (Figure 12D).

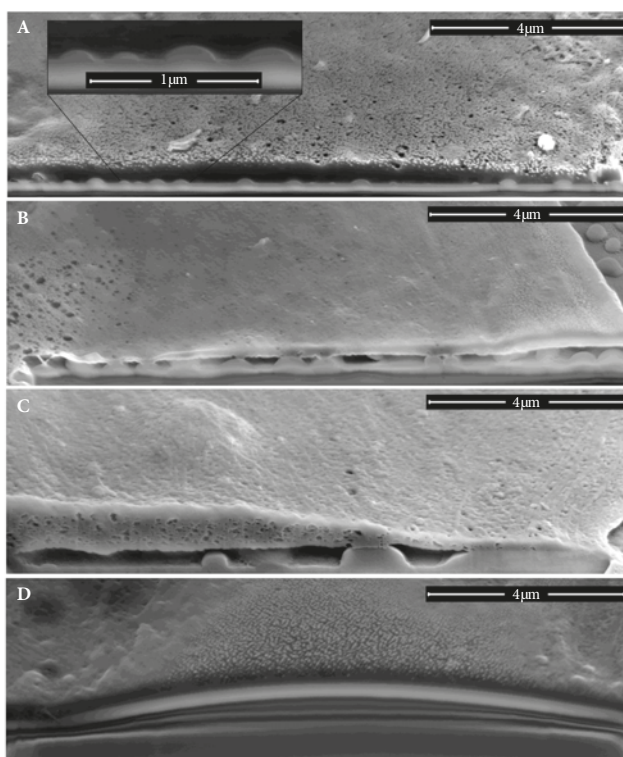


Figure 12. Cross-sectional imaging. SEM micrographs of cross sections performed with focused ion beam (FIB) of fibroblasts on silica domes S1 (A), S2 (B), S3 (C) and S4 (D) indicate cell-surface integration between different sizes of domes.

4. Design of thermally cross-linked glucose-containing electrospun gelatin meshes (Paper III)

In Paper I we found that nanopatterned silica material does support the growth of primary skin fibroblasts. However, in order to create more tissue-specific and elastic materials for skin engineering, we continued by studying *in vitro* synthesized biopolymer compositions. In Paper III we investigated the use of thermally cross-linked glucose-containing electrospun gelatin meshes as possible cell substrates for *ex vivo* growth.

Electrospinning the gelatin solutions with different glucose concentrations in the presence of acetic acid produced a smooth and uniformly structured fibrous scaffold as confirmed by SEM (Figure 13). Scaffolds with glucose concentration up to 50% were electrospun successfully. However, at glucose concentration 30% and higher, the scaffold became extremely fragile and was therefore excluded from the study.

Samples with different glucose concentrations in spinning solution differed mainly by fibre diameter. Average fibre diameters varied between 250 and 600 nm. The fibre diameter was the smallest at 5% glucose concentration and increased with higher glucose concentrations in the electrospinning solution. Additionally, the samples with lower glucose concentration tend to have more loosely packed fibres (Figure 13). Thermal cross-linking did not alter detectably the microstructure of collagen scaffolds as visualized by SEM (Figure 13).

We used FTIR spectroscopy to analyse the effect of glucose on structural changes during thermal cross-linking, to determine the optimal time of exposure to cross-linking temperature and to evaluate the extent of cross-linking. We used both type A and type B gelatin in our study. Since there were small differences between the FTIR spectra of type A and type B gelatin scaffolds, a mass spectrometry analysis was carried out to study the differences in the protein content of type A and type B gelatins. We found that the content of proteins and their fragments in gelatin type A and type B powder differed significantly, being much pronounced in the case of type A gelatin (Table 7).

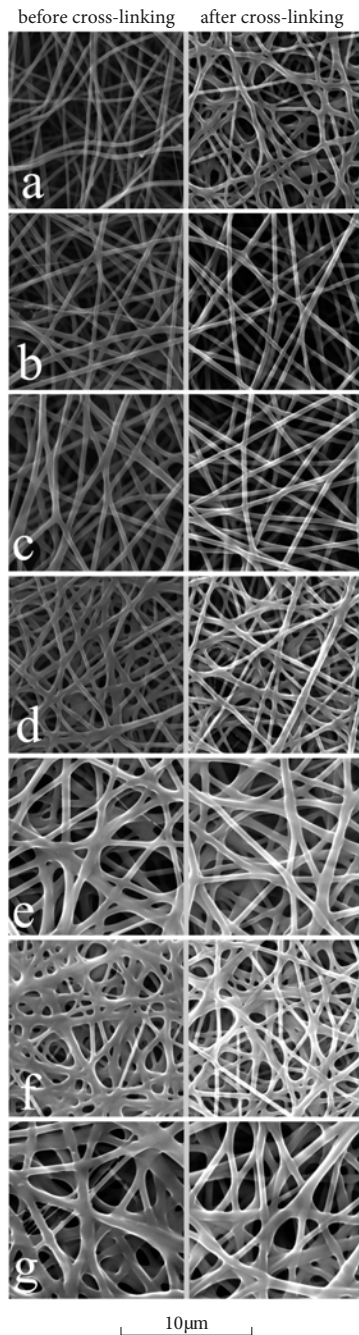


Figure 13. SEM images of gelatin scaffolds with different glucose content before (left) and after (right) thermal cross-linking: (a) 0%, (b) 5%, (c) 10%, (d) 15%, (e) 20%, (f) 25%, (g) 30% glucose. Magnification 21,000 times.

Table 7. Protein mass spectrometry results. Protein profiles of gelatin type A and type B powders. Peak intensity corresponds to the relative abundance ratio of proteins.

Gelatin, type A	Intensity	Gelatin, type B	Intensity
Protein name		Protein name	
collagen, type I, Alpha 2	7.02E+09	collagen, type I, alpha 1	1.95E+09
collagen, type I, Alpha 1	2.98E+09	collagen, type I, alpha 2	1.35E+09
fragments of collagen, type I, alpha 1 and alpha 2	1.23E+09	collagen, type III, alpha 1	1.33E+08
collagen, type III, alpha 1	7.14E+08	decorin	2.69E+06
		myosin, heavy chain 7, cardiac muscle, beta	1.61E+06
collagen, type V, alpha 2	4.93E+08	albumin	1.57E+06
albumin	1.02E+08		
decorin	4.66E+07		
collagen, type V, alpha 1	4.05E+07		
lumican	3.27E+07		
orosomuroid	3.17E+07		
transferrin	2.11E+07		
osteoglycin	1.77E+07		
transthyretin	1.34E+07		
serpin peptidase inhibitor, clade A, member 3-3	1.12E+07		
uncharacterized protein	7.41E+06		
uncharacterized protein	4.24E+06		
collagen, type V, alpha 3	2.44E+06		
fragments of serpin peptidase inhibitor, clade A, member 3-3	9.42E+05		
chitinase, acidic	8.91E+05		
serpin peptidase inhibitor, clade A, member 3-2	3.17E+05		

4.1. Glucose measurements

Next we seeded previously isolated juvenile fibroblasts onto the fibrous gelatin scaffolds prepared using different glucose concentrations. When conducting preliminary experiments, we noticed an increase in glucose concentration in the cell culture media after incubating the scaffolds in it. Since the changes in glucose concentration of the growth media could potentially influence the growth characteristics of the cells, additional experiments were carried out to find the reasons for this phenomenon. The scaffolds were incubated in DMEM and glucose concentration in the culture medium was measured. We found that after such incubation the glucose concentration in the growth media increased from 7% to 29% (Figure 14). DMEM contains normally 450 mg/dl (4.5%) glucose. The change in glucose levels for type B gelatin scaffolds was somewhat larger than for type A gelatin scaffolds (22.1% and 15.3% respectively). A probable explanation is that the degree of swelling is different for type A and type B gelatin. When the culture medium was replaced, the glucose level in the fresh medium did not increase. The amount of excess glucose in the medium did not correlate with glucose concentration present in gelatin blends. Furthermore, the glucose levels were also increased when gelatin scaffolds without

glucose addition were incubated in the media. We concluded that this effect can be attributed to water absorption during swelling of the scaffolds. Hence the swelling of scaffolds made from different types of gelatin or scaffolds with various cross-linking rate differs, the extent of increase of the glucose concentration in cell culture media were dissimilar. To avoid the changes in the media constitution, all the experiments were performed with matrices pre-incubated in the growth medium.

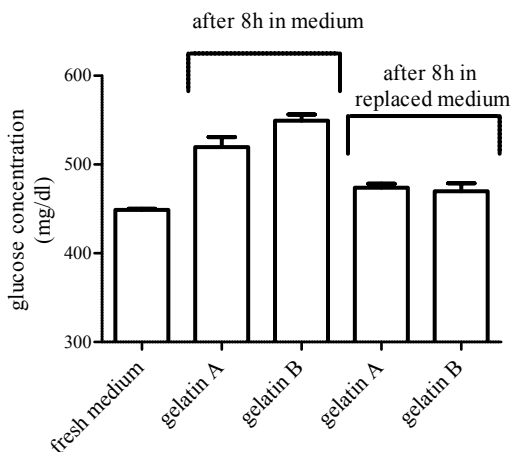


Figure 14. Changes in glucose concentration during swelling of electrospun matrices. Data is plotted as the mean of 3 replicates \pm SD (error bars).

4.2. Biological degradation

Since one of the critical properties of the matrices used for tissue engineering is their biodegradability, we tested the efficacy of a selection of ECM-degrading enzymes in degrading the electrospun collagen scaffolds.

The biological stability test of cross-linked gelatin scaffolds using digestion with collagenases (type II, IV) and trypsin showed that scaffolds with higher glucose content (25% and 30%) were resistant to digestion with all three types of enzymes, as scaffolds maintained their pre-treatment shape. Scaffolds containing 20% glucose were partially degraded. Matrices containing 15% and less glucose were totally dissolved in collagenase and trypsin solution and no undigested scaffold fragments could be observed under optical microscope.

4.3. Cell proliferation

Next, the viability and proliferation of the fibroblasts seeded onto the electrospun collagen scaffolds were studied using a luminometer-based cell viability assay. After 16 h of culturing, the number of cells attached to the scaffolds was

largely the same for all glucose concentrations. Seven days after seeding, the cells had started to proliferate and the number of fibroblasts increased remarkably. Notably, at higher glucose concentrations (25% and 30%) the number of viable cells was significantly lower (Figure 15). However, the differences between the total number of cells grown on type A and type B gelatin scaffolds containing the same amount of glucose were marginal. The number of cells started to decrease at 10% (type B gelatin) and at 25% (type A gelatin) glucose concentrations (Figure 15).

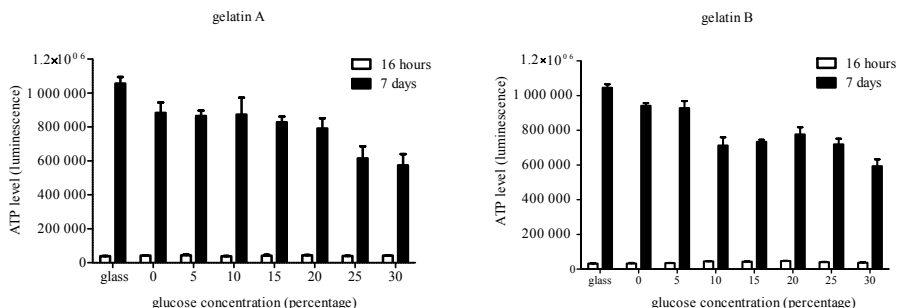


Figure 15. Dependence of ATP levels on glucose concentration 16 h and 7 days after seeding. ATP level is proportional to the number of cells grown on type A and Type B gelatin scaffold. Data is plotted as the mean of 3 replicates \pm SD (error bars).

4.4. Cell morphology

SEM images confirmed the results of the proliferation tests. Cells grown on surfaces with glucose content of 25% and 30% tended to have a polygonal shape, lacked filopodia (Figure 16C) and appeared to have a flat morphology similar to the cells grown on 2D surface like plastic or glass (Figure 16D). On these scaffolds we saw a number of cells with a morphology characteristic of stressed cells – enlarged or serrate cell body, decreased number of attachment sites to the scaffolds, and partial detachment from the scaffold. That fits well with the results of the proliferation test, where we saw the decreased proliferation at glucose 20% and higher.

The morphology of the fibroblasts grown on the scaffolds with glucose content 5–20% did not differ significantly, but displayed certain directional orientation, especially in regions where parallel ordering of fibres was evident (Figure 16B). And cells grown on the substrates with more loosely packed and disorganized fibres, were more stellate, formed more dendrites to connect to the surrounding scaffold and even localized below the fibers (Figure 16A). However the cross-sectional imaging of the scaffolds, using confocal microscopy, did not reveal any invasion of the fibroblast into the deeper layers of the scaffolds (data not shown).

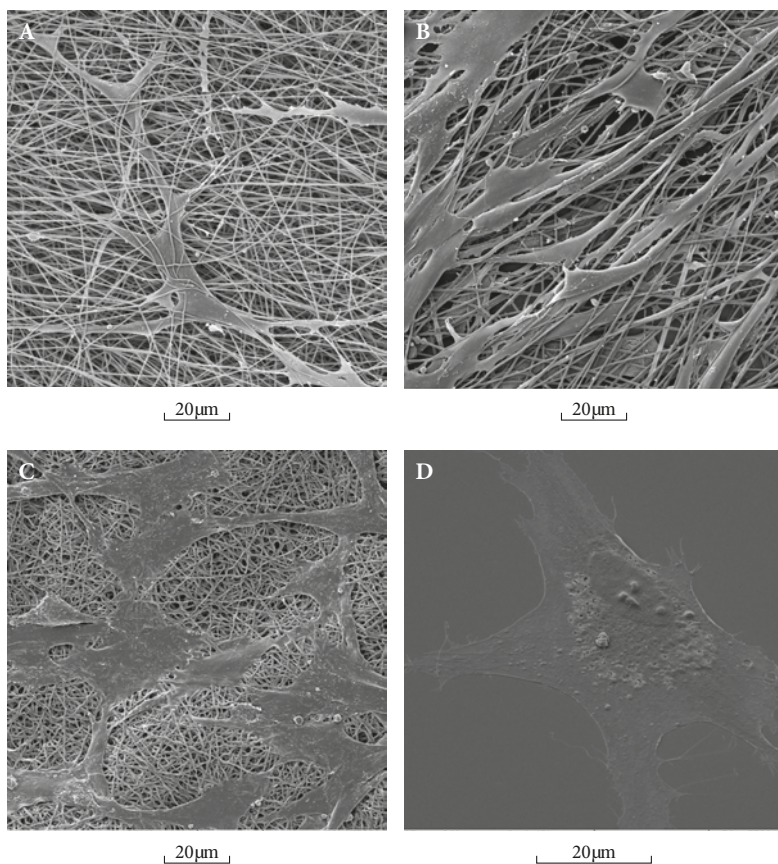


Figure 16. Morphology of fibroblasts grown on scaffolds with different porosity, fibre density, orientation and diameter (2,500 times magnification). A) 5% glucose, B) 10% glucose, C) 30% glucose, D) glass.

DISCUSSION

I. IL-10 family cytokines

The immune status of the skin plays an important role in determining the susceptibility towards a number of illnesses, but also determines the course of wound healing. Therefore the cells and immunomodulating factors produced by the cells are actively involved in regenerative processes. IL-10 family cytokines have been shown to be important players both in anti- and proinflammatory processes. As an unresolved chronic inflammation in a wound finally leads to scar formation, the resolution of the early inflammatory cascade might be crucial for successful regeneration process (Atala et al., 2010).

The aim of our study presented in Paper II was to localize cell populations with the expression of IL-10 family of cytokines in juvenile skin and to determine possible age-related differences in the expression of these genes. We found that the majority of the genes of IL-10 family and their receptors were detectable in juvenile skin (*IL10*, *IL10RA*, *IL10RB*, *IL20*, *IL20RA*, *IL20RB*, *IL22RA1*, *IL22RA2*, *IL26*, *IL28RA*). On the other hand, 50% of the genes expressed in juvenile skin were downregulated (*IL22RA1*, *IL22RA2*, *IL28RA*) or absent (*IL20*, *IL26*) in adults (Table 2). For several genes, for example *IL10RB*, we observed a significantly weaker or missing antibody reaction in juvenile samples when compared to adults (Fig 3a). In addition to *IL10RA*, *IL10RB* has been shown to be required for IL10-induced signal transduction and therefore may regulate susceptibility to various pathologies. For example, the mutations in *IL10R* genes cause severe and early childhood onset of the inflammatory bowel disease (Glocker et al., 2009).

We also found that interleukin receptors are more prominently expressed in the skin than the interleukins themselves (Figure 5). This indicates that the skin cells are to a greater degree targets for circulating cytokines than a source of these. There were also differences in the expression of cytokine receptor subunits. Interestingly, the expression level of the receptor genes correlated with the overall prevalence and selectivity of respective subunits. For example *IL10RA* is unique to *IL10R* whereas *IL10RB* is shared by several other cytokines, including *IL22*, *IL26*, and *IL28A* *IL28RB* and *IL29* (Table 1). Concurrently, there was a group of genes of the IL-10 family (*IL19*, *IL22*, *IL28B*, *IL29*), which have been shown to play a role in different skin disorders, such as psoriasis and infections (Gallagher, 2010, Sahoo and Im, 2012, Wolk et al., 2010). In healthy adult and juvenile skin their expression was undetectable (Table 2). It suggests that these cytokines are significantly expressed only in pathological conditions. For example *IL28B* and *IL29*, the newly discovered interferon-like cytokines in the IL-10 family, have been shown to exert their anti-viral, anti-proliferative, anti-tumor activity via the *IL28RA* and *IL10RB* receptor complex (Sheppard et al., 2003, Li et al., 2009). *IL28* and *IL29* can act synergistically with *IL20* (Wolk et al., 2010), which is one of the most attractive potential target cytokines for psoriasis treatment (Stenderup et al., 2007). In

agreement with previous studies (Wei et al., 2005), we found IL20 to be absent in healthy adult skin (Figure 5d). The reason for the *IL20* expression level fluctuation in juvenile whole skin (Figure 5d) and keratinocytes (Figure 4c) might be the higher proliferation activity of cells extracted from juvenile skin.

In order to localize the expression of studied cytokines in the skin we analyzed the gene expression patterns of the three main cell types found in juvenile skin – the melanocytes, keratinocytes and fibroblasts. We found that mRNAs, which were undetectable in whole skin samples of both children and adults (*IL19*, *IL22*, *IL28B* and *IL29*), were also undetectable in cultured cells (data not shown). In this regard *IL24* was exceptional as it was highly expressed in melanocytes (Figure 4g), but undetectable in juvenile and adult whole skin. Compared to fibroblasts and keratinocytes, the number of melanocytes in the skin is very small and, therefore, melanocyte-specific mRNAs are hardly detectable in whole skin samples. *IL24* has been shown to induce growth arrest and apoptosis in melanoma cells (Sarkar et al., 2002) and is also considered to be an important mediator for chronic inflammatory conditions, e.g. psoriasis (He and Liang, 2010). We treated the cells with lipopolysaccharides (LPS), which are the major components of the outer membrane of gram-negative bacteria (Karima et al., 1999). LPS preparation is a strong pro-inflammatory compound, which promotes the secretion of pro-inflammatory cytokines such as IL1 β , tumor necrosis factor alpha and IL10 from cells (Thakur et al., 2006, Ho and Ivashkiv, 2010). Interestingly, only the expression of *IL24* was increased significantly in response to LPS stimulation and that occurred only in juvenile melanocyte culture (Figure 4g). This finding shows that melanocytes can react to the inflammatory signals and are able to produce cytokines, which suggests that they play a role in the regulation of immune defense mechanisms in skin. The unresponsiveness of the rest of interleukins to LPS stimulation could be explained by the fact that neonatal cells tend to have notably lower cytokine production in response to LPS compared to adults (La Pine et al., 2003, Joyner et al., 2000). We also have to take into account that LPS could activate the secretion of the cytokines directly, and not necessarily having any influence on gene expression.

In conclusion, for the first time, we showed the difference of IL-10 family and its receptors between juvenile and adult skin. Additionally, our analysis of the expression of IL-10 family members in cultured skin cells revealed a cell type-specific cytokine production pattern, which helps to explain the roles of different cells in inflammation, regeneration and tissue rejection.

2. Cell type-specific differences in the skin transcriptome

To analyze in detail the differences between the three main cell types in skin – melanocytes, keratinocytes and fibroblasts – we determined the differences in their global gene expression profiles. Earlier, numerous gene expression

analyses of different skin cell populations have been performed using material isolated from normal and pathological samples (Lee et al., 2013, Lan et al., 2011, Liu et al., 2009, Roberts et al., 2006, Hoek et al., 2004). Various mRNA quantification methods have been used, ranging from quantitative real time polymerase chain reaction and *in situ* hybridization to high throughput methods such as serial analysis of gene expression and microarrays. However, to our knowledge, the complete transcriptome analysis of the three skin cell types has not been performed before. To achieve this goal we performed high-throughput RNA sequencing of rRNA-depleted samples, which allowed us to detect nearly all coding and non-coding RNA species in a given sample. In our analysis we concentrated on melanocytes, which are highly outnumbered by keratinocytes and fibroblasts in skin and thereby their specific properties in this regard are underestimated when using full-skin biopsies.

The data presented in Paper IV suggests that cultured melanocytes are active, motile and intensively proliferating cells. For instance, the high expression level of histone genes in melanocytes refers to intensive DNA synthesis as histones are responsible for nucleosome structure and proper DNA wrapping (Alberts et al., 2008). The kinesin genes upregulated in melanocytes are related to cell movements and intracellular trafficking, including chromosome and centrosome positioning during mitosis (Verhey et al., 2011). Calcium-binding proteins are responsible for numerous cellular processes, e.g. cell cycle regulation and differentiation, but have also been suggested to have tumor suppressor functions and are highly expressed in cells with stem cell properties (Auge et al., 2005, Chen et al., 2014). All these findings correlate well with the high proliferative activity we saw during the melanocytes cultivation process.

Previous studies have pointed out the role of melanocytes as pigment-producing cells in the skin. The gene expression profile of melanocytes has been compared to other normal skin cells, but also to pathologic melanoma cells (Lee et al., 2013, Hoek et al., 2004). We confirmed the high expression level of previously identified melanocyte-specific genes, such as *DCT*, *TYR*, *KIT*, *EDNRB*, *MITF*, and *TYRP1*, in melanocytes (Lee et al., 2013). *DCT*, *TYR* and *TYRP1* encode enzymes acting in the melanin synthesis pathway (Cichorek et al., 2013). *EDNRB* and *MITF* are crucial for melanoblast proliferation and *KIT* is needed for the differentiation of melanoblasts into *TYR*-positive melanocytes (Lee et al., 2013, Hoek et al., 2004). We also showed that *MC1R*, *PLA1A*, *NPM2* are uniquely expressed in melanocytes, but not in keratinocytes or fibroblasts (Table 4) corroborating previously published data (Roberts et al., 2006). *MC1R*, a receptor for melanocyte-stimulating hormones and adrenocorticotrophic hormone, is involved in regulating the pigmentation of the skin and hair. *PLA1A* and *NPM2* have both been shown to be essential in melanoma progression (Liu et al., 2009, Koga et al., 2009). In agreement with previous studies (Lee et al., 2013, Hoek et al., 2004) the expression of *ABCC2*, *DNAJA1*, *GPR143*, *MLANA*, *OCA2*, *QPCT*, *RRAGD*, *TBC1D7* and *GPR137B* was detected at a higher level in melanocytes compared to keratinocytes and fibroblasts. The majority of these genes are also related to the melanogenesis

pathway, controlling the growth and maturation of melanosomes. Additionally, the genes are involved in melanoma progression (Du et al., 2003, Lee et al., 1995, Gillis, 2006, de Souza et al., 2012).

We showed that a number of genes were specifically upregulated in cultured melanocytes. The exact role of these genes in studied cell types is unclear, but based on the existing biological data they can be classified into the following categories: tumorigenesis, inflammation and stemness-related processes.

2.1. Tumorigenesis

Genes belonging to the pathways involved in tumor progression are more characteristic to melanocytes than to keratinocytes and fibroblasts. High expression of known and potential tumor suppressor genes such as *ARL9*, *SLC22A18*, *DAPK1* and *BEX1* could be observed in melanocytes compared to keratinocytes and fibroblasts (Louro et al., 2004, Chu et al., 2012, Ahmed et al., 2010, Foltz et al., 2006). We detected also the expression of the members of a novel tumor suppressor family IGLON (*IGLON2*, *IGLON 3* and *IGLON4*) in melanocytes (Chen et al., 2003). *IGLON3*, also known as *LSAMP* was prominently expressed in melanocytes compared to keratinocytes and fibroblasts. A number of genes, which normally have a role in growth and cell division or in apoptosis regulation, can play a role in cancer formation (Wu et al., 2012). As an example, certain RING finger proteins – *RNF144A*, *RNF157* and *RNF187* – were specifically upregulated in melanocytes. We confirmed an increased expression of genes related to melanoma invasion and its metastatic potential (Marzook et al., 2012).

2.2. Inflammation

The susceptibility to malignancies is linked to the deregulation of inflammatory processes. Uncoordinated inflammatory response affects cancer development at different levels – predisposing to precanceroses, misleading the immune system, initiating invasion process etc. (Elinav et al., 2013). An example about the relation of immune response and tumorigenesis is the involvement of the family of tumor necrosis factors (TNFs) and their receptors in cancer formation. Being strongly engaged in both immune system modulation and apoptosis regulation, they trigger infiltration of inflammatory cells into tumor tissue (Wajant, 2009). The cross-regulation of TNF and interferon regulatory factors has been proposed recently (Cantaert et al., 2010). In line with this, the tumor necrosis factor receptors *TNFRSF14*, *TNFRSF19* and interferon regulatory factors *IFI6* and *IRF4* were highly expressed in melanocytes compared to keratinocytes and fibroblasts. Cytokines from the IL-10 family are among the key players in host defense mechanisms and bear both pro-inflammatory and anti-inflammatory roles (Burgdorf et al., 2009). In Paper II, a quantitative real-time PCR analysis of selected IL-10 family cytokines mRNAs indicated differential expression in

cultivated juvenile melanocytes relative to keratinocytes and fibroblasts. The data correlates well with the whole transcriptome analysis results. For example, *IL20RA* and *IL20RB* had significantly higher expression in keratinocytes compared to melanocytes. Also, *IL22RA1* could be found in keratinocytes and not in melanocytes, whereas *IL22RA2* gene was expressed in whole skin but not in melanocytes, keratinocytes or fibroblasts (Table 2). Among the studied IL-10 family cytokine genes (*IL10*, *IL19*, *IL20*, *IL22*, *IL24*, *IL26*, *IL28B*, *IL29*) and their receptors (*IL10RA*, *IL10RB*, *IL20RA*, *IL20RB*, *IL22RA1*, *IL22RA2*, *IL28RA*), *IL24* was the most prominent cytokine in melanocytes, which was hardly detectable in keratinocytes and fibroblasts (Table 2).

2.3. Stemness-related processes

Cultured melanocytes express many genes, which are characteristic of stem cells. Evidence shows that several pathways important in normal stem cells (BCL2 family genes, Notch, Sonic hedgehog and Wnt signaling pathways) may also act in cancer development (Reya et al., 2001, White and Zon, 2008). For instance, we saw an increased expression of antiapoptotic *BCL2* and *BCL2A1* and stem cell factor inducer *RCAN1* (Wu et al., 2013) in melanocytes when compared to keratinocytes, fibroblasts and whole skin. Interestingly, *CD200* was uniquely expressed in melanocytes (Table 4). CD200 has been proposed to be a marker of follicular stem cells, but it has been shown that cancers overexpressing CD200 expand and metastasize more rapidly (Rosenblum et al., 2004). As mentioned above, the expression of *S100* calcium-binding protein gene, which are specifically expressed in cells with stem cell properties, but have also shown to be prognostic markers for melanoma progression (Auge et al., 2005), was increased in melanocytes. Tumor cells and stem cells both possess self-renewal capacity – they have extensive proliferative potential and stem cells are often targets for malignant genetic transformations (Reya et al., 2001). These stem-cell-like properties have brought forth melanocytes as a potential source for induced pluripotent stem cells (iPSCs) (Utikal et al., 2009).

The data presented in Paper IV provided insight into the possible roles of melanocytes in the skin. As expected by the rapid growth in the cell culture, our differential gene expression and pathway analyses described melanocytes as cells with a high proliferative capacity *in vitro* compared to keratinocytes and fibroblasts. That might suggest they have preserved the readiness to regenerate and possess stem-cell-like properties to a larger extent than bulk keratinocytes and fibroblasts. However, these properties make melanocytes the most vulnerable cells in the skin and provide an explanation to their increased susceptibility to harmful environment agents (e.g. UV exposure) and high incidence rate of malignancies that originate from this cell type. On the other hand, the increased stem cell-like properties provide melanocytes with good self-renewing potential and also advocate for their use as a potential source for induced pluripotent stem cells for therapeutic purposes.

2.4. Extracellular matrix

Extracellular matrix (ECM) is a well-organized network that provides structural and biochemical support to the cells. In tissue-engineered products, the cells are embedded into artificially created ECM. The embedded cells are expected to synthesize specific components of the ECM, which are characteristic to the particular type of the tissue and thus contribute to the formation of a natural-like tissue structure. As the final goal of our work is to develop an appropriate tissue-engineered matrix for the skin, which could mimic the architecture in the normal dermis, we used fibroblasts as a model system for our next set of experiments. In the skin, the biosynthesis and degradation of the extracellular matrix is mostly conducted by fibroblasts, which are the prevailing cell type in the dermis. The importance of fibroblasts in the regulation of ECM was underlined by the results of the transcriptome analysis. We found that a number of ECM-related genes were detectable in fibroblasts (Table 5). In addition to several well-characterized collagen genes, we could detect the expression of LAMA1, LAMA2, LAMA3, LAMA4, LAMB1, LAMB2, LAMB3, LAMC1, LAMC2, which encode the α 1, 2, 3, 4, β 1, 2, 3 and γ 1 and 2 subunits of laminins in fibroblasts (Table 5). Laminins are integral parts of the extracellular matrix being the key elements of the basement membrane (Ekblom et al., 2003). Meanwhile, they also act as binding molecules between cells and other ECM components in the dermis. For instance, LAMA1 is present mostly in the embryo and is not common for adult tissues (Ekblom et al., 2003). As pointed out earlier, we detected LAMA1 gene expression in melanocytes and in fibroblasts. One has to keep in mind that these cells were harvested from juvenile skin and were cultured *in vitro*.

Nevertheless these results from the whole transcriptome analysis showed that fibroblasts are capable of producing an array of ECM constituents.

Further, our preliminary results demonstrated that fibroblasts cultivated on cross-linked glucose-containing electrospun gelatin meshes can highly express laminin β 1-chain protein, but also laminin α 4 and α 5-chain proteins to a small extent. In standard cell culture conditions the expression of laminin β 1 and α 4-chain but not α 5 chain were observable (unpublished). These results are in good correlation with the gene expression analysis (Table 5).

Whole transcriptome analysis pointed out several remarkable genes and groups of genes that we should pay attention to in our further studies. When developing substitutes for skin tissue, we can evaluate changes in gene and protein expression after transferring cells from a monolayer culture into a three-dimensional structure.

3. Biocompatible surfaces

In many cases instead of biomimicking a complicated extracellular matrix, a simple biocompatible surface is used for the cells. Hence it has been demonstrated previously, that by modifying exclusively the surface topography,

we can influence the morphology (including the placement of the cell body and spreading of the cell extensions), attachment, proliferation and growth of the cells (Poellmann et al., 2010, Altala et al., 2011). In Paper I, we studied the effect of the surface structure on the morphology and growth properties of primary human dermal fibroblasts. The novel sol-gel technique we used in our study is adaptable to a wide range of different material compositions and by its modification we can obtain different surface structures with a variety of mechanical and chemical properties. The method is extremely flexible since by variation of just solvent and sol concentrations we could generate dome-shape silica (SiO_2) structures with diameters ranging from 200 nm to 10 μm on borosilicate inserts.

Borosilicate glass inserts are commonly used for cell culturing. They compose mainly of SiO_2 , B_2O_3 , Al_2O_3 , Na_2O , K_2O , ZnO and TiO_2 and their suitability for cell culturing has been proved by numerous experiments (Altala et al., 2011). In tissue engineering practice the bioactive glasses are widely used for hard tissue culture, such as bone. The ingredients of bioglass do not differ significantly from borosilicate glass, composing SiO_2 , Na_2O , CaO and P_2O_5 in specific proportions. Meanwhile the components vary – CaO can be replaced with MgO or CaF_2 , Na_2O with K_2O . Some B_2O_3 , Al_2O_3 , $\text{Ca}(\text{PO}_3)_2$ and TiO_2 can also be added (Hollinger, 2011). The bioactive glass samples with SiO_2 content of 60% and higher are quite inert, whereas other glass constituents, which are meant to enhance the mechanical properties of the material, might turn out to be toxic for all or some specific types of cells (Hollinger, 2011). Sol-gel method and the following thermal treatment frees the material from residual solvent traces and provides a pure material with excellent bioactivity (Gupta and Kumar, 2008). At the same time the method enables to easily produce surfaces with different topography and mechanical properties and thereby modify the behaviour of the cells.

In our experiments we used domes generated by the sol-gel technique and which consisting of SiO_2 . It is important to note that the surface chemistry does not vary between the differently patterned silica surfaces, even in the flat portion of the substrates. Hence the changes in cell morphology and proliferation are caused by the structure of the surface and not by differences in the chemical composition of the materials.

It has been shown previously that the pyramidal shape of the fibroblasts is indicative of cell migration (Stockton and Jacobson, 2001). When we cultivated the fibroblasts on the nanopatterned surfaces we found that a number of cells grown on S3 and S4 surfaces had lost their pyramidal or spindle shape and become more enlarged – characteristic to senescence fibroblasts. The reason why fibroblast cultures grown on S3 and S4 surfaces contained more enlarged and senescent cells is likely related to attachment deficit and disturbance of normal cytoskeleton. The inability of the cell membrane to bend between the domes in case of S3 decreases the contact surface between the cell and the nanopatterned surface which may also lead to a decrease in the number of anchoring points. Most of the domes present in S1 and in S2 on the other hand

were successfully integrated into the cell membrane due to their smaller size and did not markedly influence the attachment of the cell to the surface. These data are in good correlation with the observation that an increase in the distances between cell's anchoring points results in enhanced differentiation of epidermal and mesenchymal stem cells (Trappmann et al., 2012). In the case of S4, the cell was able to spread over the domes due to the wide bending angle and long distance between the domes. Although this resulted in a complete attachment of the cells to the substrate, the presence of protrusions of S4 surfaces, which affect the 3D organization of the cytoplasm, affected the cells ability to proliferate and induced senescence.

Our results suggest that in addition to the chemical component of extracellular environment, the cells are influenced by the micro- and nanoscale structure of the surface. From dome size 1 μ m and higher the survival of the cells decreases, which is likely caused by the paucity on contacts between the cells and the surface and also by defects of cytoskeleton, which in its own turn leads to cellular senescence.

4. Gelatin scaffolds modified by glucose-assisted thermal cross-linking

In order to mimic the structural components of the extracellular matrix, which in a tissue are formed by micro- and nanoscale fibres, the artificial substrate should also be presented to the cells in the shape of a fibrous network. Several methods have been put forward for the formation of natural-like tissue structures including phase separation, self-assembly, surface patterning, wetspinning, biospinning, interfacial complexation, microfluidic spinning, meltspinning and electrospinning (Altala et al., 2011, Gupta and Kumar, 2008).

Gelatin is a mixture of naturally occurring collagens and thus suits well for the formation of an artificial biocompatible scaffold. To give the gelatin fibres a shape, these need to be cross-linked. It was demonstrated that glucose could be used to increase the extent of collagen cross-linking (Ohan et al., 2002). Although gelatin nanofibres can be cross-linked by thermal treatment alone, we demonstrated for the first time that combining thermal treatment with cross-linking by glucose allows us to control the extent of cross-linking to a large degree by varying glucose content in the gelatin fibres.

Glucose, albeit an essential energy source, is toxic to cells when its concentration exceeds a certain value. This phenomenon can be observed in patients with diabetes, where the high blood glucose level can cause abnormal collagen cross-linking and thereby affect structure, mechanical properties and functioning of tissues (Lubec et al., 1991). Therefore, it is necessary to keep glucose levels in physiologically suitable range during cell culture. In our study we confirmed the lack of free glucose in scaffolds, since glucose is covalently bound to the matrix proteins. Therefore the changes in the morphology and numbers of cells grown on the glucose-based cross-linked scaffolds cannot be

explained by the influence of glucose itself, but by changes in mechanical properties.

The morphological differences between cells on scaffolds with different glucose content were probably caused by variations in fibre diameter and orientation (Figure 16) and mechanical properties. The increase in fibre size can be explained by the increasing viscosity of electrospinning solution and the fact that while every electrospinning solution contained 25% gelatin, it contained a smaller and smaller percentage of solvent as glucose was added to the solution

When used in tissue engineering or wound healing applications, the scaffold should degrade over time. Before cross-linking, the scaffolds were water-soluble. Cross-linking, however, converted the scaffolds insoluble in boiling water, glacial acetic acid and cell culture media. Interestingly, the scaffolds prepared by using 20% or higher glucose content became partially or fully resistant to enzymes responsible for the degradation of extracellular matrix in the body. These results, combined with the data obtained from FTIR analysis, suggest that the maximum extent of cross-linking was achieved at approximately 20% glucose.

Although gelatin is believed to consist mainly of type I collagen the exact protein content of gelatin depends on the extraction method as well as the origin of raw material. Previous studies have shown that under the same conditions collagen type I had higher cross-linking capacity compared to mixtures of collagen types I and III. The reason for this phenomenon is related to the dissimilarities in primary structures and molecular organization of different types of collagen (Mentink et al., 2002). Protein analysis indicated a remarkable difference between type A and type B gelatin used in this work. Both high rate of additives and different protein profiles might have affected the cross-linking process, leading to differences in scaffold properties and cell growth.

5. Concluding thoughts and future prospects

Normal versus artificial condition. 2D versus 3D environment

To define pathologic alterations, the “normal” has to be defined. The same applies to defining “artificial” and “natural” (“normal”) conditions. In the past few decades the most important method for investigating the behaviour of different cell types has been based on isolating and cultivating the cells. Cells obtained via extraction from tissue followed by multiplying in cell culture have been assumed to be “normal” cells. For instance in monolayer 2D cell culture, spindle-shape morphology is assumed to be “normal” morphological shape for dermal fibroblasts. These differentiated and mostly non-proliferative cells, extracted from tissues, have been inserted to cell culture media, supplemented with different nutrients and hormones and as a result start to replicate actively.

It has been described that any manipulation with cells can cause changes in their functioning – the cell viability, proliferation, morphology, protein or gene expression etc. The smaller the change, the harder it is to interpret the effect. If

the factor causes changes in cell proliferation, viability or morphological changes, it can be measured or described relatively easily. Hence, it has been shown previously that even small changes in the environment surrounding cells might have an effect at gene expression level (Achterberg et al., 2014). In our gene expression study we have to take into account that gene expression could still be influenced by *in vitro* culture conditions (Neumann et al., 2010, Crisostomo et al., 2006). In our study this could be an issue in the case of *IL10*, *IL22RA2* and *IL26* (Paper II) where gene expression was observed in the whole skin, but was absent in the cell culture. Also, mRNA synthesis could occur in other cell types than in keratinocytes, melanocytes and fibroblasts. For instance, *IL26* and a soluble receptor *IL22RA2*, which is considered to be stored in the extracellular matrix for on demand release (Schonherr and Hausser, 2000), are produced mainly by resident T cells (Dumoutier et al., 2001, Donnelly et al., 2010). Although both subunits of *IL22R* complex and *IL10RB* are required to form the functional receptor (Table 1), *IL22RA2* is able to bind alone to *IL22* (Kotenko et al., 2001). Unlike *IL22RA2*, which is strictly an antagonist for *IL22* activity, *IL22RA1* regulates both *IL22* and *IL20* activity (Table 1) and its expression was detectable only in keratinocytes (Figure 4f).

The same phenomenon can be seen in the gene expression pattern analysis (Paper IV), which describes the cultured melanocytes as highly proliferative cells. We have to consider that the high proliferation rate is characteristic only to artificially cultured melanocytes and does not reflect the actual situation *in vivo*. The cell culture conditions include less cell-cell contacts and a high level of growth factors reminiscent of active regenerative state (like in the case of wound healing). The same precautions should be applied to cultivated keratinocytes and fibroblasts we analyzed in our study. Thus the analysis of gene expression pattern of cultured cells does not reflect the homeostatic state of the cells in a tissue but rather is expected to describe their response to an injury. On the other hand, a number of well-characterized cell type-specific genes could be readily identified from each cell population analyzed, suggesting that the low-passage cultured cells have well retained their identity. Since the cell culture has remained as a gold standard for obtaining sufficient amount of relatively homogenous cell populations for tissue engineering and toxicity testing, knowing the characteristic properties of cells in culture is instrumental for their further use in *ex-vivo* applications.

The potential technique, which eliminates influence caused by cell culture conditions is the laser capture microdissection (LCM). Although the LCM is an excellent tool for the isolation of groups of cells in the case of melanocytes, which are present as single cells located in close contact with both keratinocytes and fibroblasts, the use of LCM would result in isolation of the melanocytes and adjacent cells, which would contaminate the sample. Additionally, to obtain a sufficient amount of cells, *in vitro* cell cultivation is still necessary. The results of gene expression analysis suggest possible roles for keratinocytes, melanocytes and fibroblasts in the skin, however, further studies are needed to find out, whether the expression level of genes reflects also protein levels and

functionality of the cells. The current understanding about the functions of cells in the tissue are based largely on studies of cells cultured on flat, two-dimensional (2D) plastic or glass substrates. However, in the body, cells are embedded within a tissue-specific three-dimensional scaffold (3D) – extracellular matrix.

Some cell types lose the characteristic markers of differentiation and become actively proliferative when grown on 2D surfaces. Some cell types are able to regain partially or entirely their properties when transferred into 3D structure, which mimics their original tissue (Baker and Chen, 2012). This leads to the conclusion that 2D cell culture recapitulates active regeneration of wound healing processes. The intermediate proliferating phase is necessary to obtain the number of cells needed for tissue reconstruction, however the most important task is to achieve the natural properties, the cells have in tissue by transferring and the multiplied cells back into a physiological 3D culture. One has to make sure that the matrix used in the 3D culture recapitulates the properties of the natural matrix of the particular tissue and sustains the specific properties of the embedded cells. Cell adhesion, mechanical forces and permeability to soluble factors are important factors, which influence cells in a 3D system. The multiplicity of adhesion sites between the cells and the extracellular matrix in a 3D system, compared to flat 2D substrate, lead to the changes in cell morphology and intracellular signaling. In our study we demonstrated that gelatin scaffolds modified by glucose-assisted thermal cross-linking are promising material for skin tissue engineering due to its nontoxic components and biocompatibility. However, the matrices designed by us behaved more like 2D rather than 3D structures for the cells, therefore our future studies will concentrate on the development of three-dimensionality of the material to facilitate the entrance of the skin cells into the matrix. For that purpose, the physical properties, such as porosity, stiffness, elasticity etc. of the scaffolds should be measured to determine tissue-specific parameters needed for the growth of the skin cells.

CONCLUSIONS

1. Juvenile skin cells, due to their excellent proliferative capacity, are mostly used for tissue-engineered products. We aimed to understand cell behaviour in an artificial environment, especially pro- and anti-inflammatory markers, which play a role in tissue rejection process. Our *in vitro* analysis showed that the production of IL-10 family cytokine and their receptors is cell-specific, which helps to explain the roles of keratinocytes, melanocytes and fibroblasts in the inflammatory system.
2. We identified a number of genes and pathways, which are characteristic for melanocytes, keratinocytes and fibroblasts. We also demonstrated the difference in gene expression patterns between skin cell cultures and the whole skin. The data presented provide an insight into the various possible roles of melanocytes, keratinocytes and fibroblasts in the skin. We can conclude that the analysis of gene expression pattern of cultured cells does not reflect the homeostatic state of the cells in a tissue but is rather expected to describe their response to injury. On the other hand since the cell culture has remained as a gold standard for obtaining sufficient amount of relatively homogenous cell populations for tissue engineering and toxicity testing, knowing the characteristic properties of cells in culture is instrumental for their further use in ex-vivo applications.
3. Sol-gel based method enables to design surfaces with various structural, mechanical and chemical properties, all of which are relevant in producing biocompatible, bioactive or biomimicking materials. We applied a novel sol-gel phase separation-based method for the preparation of micro- and nanopatterned silica surfaces with round nano- and microscale domes from simple TEOS-alcohol sol compositions. We saw that microscale surface (dome size less than 1 μm) with high density of domes (more than 240,000 domes per mm^2) provides a sufficient number of attachment sites for dermal fibroblasts without causing fatal disturbances into the cytoskeleton architecture, thus being a potential biocompatible material with good potential for tissue-engineering purpose.
4. Glucose can be used as a natural non-toxic cross-linking agent, which allows to generate biocompatible electrospun fibrous gelatin scaffolds for skin cells. Rising glucose content up to 20%, the extent of cross-linking of gelatin scaffolds increases linearly. From glucose content about 20% and higher, scaffold's fibres become resistant to enzymatic digestion, suggesting their inappropriateness for biodegradable devices. Cross-linked scaffolds obtained at up to 15% glucose content supported fibroblast growth and cell-scaffold interaction.

REFERENCES

- Achterberg, VF, Buscemi, L, Diekmann, H, Smith-Clerc, J, Schwengler, H, Meister, JJ, Wenck, H, Gallinat, S, Hinz, B. 2014. The nano-scale mechanical properties of the extracellular matrix regulate dermal fibroblast function. *J Invest Dermatol*, 134: 1862–72.
- Ahmed, IA, Pusch, CM, Hamed, T, Rashad, H, Idris, A, El-Fadle, AA, Blin, N. 2010. Epigenetic alterations by methylation of RASSF1A and DAPK1 promoter sequences in mammary carcinoma detected in extracellular tumor DNA. *Cancer Genet Cytogenet*, 199: 96–100.
- Akaneya, Y, Sohya, K, Kitamura, A, Kimura, F, Washburn, C, Zhou, R, Ninan, I, Tsumoto, T, Ziff, EB. 2010. Ephrin-A5 and EphA5 interaction induces synaptogenesis during early hippocampal development. *PLoS One*, 5: e12486.
- Alberts, B, Johnson, A, Lewis, J, Raff, M, Roberts, K, Walter, P 2008. *Molecular Biology of the Cell. 5th edition.*, New York, Garland Science.
- Altala, A, Lanza, R, Thomson, JA, Nerem, R 2011. *Principles of Regenerative Medicine*, Amsterdam, Boston, Heidelberg, London, New York, Oxford Paris, San Diego, San Francisco, Singapore, Sydney, Tokyo, Academic Press, Elsevier.
- Arend, Ü, Kärner, J, Kübar, H, Pöldvere, K 1994. *Üldhistologia*, Tallinn, Valgus.
- Atala, A, Irvine, DJ, Moses, M, Shaunak, S. 2010. Wound Healing Versus Regeneration: Role of the Tissue Environment in Regenerative Medicine. *MRS Bull*, 35.
- Auge, JM, Molina, R, Filella, X, Bosch, E, Gonzalez Cao, M, Puig, S, Malveyh, J, Castel, T, Ballesta, AM. 2005. S-100beta and MIA in advanced melanoma in relation to prognostic factors. *Anticancer Res*, 25: 1779–82.
- Aziz, N, Shushan, Z 2010. Evolution of Allograft Transplantation. *Allograft Procurement, Processing and Transplantation: A Comprehensive Guide for Tissue Banks*. Singapore: World Scientific Publishing Co. Pte. Ltd.
- Azzarone, B, Macieira-Coelho, A. 1982. Heterogeneity of the kinetics of proliferation within human skin fibroblastic cell populations. *J Cell Sci*, 57: 177–87.
- Baker, BM, Chen, CS. 2012. Deconstructing the third dimension – how 3D culture microenvironments alter cellular cues. *Journal of Cell Science*, 125: 3015–24.
- Bauer, J, Bahmer, FA, Worl, J, Neuhuber, W, Schuler, G, Fartasch, M. 2001. A strikingly constant ratio exists between Langerhans cells and other epidermal cells in human skin. A stereologic study using the optical disector method and the confocal laser scanning microscope. *J Invest Dermatol*, 116: 313–8.
- Bertoni, F, Barbani, N, Giusti, P, Ciardelli, G. 2006. Transglutaminase reactivity with gelatine: perspective applications in tissue engineering. *Biotechnol Lett*, 28: 697–702.
- Birshtein, VY, Tul'chinskii, VM. 1982. A study of gelatin by IR spectroscopy. *Chemistry of Natural Compounds*, 18: 697–700.
- Burgdorf, W, Plewig, G, Wolff, HH, Landthale, M 2009. *Braun-Falco's Dermatology*, Berlin, Heidelberg, New York, Springer.
- Cantaert, T, Baeten, D, Tak, PP, van Baarsen, LG. 2010. Type I IFN and TNFalpha cross-regulation in immune-mediated inflammatory disease: basic concepts and clinical relevance. *Arthritis Res Ther*, 12: 219.
- Cao, S, Zhang, X, Edwards, JP, Mosser, DM. 2006. NF-kappaB1 (p50) homodimers differentially regulate pro- and anti-inflammatory cytokines in macrophages. *J Biol Chem*, 281: 26041–50.

- Chakrabarty, K, Von Oerthel, L, Hellemons, A, Clotman, F, Espana, A, Groot Koerkamp, M, Holstege, FC, Pasterkamp, RJ, Smidt, MP. 2012. Genome wide expression profiling of the mesodiencephalic region identifies novel factors involved in early and late dopaminergic development. *Biol Open*, 1: 693–704.
- Chen, J, Lui, WO, Vos, MD, Clark, GJ, Takahashi, M, Schoumans, J, Khoo, SK, Petillo, D, Lavery, T, Sugimura, J, Astuti, D, Zhang, C, Kagawa, S, Maher, ER, Larsson, C, Alberts, AS, Kanayama, HO, Teh, BT. 2003. The t(1;3) breakpoint-spanning genes LSAMP and NORE1 are involved in clear cell renal cell carcinomas. *Cancer Cell*, 4: 405–13.
- Chen, QM, Tu, VC, Catania, J, Burton, M, Toussaint, O, Dilley, T. 2000. Involvement of Rb family proteins, focal adhesion proteins and protein synthesis in senescent morphogenesis induced by hydrogen peroxide. *J Cell Sci*, 113 (Pt 22): 4087–97.
- Chen, YK, Hsueh, YP. 2012. Cortactin-binding protein 2 modulates the mobility of cortactin and regulates dendritic spine formation and maintenance. *J Neurosci*, 32: 1043–55.
- Chen, ZX, Wallis, K, Fell, SM, Sobrado, VR, Hemmer, MC, Ramskold, D, Hellman, U, Sandberg, R, Kenchappa, RS, Martinson, T, Johnsen, JI, Kogner, P, Schlisio, S. 2014. RNA Helicase A Is a Downstream Mediator of KIF1Bbeta Tumor-Suppressor Function in Neuroblastoma. *Cancer Discov*, 4: 434–51.
- Chu, SH, Ma, YB, Feng, DF, Zhang, H, Zhu, ZA, Li, ZQ, Jiang, PC. 2012. Correlation of low SLC22A18 expression with poor prognosis in patients with glioma. *J Clin Neurosci*, 19: 95–8.
- Cichorek, M, Wachulska, M, Stasiewicz, A, Tyminska, A. 2013. Skin melanocytes: biology and development. *Postepy Dermatol Alergol*, 30: 30–41.
- Comper, WD 1996. *Extracellular Matrix*, Amsterdam, Harwood Academic Publisher GmbH.
- Crisostomo, PR, Wang, M, Wairiuko, GM, Morrell, ED, Terrell, AM, Seshadri, P, Nam, UH, Meldrum, DR. 2006. High passage number of stem cells adversely affects stem cell activation and myocardial protection. *Shock*, 26: 575–80.
- de Souza, CF, Xander, P, Monteiro, AC, Silva, AG, da Silva, DC, Mai, S, Bernardo, V, Lopes, JD, Jasiulionis, MG. 2012. Mining gene expression signature for the detection of pre-malignant melanocytes and early melanomas with risk for metastasis. *PLoS One*, 7: e44800.
- Debacq-Chainiaux, F, Erusalimsky, JD, Campisi, J, Toussaint, O. 2009. Protocols to detect senescence-associated beta-galactosidase (SA-beta-gal) activity, a biomarker of senescent cells in culture and in vivo. *Nat Protoc*, 4: 1798–806.
- Dieckmann, C, Renner, R, Milkova, L, Simon, JC. 2010. Regenerative medicine in dermatology: biomaterials, tissue engineering, stem cells, gene transfer and beyond. *Exp Dermatol*, 19: 697–706.
- Dirè, S, Tagliazucca, V, Callone, E, Quaranta, A. 2011. Effect of functional groups on condensation and properties of sol-gel silica nanoparticles prepared by direct synthesis from organoalkoxysilanes. *Materials Chemistry and Physics*, 126: 909–17.
- Donnelly, RP, Sheikh, F, Dickensheets, H, Savan, R, Young, HA, Walter, MR. 2010. Interleukin-26: an IL-10-related cytokine produced by Th17 cells. *Cytokine Growth Factor Rev*, 21: 393–401.
- Du, J, Miller, AJ, Widlund, HR, Horstmann, MA, Ramaswamy, S, Fisher, DE. 2003. MLANA/MART1 and SILV/PMEL17/GP100 are transcriptionally regulated by MITF in melanocytes and melanoma. *Am J Pathol*, 163: 333–43.

- Dumoutier, L, Lejeune, D, Colau, D, Renaud, JC. 2001. Cloning and characterization of IL-22 binding protein, a natural antagonist of IL-10-related T cell-derived inducible factor/IL-22. *J Immunol*, 166: 7090–5.
- Dumoutier, L, Renaud, JC. 2002. Viral and cellular interleukin-10 (IL-10)-related cytokines: from structures to functions. *Eur Cytokine Netw*, 13: 5–15.
- Ekblom, P, Lonai, P, Talts, JF. 2003. Expression and biological role of laminin-1. *Matrix Biol*, 22: 35–47.
- Elinav, E, Nowarski, R, Thaiss, CA, Hu, B, Jin, C, Flavell, RA. 2013. Inflammation-induced cancer: crosstalk between tumours, immune cells and microorganisms. *Nat Rev Cancer*, 13: 759–71.
- Fickenscher, H, Hor, S, Kupers, H, Knappe, A, Wittmann, S, Sticht, H. 2002. The interleukin-10 family of cytokines. *Trends Immunol*, 23: 89–96.
- Foltz, G, Ryu, GY, Yoon, JG, Nelson, T, Fahey, J, Frakes, A, Lee, H, Field, L, Zander, K, Sibenaller, Z, Ryken, TC, Vibhakkar, R, Hood, L, Madan, A. 2006. Genome-wide analysis of epigenetic silencing identifies BEX1 and BEX2 as candidate tumor suppressor genes in malignant glioma. *Cancer Res*, 66: 6665–74.
- Gallagher, G. 2010. Interleukin-19: multiple roles in immune regulation and disease. *Cytokine Growth Factor Rev*, 21: 345–52.
- Gartner, LP, Hiatt, JL 2001. *Color Textbook of Histology*, Philadelphia, W.B. Saunders Company.
- Geneser, F 1986. *Textbook of Histology*, Copenhagen, Munksgaard.
- Gerdes, J, Lemke, H, Baisch, H, Wacker, HH, Schwab, U, Stein, H. 1984. Cell cycle analysis of a cell proliferation-associated human nuclear antigen defined by the monoclonal antibody Ki-67. *J Immunol*, 133: 1710–5.
- Gillis, JS. 2006. Microarray evidence of glutaminyl cyclase gene expression in melanoma: implications for tumor antigen specific immunotherapy. *J Transl Med*, 4: 27.
- Giudice, GJ, Emery, DJ, Zelickson, BD, Anhalt, GJ, Liu, Z, Diaz, LA. 1993. Bullous pemphigoid and herpes gestationis autoantibodies recognize a common non-collagenous site on the BP180 ectodomain. *J Immunol*, 151: 5742–50.
- Glocker, EO, Kotlarz, D, Boztug, K, Gertz, EM, Schaffer, AA, Noyan, F, Perro, M, Diestelhorst, J, Allroth, A, Murugan, D, Hatscher, N, Pfeifer, D, Sykora, KW, Sauer, M, Kreipe, H, Lacher, M, Nustede, R, Woellner, C, Baumann, U, Salzer, U, Koletzko, S, Shah, N, Segal, AW, Sauerbrey, A, Buderus, S, Snapper, SB, Griebacher, B, Klein, C. 2009. Inflammatory bowel disease and mutations affecting the interleukin-10 receptor. *N Engl J Med*, 361: 2033–45.
- Gorgieva, S, Kokol, V 2011. Collagen- vs. Gelatine-Based Biomaterials and Their Biocompatibility: Review and Perspectives In: Pignatello, R. (ed.) *Biomaterials Applications for Nanomedicine*. Maastricht: InTech.
- Gupta, R, Kumar, A. 2008. Bioactive materials for biomedical applications using sol-gel technology. *Biomed Mater*, 3: 034005.
- Haake, A, Scott, GA, Holbrook, KA 2001. Structure and function of the skin: overview of the epidermis and dermis. In: Freinkel, R.K. & Woodley, D. (eds.) *The biology of the skin*. New York: Parthenon Pub. Group.
- Harper, RA, Grove, G. 1979. Human skin fibroblasts derived from papillary and reticular dermis: differences in growth potential in vitro. *Science*, 204: 526–7.
- He, M, Liang, P. 2010. IL-24 transgenic mice: in vivo evidence of overlapping functions for IL-20, IL-22, and IL-24 in the epidermis. *J Immunol*, 184: 1793–8.

- Hill, KK, Bedian, V, Juang, JL, Hoffmann, FM. 1995. Genetic Interactions between the *Drosophila* Abelson (Abl) Tyrosine Kinase and Failed Axon Connections (Fax), a Novel Protein in Axon Bundles. *Genetics*, 141: 595–606.
- Ho, HH, Ivashkiv, LB. 2010. Downregulation of Friend leukemia virus integration 1 as a feedback mechanism that restrains lipopolysaccharide induction of matrix metalloproteases and interleukin-10 in human macrophages. *J Interferon Cytokine Res*, 30: 893–900.
- Hoath, SB, Leahy, DG. 2003. The organization of human epidermis: functional epidermal units and phi proportionality. *J Invest Dermatol*, 121: 1440–6.
- Hoek, K, Rimm, DL, Williams, KR, Zhao, H, Ariyan, S, Lin, A, Kluger, HM, Berger, AJ, Cheng, E, Trombetta, ES, Wu, T, Niinobe, M, Yoshikawa, K, Hannigan, GE, Halaban, R. 2004. Expression profiling reveals novel pathways in the transformation of melanocytes to melanomas. *Cancer Res*, 64: 5270–82.
- Hollinger, HO 2011. *An Introduction to Biomaterials*, Boca Raton, CRC Press.
- Hotta, K, Hosaka, M, Tanabe, A, Takeuchi, T. 2009. Secretogranin II binds to secretogranin III and forms secretory granules with orexin, neuropeptide Y, and POMC. *Journal of Endocrinology*, 202: 111–21.
- Itsui, Y, Sakamoto, N, Kurosaki, M, Kanazawa, N, Tanabe, Y, Koyama, T, Takeda, Y, Nakagawa, M, Kakinuma, S, Sekine, Y, Maekawa, S, Enomoto, N, Watanabe, M. 2006. Expressional screening of interferon-stimulated genes for antiviral activity against hepatitis C virus replication. *Journal of Viral Hepatitis*, 13: 690–700.
- Janson, D, Saintigny, G, Mahe, C, El Ghalbzouri, A. 2013. Papillary fibroblasts differentiate into reticular fibroblasts after prolonged in vitro culture. *Exp Dermatol*, 22: 48–53.
- Janson, DG, Saintigny, G, van Adrichem, A, Mahe, C, El Ghalbzouri, A. 2012. Different gene expression patterns in human papillary and reticular fibroblasts. *J Invest Dermatol*, 132: 2565–72.
- Jiao, Y, Yan, J, Zhao, Y, Donahue, LR, Beamer, WG, Li, XM, Roe, BA, LeDoux, MS, Gu, WK. 2005. Carbonic anhydrase-related protein VIII deficiency is associated with a distinctive lifelong gait disorder in waddles mice. *Genetics*, 171: 1239–46.
- Joyner, JL, Augustine, NH, Taylor, KA, La Pine, TR, Hill, HR. 2000. Effects of group B streptococci on cord and adult mononuclear cell interleukin-12 and interferon-gamma mRNA accumulation and protein secretion. *J Infect Dis*, 182: 974–7.
- Karima, R, Matsumoto, S, Higashi, H, Matsushima, K. 1999. The molecular pathogenesis of endotoxic shock and organ failure. *Mol Med Today*, 5: 123–32.
- Kill, IR. 1996. Localisation of the Ki-67 antigen within the nucleolus. Evidence for a fibrillar-deficient region of the dense fibrillar component. *J Cell Sci*, 109 (Pt 6): 1253–63.
- Kim, D, Pertea, G, Trapnell, C, Pimentel, H, Kelley, R, Salzberg, SL. 2013. TopHat2: accurate alignment of transcriptomes in the presence of insertions, deletions and gene fusions. *Genome Biol*, 14: R36.
- Knuchel, R, Hofstaedter, F, Sutherland, RM, Keng, PC. 1990. [Proliferation-associated antigens PCNA and Ki-67 in two- and three-dimensional experimental systems of human squamous epithelial carcinomas]. *Verh Dtsch Ges Pathol*, 74: 275–8.
- Koga, Y, Pelizzola, M, Cheng, E, Krauthammer, M, Sznol, M, Ariyan, S, Narayan, D, Molinaro, AM, Halaban, R, Weissman, SM. 2009. Genome-wide screen of promoter methylation identifies novel markers in melanoma. *Genome Research*, 19: 1462–70.

- Kos, R, Reedy, MV, Johnson, RL, Erickson, CA. 2001. The winged-helix transcription factor FoxD3 is important for establishing the neural crest lineage and repressing melanogenesis in avian embryos. *Development*, 128: 1467–79.
- Kotenko, SV, Izotova, LS, Mirochnichenko, OV, Esterova, E, Dickensheets, H, Donnelly, RP, Pestka, S. 2001. Identification, cloning, and characterization of a novel soluble receptor that binds IL-22 and neutralizes its activity. *J Immunol*, 166: 7096–103.
- Krieg, T, Aumailley, M. 2011. The extracellular matrix of the dermis: flexible structures with dynamic functions. *Exp Dermatol*, 20: 689–95.
- La Pine, TR, Joyner, JL, Augustine, NH, Kwak, SD, Hill, HR. 2003. Defective production of IL-18 and IL-12 by cord blood mononuclear cells influences the T helper-1 interferon gamma response to group B Streptococci. *Pediatr Res*, 54: 276–81.
- Lan, W, Liu, DW, Li, GH, Mao, YG, Chen, H, Yi, XF, Wang, LQ, Peng, Y, Zhong, QL. 2011. [Screening of differential expression genes of human skin epidermal stem cells at different development stages by cDNA microarray technique]. *Zhonghua Shao Shang Za Zhi*, 27: 26–31.
- Langer, JA, Cutrone, EC, Kotenko, S. 2004. The Class II cytokine receptor (CRF2) family: overview and patterns of receptor-ligand interactions. *Cytokine Growth Factor Rev*, 15: 33–48.
- Langmead, B, Trapnell, C, Pop, M, Salzberg, SL. 2009. Ultrafast and memory-efficient alignment of short DNA sequences to the human genome. *Genome Biol*, 10: R25.
- Lee, JS, Kim, DH, Choi, DK, Kim, CD, Ahn, GB, Yoon, TY, Lee, JH, Lee, JY. 2013. Comparison of Gene Expression Profiles between Keratinocytes, Melanocytes and Fibroblasts. *Ann Dermatol*, 25: 36–45.
- Lee, ST, Nicholls, RD, Jong, MT, Fukai, K, Spritz, RA. 1995. Organization and sequence of the human P gene and identification of a new family of transport proteins. *Genomics*, 26: 354–63.
- Leeson, CR, Leeson, TS, Paparo, AA 1985. *Textbook of Histology*, Toronto, W.B.Saunders Company.
- Li, M, Liu, X, Zhou, Y, Su, SB. 2009. Interferon-lambdas: the modulators of antiviral, antitumor, and immune responses. *J Leukoc Biol*, 86: 23–32.
- Liu, DW, Lan, W, Mao, YG. 2009. Detection of Differentially Expressed Genes in Cultured Epidermal Stem Cells Derived From Children and Adult Skins by cDNA Microarray Technique. *2009 3rd International Conference on Bioinformatics and Biomedical Engineering, Vols 1–11*: 1609–12.
- Livak, KJ, Schmittgen, TD. 2001. Analysis of relative gene expression data using real-time quantitative PCR and the 2(-Delta Delta C(T)) Method. *Methods*, 25: 402–8.
- Louro, R, Nakaya, HI, Paquola, AC, Martins, EA, da Silva, AM, Verjovski-Almeida, S, Reis, EM. 2004. RASL11A, member of a novel small monomeric GTPase gene family, is down-regulated in prostate tumors. *Biochem Biophys Res Commun*, 316: 618–27.
- Lubec, G, Vierhapper, H, Bailey, AJ, Damjancic, P, Fasching, P, Sims, TJ, Kampel, D, Popow, C, Bartosch, B. 1991. Influence of L-arginine on glucose mediated collagen cross link precursors in patients with diabetes mellitus. *Amino Acids*, 1: 73–80.
- Marzook, H, Li, DQ, Nair, VS, Mudvari, P, Reddy, SD, Pakala, SB, Santhoshkumar, TR, Pillai, MR, Kumar, R. 2012. Metastasis-associated protein 1 drives tumor cell migration and invasion through transcriptional repression of RING finger protein 144A. *J Biol Chem*, 287: 5615–26.

- Mentink, CJ, Hendriks, M, Levels, AA, Wolffenbuttel, BH. 2002. Glucose-mediated cross-linking of collagen in rat tendon and skin. *Clin Chim Acta*, 321: 69–76.
- Miller, CC, Godeau, G, Lebreton-DeCoster, C, Desmouliere, A, Pellat, B, Dubertret, L, Coulomb, B. 2003. Validation of a morphometric method for evaluating fibroblast numbers in normal and pathologic tissues. *Exp Dermatol*, 12: 403–11.
- Mine, S, Fortunel, NO, Pageon, H, Asselineau, D. 2008. Aging alters functionally human dermal papillary fibroblasts but not reticular fibroblasts: a new view of skin morphogenesis and aging. *PLoS One*, 3: e4066.
- Mosser, DM, Zhang, X. 2008. Interleukin-10: new perspectives on an old cytokine. *Immunol Rev*, 226: 205–18.
- Neumann, E, Riepl, B, Knedla, A, Lefevre, S, Tarner, IH, Grifka, J, Steinmeyer, J, Scholmerich, J, Gay, S, Muller-Ladner, U. 2010. Cell culture and passaging alters gene expression pattern and proliferation rate in rheumatoid arthritis synovial fibroblasts. *Arthritis Res Ther*, 12: R83.
- Ohan, MP, Weadock, KS, Dunn, MG. 2002. Synergistic effects of glucose and ultraviolet irradiation on the physical properties of collagen. *J Biomed Mater Res*, 60: 384–91.
- Ouyang, W, Rutz, S, Crellin, NK, Valdez, PA, Hymowitz, SG. 2011. Regulation and functions of the IL-10 family of cytokines in inflammation and disease. *Annu Rev Immunol*, 29: 71–109.
- Panzavolta, S, Gioffre, M, Focarete, ML, Gualandi, C, Foroni, L, Bigi, A. 2011. Electrospun gelatin nanofibers: optimization of genipin cross-linking to preserve fiber morphology after exposure to water. *Acta Biomater*, 7: 1702–9.
- Park, H-Y, Pongpudpunth, M, Lee, J, Yaar, M. 2012. Biology of Melanocytes. In: Lowell Goldsmith, S.K., Barbara Gilchrist, Amy Paller, David Leffell, Klaus Wolff (ed.) *Fitzpatrick's Dermatology in General Medicine*. New York: McGraw-Hill.
- Place, ES, George, JH, Williams, CK, Stevens, MM. 2009. Synthetic polymer scaffolds for tissue engineering. *Chem Soc Rev*, 38: 1139–51.
- Poellmann, MJ, Harrell, PA, King, WP, Wagoner Johnson, AJ. 2010. Geometric microenvironment directs cell morphology on topographically patterned hydrogel substrates. *Acta Biomater*, 6: 3514–23.
- Ramskold, D, Wang, ET, Burge, CB, Sandberg, R. 2009. An abundance of ubiquitously expressed genes revealed by tissue transcriptome sequence data. *PLoS Comput Biol*, 5: e1000598.
- Randolph, RK, Simon, M. 1998. Dermal fibroblasts actively metabolize retinoic acid but not retinol. *J Invest Dermatol*, 111: 478–84.
- Reimand, J, Arak, T, Vilo, J. 2011. g:Profiler—a web server for functional interpretation of gene lists (2011 update). *Nucleic Acids Research*, 39: W307–W15.
- Reya, T, Morrison, SJ, Clarke, MF, Weissman, IL. 2001. Stem cells, cancer, and cancer stem cells. *Nature*, 414: 105–11.
- Roberts, A, Trapnell, C, Donaghey, J, Rinn, JL, Pachter, L. 2011. Improving RNA-Seq expression estimates by correcting for fragment bias. *Genome Biol*, 12: R22.
- Roberts, DW, Newton, RA, Beaumont, KA, Helen Leonard, J, Sturm, RA. 2006. Quantitative analysis of MC1R gene expression in human skin cell cultures. *Pigment Cell Res*, 19: 76–89.
- Robinson, MD, McCarthy, DJ, Smyth, GK. 2010. edgeR: a Bioconductor package for differential expression analysis of digital gene expression data. *Bioinformatics*, 26: 139–40.

- Rosenblum, MD, Olasz, E, Woodliff, JE, Johnson, BD, Konkol, MC, Gerber, KA, Orentas, RJ, Sandford, G, Truitt, RL. 2004. CD200 is a novel p53-target gene involved in apoptosis-associated immune tolerance. *Blood*, 103: 2691–8.
- Saal, K, Tätte, T, Järvekülg, M, Reedo, V, Lohmus, A, Kink, I. 2011. Micro- and nanoscale structures by sol-gel processing. *International Journal Of Materials & Product Technology*, 40: 2–14.
- Sahoo, A, Im, SH. 2012. Molecular Mechanisms Governing IL-24 Gene Expression. *Immune Netw*, 12: 1–7.
- Sarkar, D, Su, ZZ, Lebedeva, IV, Sauane, M, Gopalkrishnan, RV, Valerie, K, Dent, P, Fisher, PB. 2002. mda-7 (IL-24) Mediates selective apoptosis in human melanoma cells by inducing the coordinated overexpression of the GADD family of genes by means of p38 MAPK. *Proc Natl Acad Sci U S A*, 99: 10054–9.
- Schönherr, E, Hausser, HJ. 2000. Extracellular matrix and cytokines: a functional unit. *Dev Immunol*, 7: 89–101.
- Sheppard, P, Kindsvogel, W, Xu, W, Henderson, K, Schlusmeyer, S, Whitmore, TE, Kuestner, R, Garrigues, U, Birks, C, Roraback, J, Ostrand, C, Dong, D, Shin, J, Presnell, S, Fox, B, Haldeman, B, Cooper, E, Taft, D, Gilbert, T, Grant, FJ, Tackett, M, Krivan, W, McKnight, G, Clegg, C, Foster, D, Klucher, KM. 2003. IL-28, IL-29 and their class II cytokine receptor IL-28R. *Nat Immunol*, 4: 63–8.
- Shi, GX, Rouabhia, M, Wang, ZX, Dao, LH, Zhang, Z. 2004. A novel electrically conductive and biodegradable composite made of polypyrrole nanoparticles and polylactide. *Biomaterials*, 25: 2477–88.
- Slominski, A. 2009. Neuroendocrine activity of the melanocyte. *Exp Dermatol*, 18: 760–3.
- Sonnenberg, GF, Nair, MG, Kim, TJ, Zaph, C, Fouser, LA, Artis, D. 2010. Pathological versus protective functions of IL-22 in airway inflammation are regulated by IL-17A. *J Exp Med*, 207: 1293–305.
- Sorrell, JM, Caplan, AI. 2004. Fibroblast heterogeneity: more than skin deep. *J Cell Sci*, 117: 667–75.
- Stenderup, K, Rosada, C, Worsaae, A, Clausen, JT, Dam, TN. 2007. Interleukin-20 as a target in psoriasis treatment. *Autoimmunity, Pt B: Novel Applications of Basic Research*, 1110: 368–81.
- Stockton, RA, Jacobson, BS. 2001. Modulation of cell-substrate adhesion by arachidonic acid: lipoxygenase regulates cell spreading and ERK1/2-inducible cyclooxygenase regulates cell migration in NIH-3T3 fibroblasts. *Mol Biol Cell*, 12: 1937–56.
- Szatanik, M, Vibert, N, Vassias, I, Guenet, JL, Eugene, D, de Waele, C, Jaubert, J. 2008. Behavioral effects of a deletion in *Kcnn2*, the gene encoding the SK2 subunit of small-conductance Ca²⁺-activated K⁺ channels. *Neurogenetics*, 9: 237–48.
- Tammi, R, Ripellino, JA, Margolis, RU, Tammi, M. 1988. Localization of epidermal hyaluronic acid using the hyaluronate binding region of cartilage proteoglycan as a specific probe. *J Invest Dermatol*, 90: 412–4.
- Thakur, V, Pritchard, MT, McMullen, MR, Nagy, LE. 2006. Adiponectin normalizes LPS-stimulated TNF-alpha production by rat Kupffer cells after chronic ethanol feeding. *Am J Physiol Gastrointest Liver Physiol*, 290: G998–1007.
- Thingnes, J, Lavelle, TJ, Hovig, E, Omholt, SW. 2012. Understanding the Melanocyte Distribution in Human Epidermis: An Agent-Based Computational Model Approach. *PLoS One*, 7.

- Thomas, WE, Discher, DE, Shastri, VP. 2010. Mechanical Regulation of Cells by Materials and Tissues. *Mrs Bulletin*, 35: 578–83.
- Trappmann, B, Gautrot, JE, Connelly, JT, Strange, DG, Li, Y, Oyen, ML, Cohen Stuart, MA, Boehm, H, Li, B, Vogel, V, Spatz, JP, Watt, FM, Huck, WT. 2012. Extracellular-matrix tethering regulates stem-cell fate. *Nat Mater*, 11: 642–9.
- Trivella, DB, Ferreira-Junior, JR, Dumoutier, L, Renaud, JC, Polikarpov, I. 2010. Structure and function of interleukin-22 and other members of the interleukin-10 family. *Cell Mol Life Sci*, 67: 2909–35.
- Utikal, J, Maherali, N, Kulalert, W, Hochedlinger, K. 2009. Sox2 is dispensable for the reprogramming of melanocytes and melanoma cells into induced pluripotent stem cells. *J Cell Sci*, 122: 3502–10.
- Verhey, KJ, Kaul, N, Soppina, V. 2011. Kinesin Assembly and Movement in Cells. *Annual Review of Biophysics*, Vol 40, 40: 267–88.
- Wajant, H. 2009. The role of TNF in cancer. *Results Probl Cell Differ*, 49: 1–15.
- Wei, CC, Chen, WY, Wang, YC, Chen, PJ, Lee, JY, Wong, TW, Chen, WC, Wu, JC, Chen, GY, Chang, MS, Lin, YC. 2005. Detection of IL-20 and its receptors on psoriatic skin. *Clin Immunol*, 117: 65–72.
- White, RM, Zon, LI. 2008. Melanocytes in development, regeneration, and cancer. *Cell Stem Cell*, 3: 242–52.
- Wolk, K, Witte, K, Sabat, R. 2010. Interleukin-28 and interleukin-29: novel regulators of skin biology. *J Interferon Cytokine Res*, 30: 617–28.
- Wu, S, Singh, S, Varney, ML, Kindle, S, Singh, RK. 2012. Modulation of CXCL-8 expression in human melanoma cells regulates tumor growth, angiogenesis, invasion, and metastasis. *Cancer Med*, 1: 306–17.
- Wu, Z, Li, Y, MacNeil, AJ, Junkins, RD, Berman, JN, Lin, TJ. 2013. Calcineurin-Rcan1 interaction contributes to stem cell factor-mediated mast cell activation. *J Immunol*, 191: 5885–94.
- Yim, YS, Kwon, Y, Nam, J, Yoon, HI, Lee, K, Kim, DG, Kim, E, Kim, CH, Ko, J. 2013. Slitrks control excitatory and inhibitory synapse formation with LAR receptor protein tyrosine phosphatases. *Proc Natl Acad Sci U S A*, 110: 4057–62.
- Young, B, Heath, JW 2000. *Wheater's Functional Histology: A Text and Colour Atlas*, Edinburgh, Churchill Livingstone.
- Zhang, X, Do, MD, Casey, P, Sulistio, A, Qiao, GG, Lundin, L, Lillford, P, Kosaraju, S. 2010. Chemical cross-linking gelatin with natural phenolic compounds as studied by high-resolution NMR spectroscopy. *Biomacromolecules*, 11: 1125–32.
- Zhang, Z, Michniak-Kohn, BB. 2012. Tissue engineered human skin equivalents. *Pharmaceutics*, 4: 26–41.

SUMMARY IN ESTONIAN

Mikrokeskkonna mõju naharakkudele

Vajadus nahakoe siirdamise järele on maailmas üha suurenevas. Biotehnoloogilisel teel saadud nahakoest soovitakse leida abi nii suurte põletuste, krooniliste haavandite kui ka kaasasündinud ja omandatud nahadefektide ravis. Füsioloogilisele nahale võimalikult sarnase nahaanalooži valmistamiseks on vajalik nii funktsioonivõimeliste naharakkude kui rakke ümbritseva tugisüsteemi olemasolu.

Inimese naha rakulise komponendi moodustavad peamiselt epidermises paiknevad keratinotsüüdid ja melanotsüüdid ning dermises paiknevad fibroblastid. Kõigil kolmel rakutüübil on oma spetsiifilised ülesanded nahakoos: tihedalt mitmekihilise struktuurina paiknevad keratinotsüüdid tagavad organismile esmase kaitse väliste keskkonnamõjude, sealhulgas patogeenide eest; pigmendisünteesi eest vastutavad melanotsüüdid; ning fibroblastid on peamiseks rakuvälise valkude tootjateks. Selleks et naharakud oma spetsiifilisi funktsioone täita saaksid, on vajalik koele omase tugisüsteemi – rakuvälise maatriksi olemasolu. Rakuväline maatriks koosneb paljudest valkudest ning polüsahhariididest, mis on omavahel põimunud võrgustikuks. Varasemates uuringutes on näidatud, et ka väikseimad muutused rakke ümbritsevas keskkonnas mõjutavad oluliselt rakkude toimimist, seega vajavad rakud tehiskudedes oma funktsioonide täitmiseks füsioloogilisele võimalikult sarnast keskkonda. Ülesandeid, mida naharakud peavad täitma, on kordades rohkem kui ülalmainitud ning paljud neist pole veel teada või vajavad täiendavaid uuringuid.

Väga oluline on rakkude õige funktsioneerimine tagada tehiskudedes arendamisel. Meie teadustöö laiemaks eesmärgiks on töötada välja nahale iseloomulike keemiliste ja füüsikaliste omadustega struktuurne materjal, mis võimalikult hästi imiteeriks füsioloogilist rakuvälist maatriksit.

Käeolev doktoritöö hõlmab nelja artiklit, milles uurisime naharakkude geeniekspressiooni muustrite erinevusi ning rakuvälise nano- ja mikrokeskkonna muutuste mõju rakkude morfoloogiale ja molekulaarsetele omadustele.

Esimene artikkel kirjeldab interleukiin-10 (IL-10) perekonna tsütokiinide (*IL10*, *IL19*, *IL20*, *IL22*, *IL24*, *IL26*, *IL28B*, *IL29*) ja nende retseptorite (*IL10RA*, *IL10RB*, *IL20RA*, *IL20RB*, *IL22RA1*, *IL22RA2*, *IL28RA*) geeniekspressioonide erinevusi keratinotsüütide, melanotsüütide ja fibroblastide rakukultuurides, kasutades selleks qRT-PCR meetodit. IL-10 perekonda kuuluvad nii põletikku soodustavad kui ka põletikuvastased interleukiinid. Lisaks on selle perekonna tsütokiinidel oluline roll nii haavade paranemisel kui ka doonorkudedes äratõukereaktsioonide väljakujunemisel. Kuna koedisainis kasutatakse sageli just juveniilseid rakke, siis üheks meie eesmärgiks oli hinnata laste nahakoos eraldatud rakkude põletikulist potentsiaali. Uurisime geeniekspressiooni ka terves nahakoos ning leidsime, et IL-10 perekonna tsütokiinid ning nende retseptorid on erinevalt ekspresseerunud laste ja täiskasvanute nahas, mis võib olla tingitud lapsea immuunsüsteemi ebaküpsusest ning mida peab arvesse võtma, kui

kasutame juveniilseid rakke ka täiskasvanud inimestele mõeldud tehiskude arendamisel.

Teine artikkel kirjeldab keratinotsüütide, melanotsüütide ja fibroblastide geeniekspressiooni mustrite erinevusi kogu transkriptoomi tasemel. Transkriptoomi sekveneerimiseks kasutasime SOLiD 5500xl platformi. Lisaks rakutüübi spetsiifilistele geeniekspressiooni mustritele nägime, et kultuuri viidud rakkudes, eeskätt just melanotsüütides, oli ekspresseerunud mitmeid rakkude proliferatsiooni eest vastutavaid gene. Selline leid viitab asjaolule, et rakukultuur kirjeldab pigem koe vigastuse järgset seisundit ning ei peegelda täpselt rakkude homöostaatilist seisundit. Samas leidsime, et varasemalt põhjalikult kirjeldatud rakuspetsiifiliste geenide ekspressiooni (nt. melanotsüütide pigmentisünteesi radadega seotud geenid) kultiveerimine oluliselt ei muutnud, kuna uuringus kasutasime ainult minimaalselt ümberkülvatud (2 – 3x) rakke.

Kolmanda artikli eesmärgiks oli hinnata uudsel sool-geel meetodil valmistatud SiO₂ nano- ja mikrostruktuursete pindade biosobivust. Selleks kasvasime erineva struktuursusega pindadel nahakoest eraldatud fibroblaste. Uuringu tulemustest selgus, et rakkude kasv ja paljunemine pindadel sõltub suuresti nano- ja mikrostruktuuride paigutuse tihedusest, samuti struktuuride läbimõõdust. Uuritud pinnad, mille struktuuride läbimõõt ei ületanud 1 µm ja struktuuride tihedus oli üle 240,000/mm², tagasid rakkudele piisavalt adhesiooni punkte ning ei häirinud tsütoskeleti ülesehitust ning toetasid rakkude kasvu ja paljunemist. Seetõttu on nimetatud pinnad potentsiaalselt sobilikud koetehnoloogiates kasutamiseks.

Neljas artikkel keskendub naturaalse biopolümeeri – želatiini – kasutamise võimaluste välja selgitamisele rakuvälise maatriksi arendamisel. Uurisime elektroformeeritud ning erineva kontsentratsiooniga glükoosi ning temperatuuri koosmõjul ristsidestatud želatiinmattide bioloogilisi omadusi – biolagunevust, neil kasvatatud fibroblastide proliferatsiooni, morfoloogiat ja paiknemist. Uuringu tulemusena selgus, et kuni 15% glükoosi abil valmistatud maatriksid toetasid rakkude kasvu ning paljunemist. Üle 20% glükoosi abil ristsidestatud želatiinmattid enam rakuvälise maatriksi valke lõhustavate ensüümide (kollageenaas II, IV ja trüpsiin) toimel ei lagunenu, samuti oli näha neil pindadel rakkude kasvu pidurdumine.

Käesoleva töö raames näitasime, et rakuvälise keskkonna omadused mõjutavad oluliselt rakkude kasvu, paljunemist ning morfoloogiat. Arendasime välja erinevad potentsiaalsed biosobivad materjalid koeanalogoide valmistamiseks. Edaspidises töös keskendume biomaterjalide omaduste – poorsus, elastsus, venitatavus jne. mõõtmistele ning selle põhjal materjalide edasi arendamistele, et saavutada füsioloogilisele nahale võimalikult sarnaselt funktsioneeriv nahaanaloo.

ACKNOWLEDGEMENTS

This thesis could not have been completed without the help of a number of people.

First of all, I would like to thank my supervisors Viljar Jaks, Külli Kingo, Sulev Kõks and Olavi Vasar for their support, valuable advices and scientific freedom during these years of research. Especially, I am grateful to Eero Vasar for his kind support.

Thanks to these people our new interdisciplinary working group became possible and I am very delighted to belong to this youthful team with endless enthusiasm and bright ideas. I want to thank Martin Järvekülg, Triin Kangur, Martin Pook and Kaido Siimon, who are not just excellent colleagues but also dear friends and companions.

In particular, I would like to thank Jürgen Innos and Hendrik Luuk for reviewing my paper manuscripts and dissertation. I am also grateful to the peer-reviewers Pille Säälük and Tarmo Annilo for their numerous comments, useful suggestions and constructive criticism. I need to express my sincere appreciation to Dr. Orm Porosaar at Tallinn Children's Hospital, and the Department of Dermatology of Tartu University Hospital for providing all the tissue samples for this study.

I owe all my colleagues from the Institute of Biomedicine and Translational Medicine many thanks for creating a warm and inspiring atmosphere. I absolutely cherish our “Ümarlaua bänd” for its special sense of humour.

And I shall never forget the moments I shared with my coursemate Ene Reimann – all the ups and downs in the unpredictable field on Science. These memories warm my heart and keep bringing a smile to my face.

From the bottom of my heart, I am thankful to my friends for their round-the-clock availability for vital talks and a cup of coffee.

And finally, I would like to thank my closest family. My warmest thanks belong to my parents Vaike and Madis for all the kindness and silent concern and to my beloved Kalev for continuous encouragement and patience.

ORIGINAL PUBLICATIONS

CURRICULUM VITAE

Name: Paula Reemann
Date of birth: June 4, 1982, Tartu
Citizenship: Estonian
Address: University of Tartu, Institute of Biomedicine and Translational Medicine, Department of Physiology, Ravila 19, Tartu 50411, Estonia
Phone: (+372) 53 468 351
E-mail: paula.reemann@ut.ee

Education:

2014–... University of Tartu, Faculty of Medicine, residency program in radiology
2008–... University of Tartu, Faculty of Medicine, doctoral studies in neuroscience
2001–2007 University of Tartu, Faculty of Medicine, M.D
2000–2001 Estonian University of Life Sciences, veterinary medicine
1994–2000 Hugo Treffner Gymnasium
1988–1994 Tartu Kesklinna School

Career:

2014–... Tartu University Hospital, Clinic of Radiology, residency in radiology
2013–... University of Tartu, Faculty of Medicine, Institute of Biomedicine and Translational Medicine, Department of Physiology; specialist (0.75)
01.10.11–29.02.12 Project *Regenerative medicine and tissue engineering* (IARFS11188K); project manager
2011–2012 University of Tartu, Faculty of Medicine, Institute of Physiology; specialist (1.00)
2010–2011 Competence Centre on Reproductive Medicine and Biology; research fellow (0.25)
2009–2011 University of Tartu, Faculty of Medicine, Department of Dermatology; specialist (0.50)
2009–2009 Estonian University of Life Sciences; specialist (0.50)
2007–2009 Tallinn Ambulance Service; doctor (1.00)

Research:

My scientific work has focused on investigation of interaction between cells and extracellular environment and development of three-dimensional substitute for skin tissue.

Special courses:

- *Estonian Cell Therapy Cluster, Good Manufactory Practice (GMP) Training*; Regea, Tampere, Finland; 10.–12.04.2012
- *Introductory Course on the Biology of the Skin*; Downing College, Cambridge, UK; 6.–10.12.2010
- *SOLiD™ Instrument Training* Darmstadt, Germany; 13.–17.12.2010
- *Frame Symposium – Human alternatives to animal studies*; University of Nottingham, UK; 8.–10.09.2009

Dissertations supervised

Annika Pöder, Master of Science in Pharmacy, 2014, (sub) Paula Reemann, Fibroblastide morfoloogia ja funktsionaalsete omaduste hindamine elektroformeerimise meetodil valmistatud kiulistel želatiinmaatriksitel, University of Tartu, Faculty of Medicine, Institute of Biomedicine and Translational Medicine, Department of Physiology and Department of Pharmacy.

List of publications

1. Reemann P, Reimann E, Ilmjarv S, Porosaar O, Silm H, et al. (2014). Melanocytes in the skin – comparative whole transcriptome analysis of main skin cell types. *PLoS One* 9: e115717.
2. Siimon K, Reemann P, Pöder A, Pook M, Kangur T, et al. (2014). Effect of glucose content on thermally cross-linked fibrous gelatin scaffolds for tissue engineering. *Mater Sci Eng C Mater Biol Appl* 42: 538–545.
3. Reemann P, Reimann E, Suutre S, Paavo M, Loite U, et al. (2014). Expression of class II cytokine genes in children's skin. *Acta Derm Venereol* 94: 386–392.
4. Reimann E, Kingo K, Karelson M, Reemann P, Vasar E, et al. (2014). Whole Transcriptome Analysis (RNA Sequencing) of Peripheral Blood Mononuclear Cells of Vitiligo Patients. *Dermatopathology* 1: 11–23.
5. Kõks S, Reimann E, Lilleoja R, Lattekivi F, Salumets A, et al. (2014). Sequencing and annotated analysis of full genome of Holstein breed bull. *Mamm Genome* 25: 363–373.
6. Reemann P, Kangur T, Pook M, Paalo M, Nurmis L, et al. (2013). Fibroblast growth on micro- and nanopatterned surfaces prepared by a novel sol-gel phase separation method. *J Mater Sci Mater Med* 24: 783–792.
7. Loite U, Kingo K, Reimann E, Reemann P, Vasar E, et al. (2013). Gene expression analysis of the corticotrophin-releasing hormone-proopiomelanocortin system in psoriasis skin biopsies. *Acta Derm Venereol* 93: 400–405.
8. Kõks S, Lilleoja R, Reimann E, Salumets A, Reemann P, et al. (2013). Sequencing and annotated analysis of the Holstein cow genome. *Mamm Genome* 24: 309–321.

9. Reimann E, Kingo K, Karelson M, Reemann P, Loite U, et al. (2012). The mRNA expression profile of cytokines connected to the regulation of melanocyte functioning in vitiligo skin biopsy samples and peripheral blood mononuclear cells. *Hum Immunol* 73: 393–398.
10. Lilleoja R, Sarapik A, Reimann E, Reemann P, Jaakma U, et al. (2012). Sequencing and annotated analysis of an Estonian human genome. *Gene* 493: 69–76.
11. Reimann E, Kingo K, Karelson M, Reemann P, Loite U, et al. (2012). Expression profile of genes associated with the dopamine pathway in vitiligo skin biopsies and blood sera. *Dermatology* 224: 168–176.
12. Innos J, Philips MA, Leidmaa E, Heinla I, Raud S, et al. (2011). Lower anxiety and a decrease in agonistic behaviour in Lsamp-deficient mice. *Behav Brain Res* 217: 21–31.
13. Philips MA, Kingo K, Karelson M, Ratsep R, Aunin E, et al. (2010). Promoter polymorphism -119C/G in MYG1 (C12orf10) gene is related to vitiligo susceptibility and Arg4Gln affects mitochondrial entrance of Myg1. *BMC Med Genet* 11: 56.
14. Reimann E, Kingo K, Karelson M, Salum T, Aunin E, et al. (2010). Analysis of the expression profile of CRH-POMC system genes in vitiligo skin biopsies. *J Dermatol Sci* 60: 125–128.

ELULOOKIRJELDUS

Nimi: Paula Reemann
Sünniaeg: 6. juuni, 1982, Tartu
Kodakondsus: Eesti
Aadress: TÜ bio- ja siirdemeditsiini instituut, füsioloogia osakond, Ravila 19, Tartu 50411, Eesti
Telefon: (+372) 5346 8351
E-post: paula.reemann@ut.ee

Haridustee:

2014–... TÜ, arstiteaduskond, radioloogia residentuur
2008–... TÜ arstiteaduskonna neuroteaduste doktorant
2001–2007 TÜ arstiteaduskond, ravi eriala
2000–2001 EPMÜ veterinaarmeditsiini eriala
1994–2000 Hugo Treffneri Gümnaasium (keskkool)
1988–1994 Tartu Kesklinna Kool (algkool)

Töökogemus:

2014–... SA Tartu Ülikooli Kliinikum, radioloogia kliinik, radioloogia resident
2013–... Tartu Ülikool, arstiteaduskond, bio- ja siirdemeditsiini instituut, füsioloogia osakond; spetsialist (0.75)
01.10.11–29.02.12 Projekt “Regeneratiivne meditsiin ja tehiskudede kasvatamine” (IARFS11188K); projektijuht
2011–2012 Tartu Ülikool, arstiteaduskond, füsioloogia instituut, füsioloogia õppetool; spetsialist (1.00)
2010–2011 Reproductiivmeditsiini tehnoloogia arenduskeskus AS; teadur (0.25)
2009–2011 Tartu Ülikool, arstiteaduskond, nahahaiguste kliinik; spetsialist (0.50)
2009–2009 Eesti Maaülikool; spetsialist (0.50)
2007–2009 Tallinna Kiirabi; arst (1.00)

Teadustöö:

Teadustöös olen keskendunud rakkude ja rakuvälise keskkonna omavaheliste interaktsioonide uurimisele ning kolmedimensionaalse nahaanloogi välja-töötamisele.

Juhendamised:

Annika Pöder, magistrikraad farmaatsias 2014, juhendajad: Paula Reemann, Fibroblastide morfoloogia ja funktsionaalsete omaduste hindamine elektroformeerimise meetodil valmistatud kiulistel želatiinmaatriksitel, Tartu Ülikool, Bio- ja siirdemeditsiini instituut, füsioloogia osakond; farmaatsia instituut.

Erialane enesetäiendus:

- *Estonian Cell Therapy Cluster, Good Manufactory Practice (GMP) Training*; Regea, Tampere, Soome; 10.–12.04.2012
- *Introductory Course on the Biology of the Skin*; Downing College, Cambridge, Suurbritannia; 6.–10.12.2010
- *SOLiD™ Instrument Training* Darmstadt, Saksamaa; 13.–17.12.2010
- *Frame Symposium – Human alternatives to animal studies*; Nottinghami ülikool, Suurbritannia; 8.–10.09.2009

Publikatsioonid:

1. Reemann P, Reimann E, Ilmjarv S, Porosaar O, Silm H, et al. (2014). Melanocytes in the skin – comparative whole transcriptome analysis of main skin cell types. *PLoS One* 9: e115717.
2. Siimon K, Reemann P, Pöder A, Pook M, Kangur T, et al. (2014). Effect of glucose content on thermally cross-linked fibrous gelatin scaffolds for tissue engineering. *Mater Sci Eng C Mater Biol Appl* 42: 538–545.
3. Reemann P, Reimann E, Suutre S, Paavo M, Loite U, et al. (2014). Expression of class II cytokine genes in children's skin. *Acta Derm Venereol* 94: 386–392.
4. Reimann E, Kingo K, Karelson M, Reemann P, Vasar E, et al. (2014). Whole Transcriptome Analysis (RNA Sequencing) of Peripheral Blood Mononuclear Cells of Vitiligo Patients. *Dermatopathology* 1: 11–23.
5. Kõks S, Reimann E, Lilleoja R, Lattekivi F, Salumets A, et al. (2014). Sequencing and annotated analysis of full genome of Holstein breed bull. *Mamm Genome* 25: 363–373.
6. Reemann P, Kangur T, Pook M, Paalo M, Nurmis L, et al. (2013). Fibroblast growth on micro- and nanopatterned surfaces prepared by a novel sol-gel phase separation method. *J Mater Sci Mater Med* 24: 783–792.
7. Loite U, Kingo K, Reimann E, Reemann P, Vasar E, et al. (2013). Gene expression analysis of the corticotrophin-releasing hormone-proopiomelanocortin system in psoriasis skin biopsies. *Acta Derm Venereol* 93: 400–405.
8. Kõks S, Lilleoja R, Reimann E, Salumets A, Reemann P, et al. (2013). Sequencing and annotated analysis of the Holstein cow genome. *Mamm Genome* 24: 309–321.
9. Reimann E, Kingo K, Karelson M, Reemann P, Loite U, et al. (2012). The mRNA expression profile of cytokines connected to the regulation of melanocyte functioning in vitiligo skin biopsy samples and peripheral blood mononuclear cells. *Hum Immunol* 73: 393–398.
10. Lilleoja R, Sarapik A, Reimann E, Reemann P, Jaakma U, et al. (2012). Sequencing and annotated analysis of an Estonian human genome. *Gene* 493: 69–76.
11. Reimann E, Kingo K, Karelson M, Reemann P, Loite U, et al. (2012). Expression profile of genes associated with the dopamine pathway in vitiligo skin biopsies and blood sera. *Dermatology* 224: 168–176.

12. Innos J, Philips MA, Leidmaa E, Heinla I, Raud S, et al. (2011). Lower anxiety and a decrease in agonistic behaviour in *Lsamp*-deficient mice. *Behav Brain Res* 217: 21–31.
13. Philips MA, Kingo K, Karelson M, Ratsep R, Aunin E, et al. (2010). Promoter polymorphism -119C/G in *MYG1* (*C12orf10*) gene is related to vitiligo susceptibility and Arg4Gln affects mitochondrial entrance of Myg1. *BMC Med Genet* 11: 56.
14. Reimann E, Kingo K, Karelson M, Salum T, Aunin E, et al. (2010). Analysis of the expression profile of CRH-POMC system genes in vitiligo skin biopsies. *J Dermatol Sci* 60: 125–128.

DISSERTATIONES NEUROSCIENTIAE UNIVERSITATIS TARTUENSIS

1. **Sirli Raud.** Cholecystokinin₂ receptor deficient mice: changes in function of GABA-ergic system. Tartu, 2005.
2. **Kati Koido.** Single-nucleotide polymorphism profiling of 22 candidate genes in mood and anxiety disorders. Tartu, 2005.
3. **Dzhamilja Safiulina.** The studies of mitochondria in cultured cerebellar granule neurons: characterization of mitochondrial function, volume homeostasis and interaction with neurosteroids. Tartu, 2006.
4. **Tarmo Areda.** Behavioural and neurogenetic study of mechanisms related to cat odour induced anxiety in rodents. Tartu, 2006.
5. **Aleksei Nelovkov.** Behavioural and neurogenetic study of molecular mechanisms involved in regulation of exploratory behaviour in rodents. Tartu, 2006.
6. **Annika Vaarmann.** The studies on cystatin B deficient mice: neurochemical and behavioural alterations in animal model of progressive myoclonus epilepsy of Unverricht-Lundborg type. Tartu, 2007.
7. **Urho Abramov.** Sex and environmental factors determine the behavioural phenotype of mice lacking CCK₂ receptors: implications for the behavioural studies in transgenic lines. Tartu, 2008.
8. **Hendrik Luuk.** Distribution and behavioral effects of WFS1 protein in the central nervous system. Tartu, 2009.
9. **Anne Must.** Studies on molecular genetics of male completed suicide in Estonian population. Tartu, 2009.
10. **Kaido Kurrikoff.** Involvement of cholecystokinin in chronic pain mechanisms and endogenous antinociception. Tartu, 2009.
11. **Anu Aonurm-Helm.** Depression-like phenotype and altered intracellular signalling in neural cell adhesion molecule (NCAM)-deficient mice. Tartu, 2010.
12. **Silva Sütt.** Role of endocannabinoid system and *Wfs1* in regulation of emotional behaviour: behavioural, pharmacological and genetic studies. Tartu, 2010.
13. **Mari-Anne Philips.** Characterization of *Myg1* gene and protein: expression patterns, subcellular localization, gene deficient mouse and functional polymorphisms in human. Tartu, 2010.
14. **Ranno Rätsep.** Genetics of psoriasis and vitiligo, focus on IL10 family cytokines. Tartu, 2010.
15. **Kairit Joost.** Selective screening of metabolic diseases in Estonia: the application of new diagnostic methods. Tartu, 2012, 143 p.
16. **Monika Jürgenson.** A complex phenotype in mice with partial or complete deficiency of the NCAM protein. Tartu, 2012, 117 p.

17. **Ene Reimann.** Description of the cytokines and cutaneous neuroendocrine system in the development of vitiligo. Tartu, 2012, 117 p.
18. **Jürgen Innos.** Behavioural, pharmacological and neurochemical characterisation of limbic system-associated membrane protein (LSAMP) deficient mice. Tartu, 2013, 113 p.
19. **Kaili Anier.** The role of DNA methylation in the development of cocaine-induced behavioural sensitisation. Tartu, 2013, 147 p.
20. **Maarika Liik.** Cognitive functioning, perceived cognition, subjective complaints and symptoms of depression in patients with epilepsy: neuropsychological assessment and spet brain imaging study. Tartu, 2014, 124 p.
21. **Sten Ilmjärv.** Estimating differential expression from multiple indicators. Tartu, 2015, 125 p.